

## Chapter 4

### THE HIGH TEMPERATURE GAS COOLED REACTOR TEST MODULE CORE PHYSICS BENCHMARKS

#### 4.1 HTR-10 GENERAL INFORMATION

China has a substantial programme for the development of advanced reactors that have favorable safety features, economic competitiveness and uranium resource availability. Their assessment is that the HTGR, with its unique capability to provide coolant temperatures to 950°C, provides two significant benefits; 1.) efficient electrical power generation, and 2.) the capability to supply process heat for a variety of industrial applications. China recognizes the advantages of the modular HTGR, particularly in the area of safety and has decided to develop this technology [4-2].

The objective of the HTR-10 is to verify and demonstrate the technical and safety features of the modular HTGR and to establish an experimental base for developing nuclear process heat applications. The specific aims of the HTR-10 have been defined as follows:

- To acquire the experience of HTGR design, construction and operation.
- To carry out the irradiation tests for fuel elements.
- To verify the inherent safety features of the modular HTGR.
- To demonstrate the electricity/heat co-generation and steam/gas turbine combine cycle.
- To develop the high temperature process heat utilizations [4-5].

The design of the HTR-10 reactor represents the design features of the modular HTGR which is primarily characterized by inherent safety features. The safety design philosophy deviates from the traditional approach which relies on highly reliable redundant and diversified active components and systems as well as their power supply. How much credit is given to the new safety design approach which is based on inherent safety philosophy affects the plant economy balance very much. The HTR-10 test reactor should serve as a test facility to demonstrate the inherent safety features of the modular reactor design and to help win the credit from regulatory bodies, utilities and the public [4-3].

#### 4.1.1. Facility Description

##### 4.1.1.1. Background

The HTR-10 is China's first major step of modular HTGR development. It is projected as part of the framework of China's High Technology R&D Programme, and was approved by the State Council in March 1992 for construction on a site of Tsinghua University's Institute of Nuclear Energy Technology (INET) approximately 40km north of Beijing. INET has the responsibility for overall design, construction and operation of this test reactor. Construction of the plant was completed in 2000 and initial criticality took place in December 2000.

The Design Criteria and the Safety Analysis Report for the HTR-10 were approved in August 1992 and March 1993, respectively. The basic design and budget estimate were carried out and subsequently approved by the State Education Commission and the State Science and Technology Commission in 1994. The detailed design of the components,

systems and buildings was then carried out by INET under cooperation with sub-contractors responsible for the helium auxiliary systems and the turbine generator system. For the detailed design of the main components e.g. the reactor pressure vessel, the steam generator and the helium circulator, design engineers of INET closely interfaced with manufacturing engineers to evaluate and finalize these designs.

The major technical features incorporated into the design of the HTR-10 include the following:

- Use of spherical fuel elements, which are formed with coated particles.
- A reactor core design which ensures that the maximum fuel element temperature limit cannot be exceeded in any accident.
- The reactor and the steam generator are housed in two separate steel pressure vessels. They are connected by the hot gas duct pressure vessel and arranged side by side.
- An active core cooling system is not required for residual heat removal in case of accident. Residual heat can be dissipated by means of passive heat transfer mechanism to the surrounding atmosphere
- The reactor core is entirely constructed by graphite materials, no metallic component are used in the region of the core.
- The two reactor shut down systems, i.e. ten control rods and seven small absorber ball systems, are all positioned in the side reflector. They can drop into borings by means of gravity. In-core control rods are not needed.
- Spherical fuel elements go through the reactor core in a “multi-pass” pattern. Thus all fuel elements attain a relatively uniform burn up distribution in the core. Fuel pebbles are continuously discharged via a pneumatic pulse single-exit gate which is placed inside the reactor pressure vessel.
- A design incorporating an integrated steam generator and intermediate heat exchanger (IHX). The steam generator is a once through, modular small helical tube type. The helium circulator is installed in the steam generator pressure vessel and positioned above the steam generator.
- A ventilated primary cavity is designed as a confinement to restrict the radioactivity release into the environment, it does not serve the function of gas-tight and pressure retaining containment.
- A digital reactor protection system is utilized.
- Use of a domestic standard turbine-generator unit in the secondary circuit provides electrical power.

The HTR-10 project is to be carried out in two phases. In the first phase, the reactor, with a coolant outlet temperature of 700°C, is coupled with a steam generator providing steam for a steam turbine cycle which operates on an electricity/heat co-generation basis. In the second phase, the gas turbine cycle will then be coupled to the reactor in addition to the steam turbine cycle [4-1].

#### *4.1.1.2 General design features of the HTR-10*

Design of the HTR-10 test reactor represents the basic features of the modular HTGR. The reactor core and steam generator are housed in two steel pressure vessels arranged in a “side-by-side” configuration as shown in Figure 4.1. These vessels are tied together by a connecting cross-vessel which contains the hot gas duct. All pressure vessels are subjected to cold helium discharged from the circulator at approximately 250°C. Table 4-1 provides the design parameters for the HTR-10.

Table 4-1. Key Design Parameters of the HTR-10 [4-1]

Reactor thermal power	MW	10
Primary helium pressure	MPa	3.0
Reactor core diameter	cm.	180
Average core height	cm.	197
Average helium temperature at reactor outlet	°C	700
Average helium temperature at reactor inlet	°C	250
Helium mass flow rate at full power	kg/s	4.3
Main steam pressure at steam generator outlet	MPa	4.0
Main steam temperature at steam generator outlet	°C	440
Feed water temperature	°C	104
Main steam flow rate	t/hr	12.5
Number of control rods in side reflector		10
Number of absorber ball units in side reflector		7
Nuclear fuel		UO <sub>2</sub>
Heavy metal loading per fuel element	g	5
Enrichment of fresh fuel element	%	17
Number of fuel elements in equilibrium core		27,000
Fuel loading mode		multi-pass

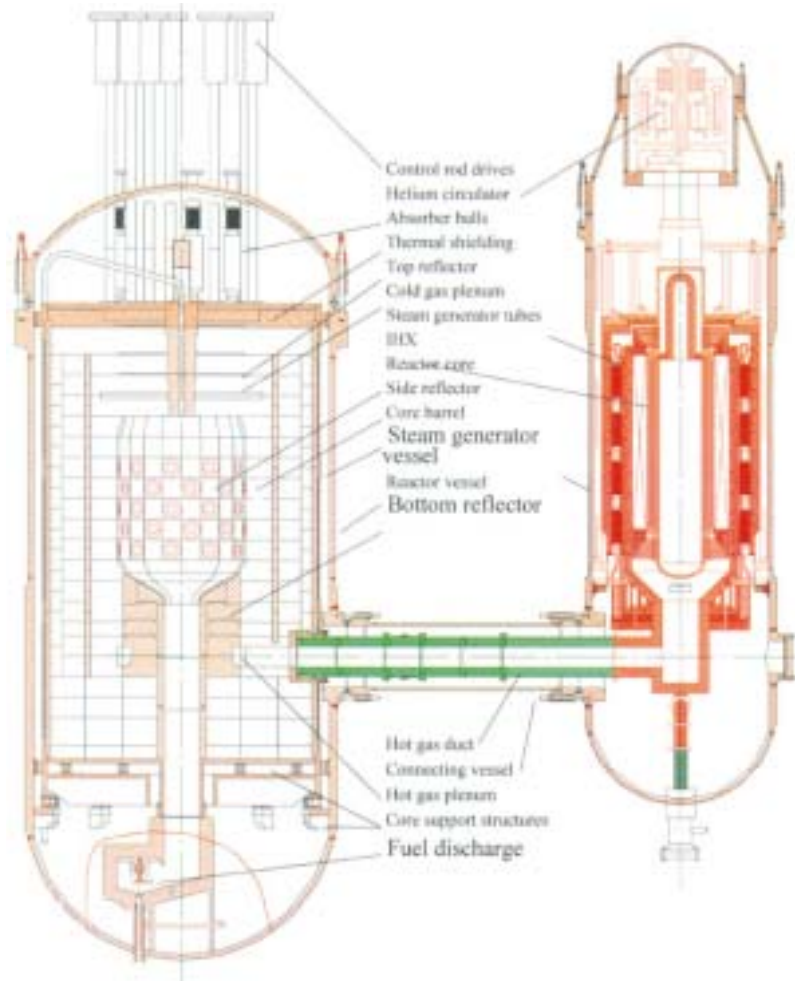


FIG. 4.1. HTR-10 primary system configuration [4-1].

#### 4.1.1.3. HTR-10 plant layout and confinement system

The HTR-10 plant includes the reactor building, a turbine/generator building, two cooling towers and a ventilation center and stack. These buildings are arranged and constructed on an area of 100x130m<sup>2</sup> as shown in Figure 4.2. The civil engineering on these buildings was contracted to companies associated with the China National Nuclear Corporation. Ground excavation was completed in late 1994 with the initial concrete poured for the reactor building foundation on 14 June 1995.

The HTR-10 plant does not contain a leak-tight pressure containing system. The concrete compartments that house the reactor and the steam generator as well as other parts of the primary pressure boundary are preferably regarded as confinement (See Figure 4.3). This confinement together with the accident ventilation system, serve as the last barrier to the release of radioactivity into the environment. During normal operation, the confinement is ventilated to be kept sub-atmospheric. In the event that the integrity of the primary pressure boundary is lost, the primary helium coolant is allowed to be released into the environment without filtering because of its low radioactivity content. Afterwards, the confinement is again ventilated and the gases in it are filtered before reaching the environment [4-3].

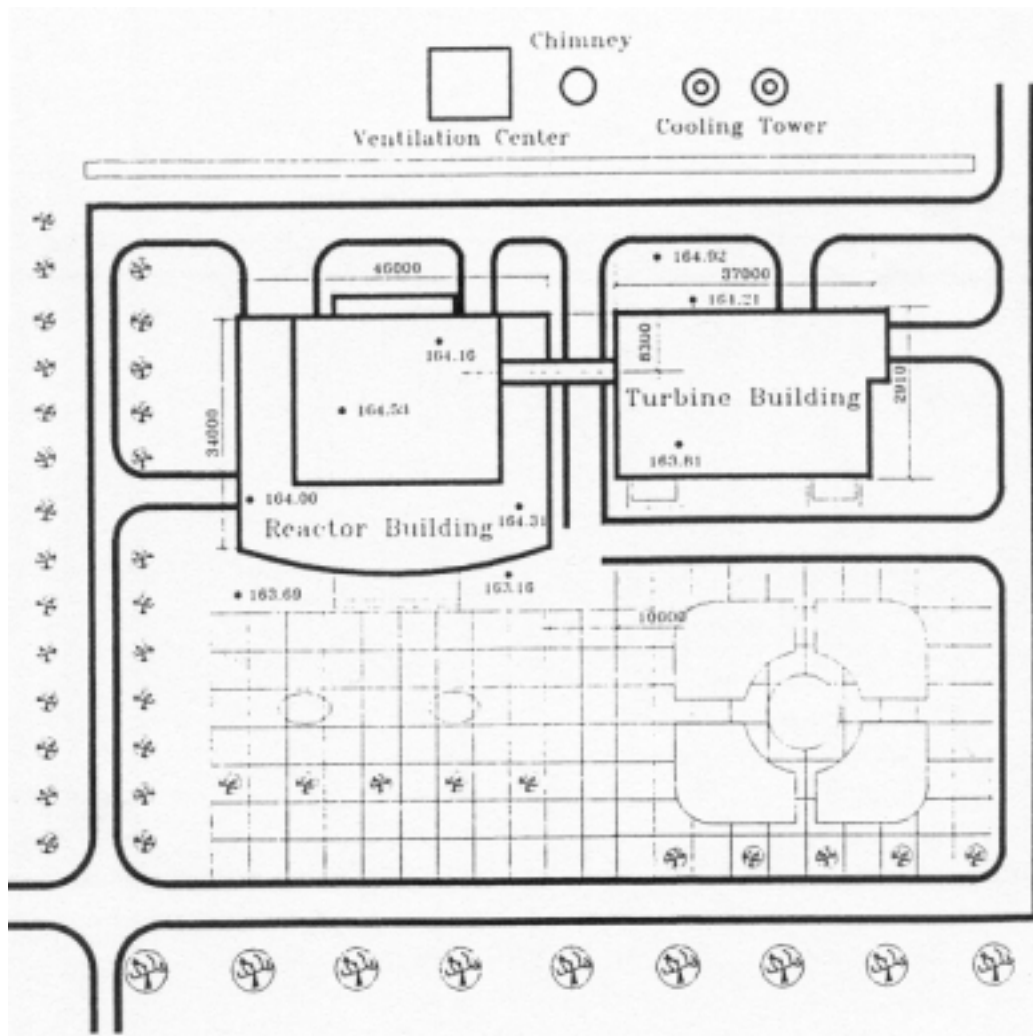


FIG. 4.2. HTR-10 site layout[4-4].

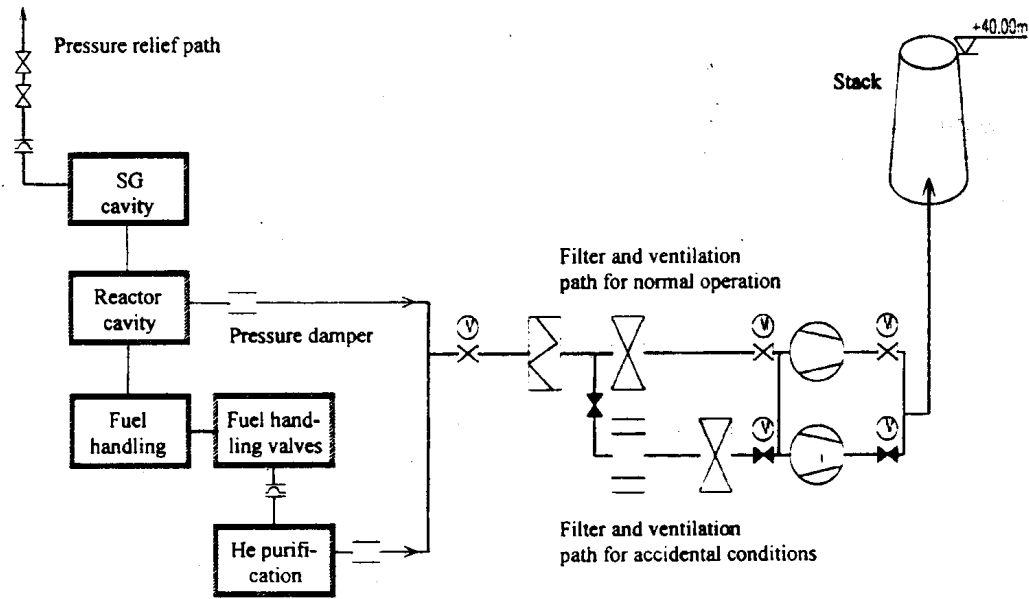


FIG. 4.3. Schematic of the HTR-10 confinement system [4-3].

#### 4.1.1.4. HTR-10 test phases

There are two operational phases for the HTR-10. In the first phase, the plant will be operated at a core outlet temperature of 700°C and inlet of 250°C. The secondary circuit will include a steam turbine cycle for electricity generation with the capability for district heating. The steam generator will produce steam at temperature of 440°C and pressure of 4.0 MPa to supply a standard turbine-generator unit. The process flow diagram for this phase is provided in Figure 4.4 (steam conditions given in the figure are for the turbine inlet).

In the second phase, the HTR-10 will be operated with a core outlet temperature of 900°C and an inlet of 300°C. A gas turbine (GT) and steam turbine (ST) combined cycle for electricity generation is in preliminary design. The intermediate heat exchanger (IHX), with a thermal power of 5MW, provides high temperature nitrogen gas of 850°C for the GT cycle. The steam generator (SG), with the remaining thermal power of 5MW, produces the steam at a temperature of 435°C for the ST cycle. Figure 4.5 depicts the flow scheme for the combined cycle [4-2].

The testing programme on the HTR-10 is divided into two power levels, 0 to 30% and 30 to 100% rated power. The 0 to 30% tests include:

- Determination of the HTR-10 response characteristics
- Performance test at operating temperature for the power conversion system, start up and shut down system
- Measurement of reactor physical and thermal hydraulic parameters
- Helium circulator test

The 30 to 100% rated power testing programme includes:

- Determination of the plants' response characteristics for this power range
- Measurement of irradiation dose distribution
- Measurement of the main parameters for the entire plant [4-8].

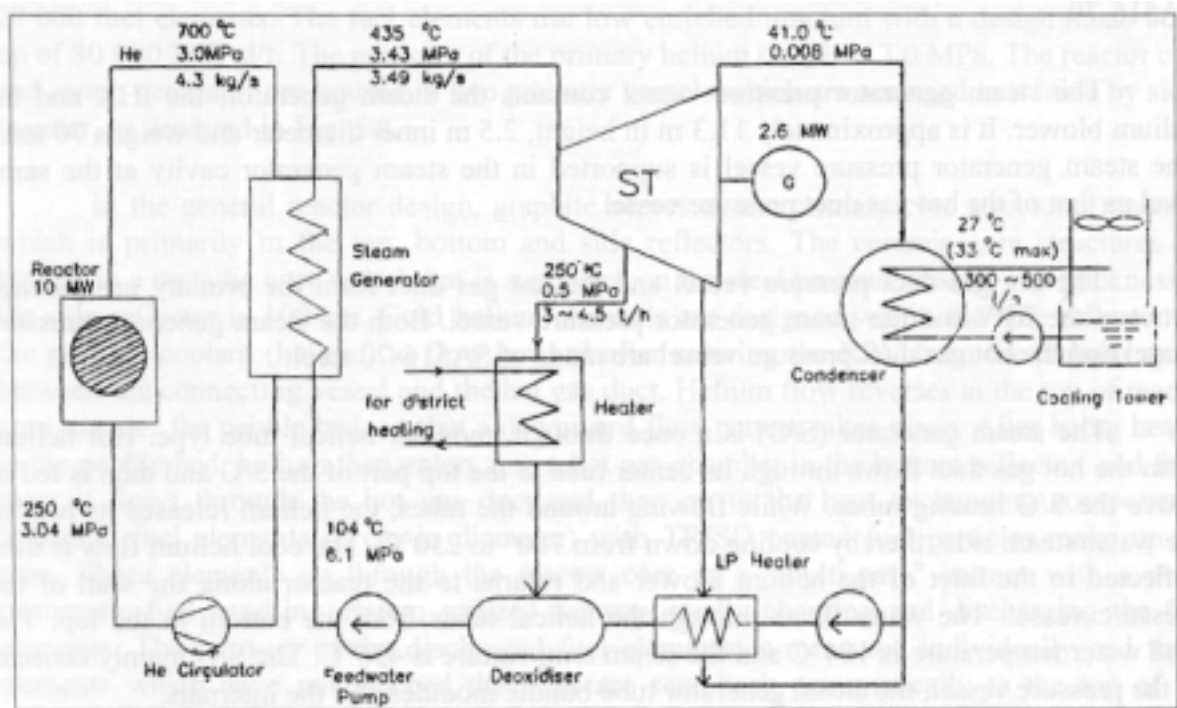


FIG. 4.4. Flow diagram for the first phase of HTR-10 operation.

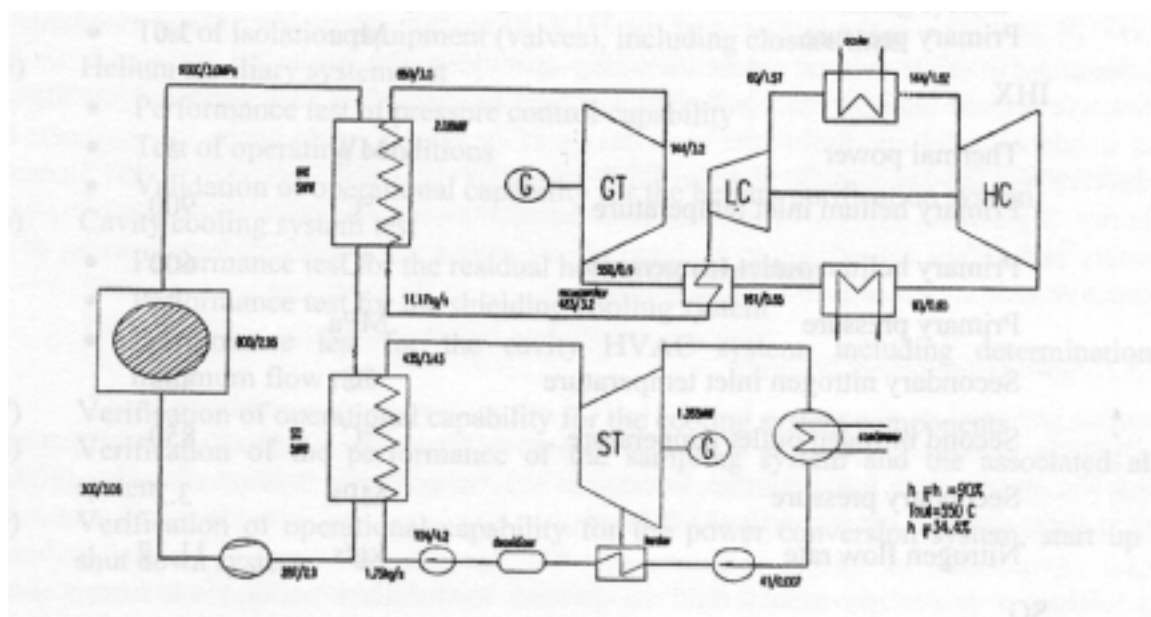


FIG. 4.5. Flow scheme for the steam turbine/gas turbine combined cycle.

#### 4.1.1.5. Core configuration

The HTR-10 is a pebble bed HTGR utilizing spherical fuel elements with ceramic coated fuel particles. The reactor core has a diameter of 1.8 m, a mean height of 1.97 m and the volume of 5.0 m<sup>3</sup>, and is surrounded by graphite reflectors. The core is composed of 27,000 fuel elements. The fuel elements use low enriched uranium with a design mean burn-up of 80,000 MWd/t. The pressure of the primary helium circuit is 3.0 Mpa.

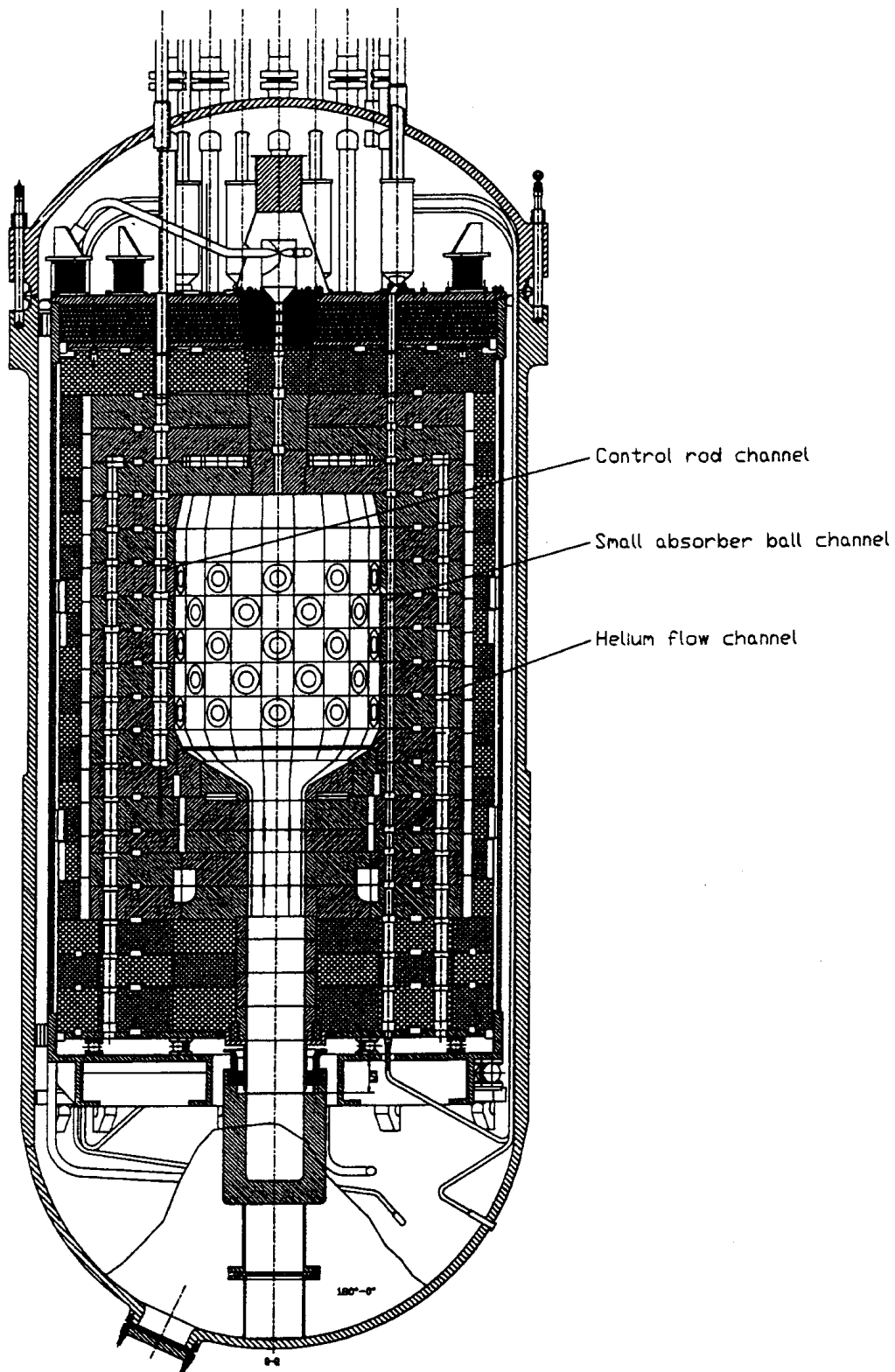


FIG. 4.6. HTR-10 reactor vertical cross-section.

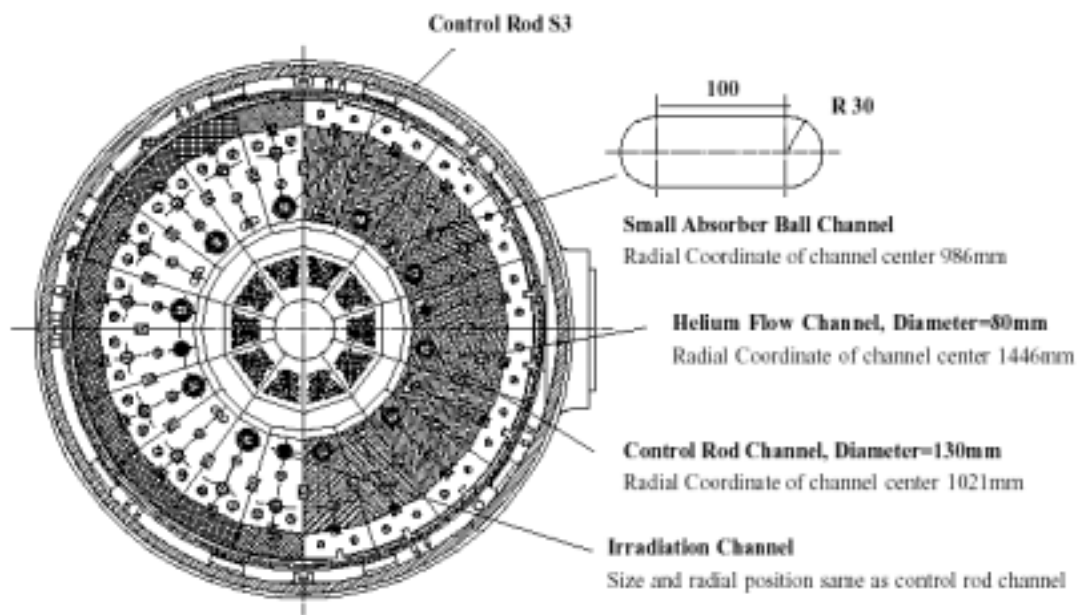


FIG. 4.7. HTR-10 reactor horizontal cross-section.

In the general reactor design, graphite serves as the primary core structural material, which is primarily in the top, bottom and side reflectors. The ceramic core structures are housed in a metallic core vessel that is supported on the steel pressure vessel. The thickness of the side reflector is 100 cm; including a layer of carbon bricks. Cold helium channels are designed within the side reflector for the primary coolant (helium) to flow upward after entering the reactor pressure vessel from the annular space between the connecting vessel and the hot gas duct. Helium flow reverses at the top of reactor core to enter the pebble bed, so that a downward flow pattern takes place. After being heated in the pebble bed, helium then enters into a hot gas chamber in the bottom reflector, and from there it flows through the hot gas duct and then on to the heat exchanging components. Spherical fuel elements (6 cm in diameter) with TRISO coated fuel particles make up the core. These elements go through the reactor core in a “multi-pass” pattern with a pulse pneumatic fuel handling system utilized for continually charging and discharging the fuel elements. The burn-up of the discharged fuel elements is measured individually and those elements which have not reached the limit are sent back pneumatically to the top of the reactor core [4-2].

Cross-sectional views of the HTR-10 reactor are shown in Figures 4.6 and 4.7. In the side reflector near the active core, there are ten borings (diameter = 130mm) for control rods, seven borings for small absorber balls and three borings (diameter = 130 mm) for irradiation purposes. There are twenty flow channels (borings with a diameter of 80 mm) in the side reflector for reactor inlet helium. The active reactor core containing spherical balls is surrounded by graphite reflectors and the graphite reflectors are surrounded by a layer (or layers) of boronated carbon bricks.

### ***HTR-10 Fuel***

Fuel elements used are the German type spherical fuel elements (6cm in diameter) with coated particles. The reactor equilibrium core contains about 27,000 fuel elements forming a pebble bed that is 180cm in diameter and 197cm in average height. The spherical fuel elements move through the reactor core in a multi-pass” pattern.

For the initial core loading, dummy balls (graphite balls without nuclear fuel) will be firstly placed into the discharge tube and the bottom conus region of the reactor core. Then, a mixture of fuel balls and dummy balls will be loaded gradually to approach first criticality. The percentages of fuel balls and dummy balls are envisaged to be 57% and 43% respectively. After the first criticality is reached, mixed balls of the same ratio will be further loaded to full core in order to make the reactor capable of being operated at full power. The full core (including the conus region) is estimated to have a volume of  $5\text{m}^3$  [4-1]. Table 4-2 and Figure 4.8 illustrate the basic characteristics and schematic of the fuel elements.

Table 4-2: Fuel element characteristics [4-1]

Diameter of ball	6.0 cm
Diameter of fuel zone	5.0 cm
Density of graphite in matrix and outer shell	$1.73\text{ g/cm}^3$
Heavy metal (uranium) loading (weight) per ball	5.0 g
Enrichment of $^{235}\text{U}$ (weight)	17 %
Equivalent natural boron content of impurities in uranium	4 ppm
Equivalent natural boron content of impurities in graphite	1.3 ppm
Volumetric filling fraction of balls in the core	0.61
<i>Fuel kernel</i>	
Radius of the kernel(mm)	0.25
$\text{UO}_2$ density( $\text{g/cm}^3$ )	10.4
<i>Coatings</i>	
Coating layer materials (starting from kernel)	PyC/PyC/SiC/PyC
Coating layer thickness(mm)	0.09/0.04/0.035/0.04
Coating layer density( $\text{g/cm}^3$ )	1.1/1.9/3.18/1.9
<i>Dummy (no fuel) elements</i>	
Diameter of ball	6.0 cm
Density of graphite	$1.73\text{ g/cm}^3$
Equivalent natural boron content of impurities in graphite	1.3 ppm

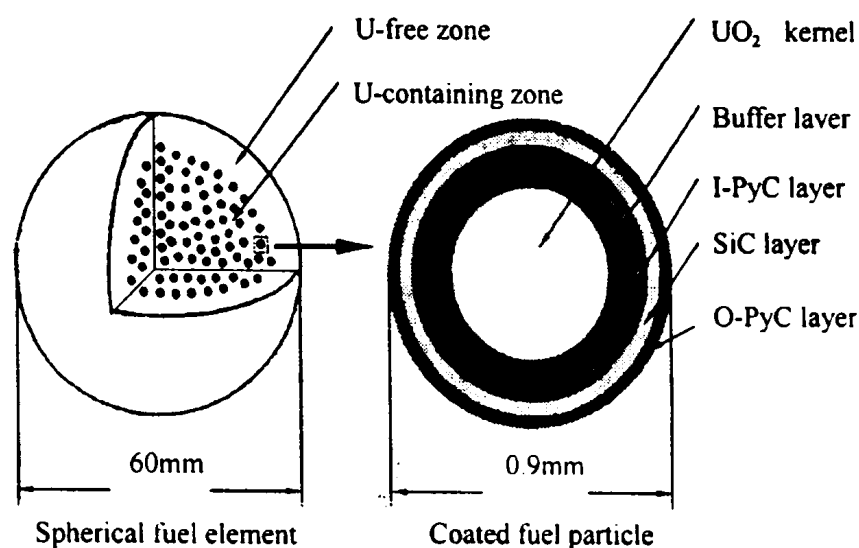


FIG. 4.8. HTR-10 spherical fuel element [4-6].

## Control of HTR-10

There are ten control rods placed in the side reflector of the HTR-10. Boron carbide ( $B_4C$ ) is used as the neutron absorber. Each control rod contains five  $B_4C$  ring segments which are housed in the area between an inner and an outer sleeve of stainless steel. These are then connected together by metallic joints. The inner and outer diameter of the  $B_4C$  ring is 60mm and 105mm respectively, while the length of each ring segment is 487mm. The inner/outer diameters of the inner and outer stainless steel sleeves are 55mm/59mm and 106mm/110mm, respectively. The length of each joint is 36mm. The lengths of the lower and upper metallic end are 45mm and 23mm, respectively (Figure 4.9). The following includes the geometry and material descriptions of one control rod:

- Control rod channel diameter/Radial coordinate of channel center: 13 cm/102.1 cm
- Axial section length and material description of the control rod from lower to upper end in sequence (mm): 45/487/36/487/36/487/36/487/36/487/23 {The 487mm long sections are the  $B_4C$  segments, other sections are stainless steel (ss) structures}
- Radial zone and thickness(mm) description of control rod in sequence: 27.5(void) / 2(ss) / 0.5(void) / 22.5( $B_4C$ ) / 0.5(void) / 2(ss)
- Density of boron carbide in the rod:  $1.7 \text{ g/cm}^3$
- Axial coordinate of control rod lower end when fully withdrawn: 119.2 cm
- Axial coordinate of control rod lower end when fully inserted: 394.2 cm
- Metallic structures of a control rod are suggested to be treated as follows:
  - 1) For the steel sleeves housing the  $B_4C$ , a density of  $7.9 \text{ g/cm}^3$  is assumed. The material chemical compositions are: Cr-18%, Fe-68.1%, Ni-10%, Si-1%, Mn-2%, C-0.1%, Ti-0.8%.
  - 2) For the metallic joints as well as the upper and lower end, it is assumed that only Fe exists in the region of  $27.5 \text{ mm} < R < 55 \text{ mm}$ , and its atom density is taken as  $0.04 \text{ cm}^{-1} \text{ barn}^{-1}$ .

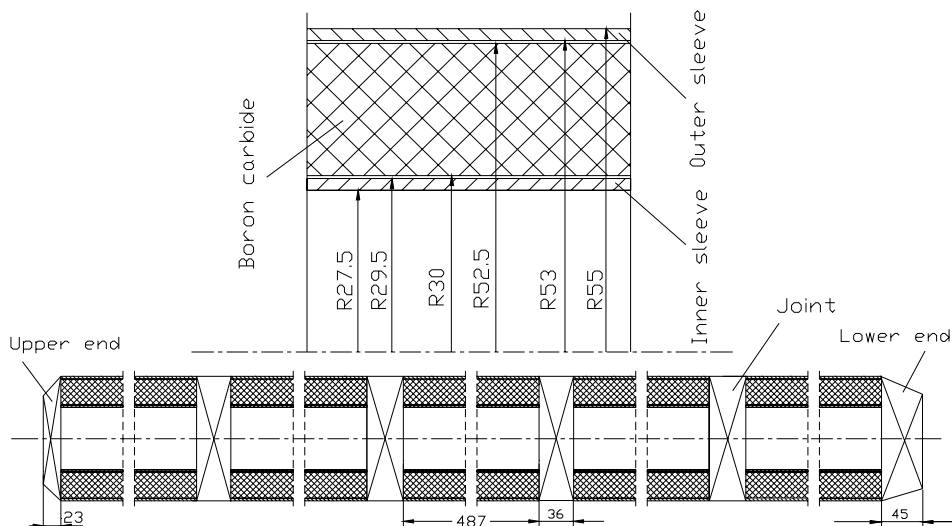


Fig.5 Simplified Structure of the HTR-10 Control Rod

FIG. 4.9. Simplified structure of the HTR-10 control rod [4-7].

There are two reactor shutdown systems, one control rod system and one small absorber ball system. They are all designed in the side reflector. Both systems are able to bring the reactor to cold shutdown conditions. Since the reactor has strong negative temperature coefficients and decay heat removal does not require any circulation of the helium coolant, the turn-off of the helium circulator can also shut down the reactor from power operating conditions [4-7].

#### *4.1.1.6 HTR-10 vessel system*

The pressure vessel unit consists of the reactor pressure vessel, the steam pressure vessel and the hot gas duct pressure vessel. The upper part of the reactor pressure vessel is a cover which is connected via eighty bolts, and its lower part is a cylindrical shelf with a lower closure head. A metallic O-ring and an  $\Omega$ -ring are used for sealing between the upper and lower parts. The tube nozzle for irradiation channels and the control rods driving system are mounted on the cover.

At the level of the hot gas duct there is a 900 mm diameter opening in the wall of the RPV. This opening is connected to the steam generator pressure vessel by the hot gas duct pressure vessel. The fuel element discharge tube penetrates through the lower closure head of the reactor pressure vessel. The reactor pressure vessel is supported in the reactor cavity by four brackets at the same level as the hot gas duct pressure vessel. The inner diameter is 4.2 m, and its height is 11.1 m. The net weight of the vessel is approximate 142 tons. The vessel material is steel SA516-70.

The steam generator pressure vessel contains the steam generator, the IHX and the helium blower. It is approximately 11.3 m in height, 2.5 m inner diameter and weighs 70 tons. The steam generator pressure vessel is supported in the steam generator cavity at the same level as that of the hot gas duct pressure vessel.

The hot gas duct pressure vessel and the hot gas duct form the primary gas passage between the reactor pressure vessel and the steam generator pressure vessel. Both the steam generator pressure vessel and the hot gas duct pressure vessel are made of SA516-70 steel.

#### *4.1.1.7. HTR-10 cooling system*

The steam generator (S-G) is a once through, modular helical tube type. Hot helium from the hot gas duct flows through its center tube to the top part of the S-G and then is fed in above the S-G heating tubes. While flowing around the tubes, the helium releases its heat to the water/steam side, thereby cooling down from 700° to 250°C. The cool helium flow is then deflected to the inlet of the helium blower and returns to the reactor along the wall of the pressure vessel. The water flows through the helical tubes from the bottom to the top. The feed water temperature is 104°C and the steam temperature at the turbine inlet is 435°C. The S-G mainly consists of the pressure vessel, the steam generator tube bundle modules and the internals.

Because the arrangement of an integrated IHX and S-G is used, the S-G adopts modular structure. There are 30 helical tube bundle modules arranged in the outer space around the IHX. Each module consists of the heat transfer tube, central pipe, fixed support structure, outer case and leak preventer. The material of the heat transfer tubes is 2-1/4Cr1Mo. The tube diameter is changed in the different heat transfer areas to improve hydrodynamic stability of steam/water two-phase flow. Also, throttle orifices are installed in the inlet of the

feed water connection tubes. The tube bundle is formed by 4 series connected helical coils wound around a circular central pipe. There are 92 coils in each heat transfer tube for a total heat transfer area of  $\sim 53 \text{ m}^2$ .

The primary circuit blower is a single stage centrifugal unit with an impeller at the end of the shaft. The drive motor is assembled on the blower shaft. The blower with its drive motor is installed on the top of the S-G pressure vessel and connected to the S/G through the connecting tube. There is an isolation valve in the connecting tube to avoid natural circulation during blower hot standby. Oil-lubricated ball bearings are utilized. The blower has the flow rate of 4.3 kg/s at a pressure of 3.0 MPa and temperature of 250°C and the pressure head is 0.06 MPa. The flow rate can be regulated down to 30% by means of changing the drive motor speed (a squirrel-case induction motor) through a frequency converter.

#### *4.1.1.8. HTR-10 safety*

##### ***Systems important to safety***

Systems important to safety are those that perform safety functions including reactor shutdown, decay heat removal and limitations on radioactivity release. For the HTR-10 reactor, these systems are primarily the following:

- Reactor protection system and its related instrumentation and associated power supplies
- Reactor shutdown systems (the control rod system and the small neutron absorber reserve shutdown system)
- Decay heat removal system
- Primary coolant pressure boundary and its pressure relief system

Definition of the functions and configuration of the systems important to safety which take proper credit for the safety features of the modular reactor design are key issues in terms of maintaining nuclear safety and cost effectiveness. The safety classification and related Quality Assurance requirements and seismic categorization of components is an associated important issue. For the HTR-10 test reactor, safety classification of components departs significantly from the LWR. For example, the primary pressure boundary is defined to the first isolation valve. Steam generator tubes are classified as Safety Class 2 components. Diesel generators are not required to be as highly qualified as those used for the LWRs, since no systems or components with large power demands would require an immediate start of the diesel engines in a plant black-out accident.

##### ***Accident identification***

The design basis accidents (DBA) are classified into several categories for the HTR-10. These categories include situations that result in:

- Increase of the heat removal capacity in the primary circuit
- Decrease of the heat removal capacity in the primary circuit
- Decrease of the primary flow rate
- Abnormality of core reactivity and power distribution
- Rupture of the primary pressure boundary tubes
- Anticipated transients without scram (ATWS)

The reactor has been designed against these accidents with conservative analysis. The results of these analyses have indicated excellent safe response of the reactor to these events. Within the framework of the DBAs, no accident will lead to the relevant release of fission products from the fuel elements.

The issue of severe accidents was also addressed for the HTR-10. A number of postulated accidents were selected to be analyzed including:

- Simultaneous withdrawal of all control rods at power operation and at reactor start-up
- Long term failure of the decay heat removal system
- Failure and shut down of the helium circulator
- Simultaneous rupture of all steam generator tubes
- Rupture of the connecting vessel and the hot gas duct

These accidents were chosen for the HTR-10 based on input from licensing authorities and on the reference to practices in Germany and U.S. For the HTR-10 reactor, as long as the reactor protection system operates, most of the above accidents lead to no damage of the fuel elements. The rupture of the connecting vessel and the hot gas duct is seen as the most severe accident leading to some fuel damage, but non-permitted release of radioactivity into the environment is not anticipated. A required action, within a relatively long time scale of a few days, is the need to block the rupture area in order to prevent air from continuously entering into the reactor core.

### ***Source term***

A mechanistic approach is adopted for determining the radioactive source term. Severe core damage is not arbitrarily postulated in the siting evaluation, as is common for large LWRs. The release of radioactivity is calculated specifically for those individually demanding accidents that lead to the most release of radioactive nuclides from the fuel elements. The calculated results serve as the basis for off-site dose evaluation. This mechanistic approach is taken primarily based on the plants' safety features, and it is directly related to the quality of the fuel elements and to the knowledge of fission product release behavior during normal operation and accident conditions. The HTR-10 reactor will serve as a test bed for fuel elements and as a facility to study fission product behavior [4-3].

### **4.1.2. Benchmark Problem Descriptions**

The benchmark problems associated with the HTR-10 addressed within this CRP include core physics evaluation of initial criticality, control rod worth (for initial and full core) and the temperature coefficient. The reactor core physics model is recommended to include core structures only until the carbon bricks. Figure 4.10 provides the two-dimensional reactor physics calculation model with zone identification numbers, while Table 4-3 gives material description and atom densities of these specific zones. The atom densities given in Table 3.3 are spatially homogenized densities. If one is to consider three-dimensional effects, the homogenized densities are to be corrected by taking into consideration of the boring geometries. Additional parameters of the reactor core include:

Density of reflector graphite	1.76 g/cm <sup>3</sup>
Equivalent natural boron impurity in reflector graphite	4.8366 ppm
Density of boronated carbon brick including B <sub>4</sub> C	1.59 g/cm <sup>3</sup>
Weight ratio of B <sub>4</sub> C in boronated carbon brick	5 %

Table 4-3. The homogenized atom density of nuclide in reflector zones under two-dimensional R-Z geometry (cm<sup>-1</sup> barn<sup>-1</sup>) per Figure 4.10

No. of zone	Carbon	Natural boron	Remarks
0	0.851047E-01	0.456926E-06	Bottom reflector with hot helium flow borings
1	0.729410E-01	0.329811E-02	Boronated carbon bricks
2	0.851462E-01	0.457148E-06	Top graphite reflector
3	0.145350E-01	0.780384E-07	Cold helium chamber
4	0.802916E-01	0.431084E-06	Top reflector
5			Top core cavity
6, 7	0.538275E-01	0.288999E-06	Dummy balls, simplified as graphite of lower density
8	0.781408E-01	0.419537E-06	Bottom reflector structures
9	0.823751E-01	0.442271E-06	Bottom reflector structures
10	0.843647E-01	0.298504E-03	Bottom reflector structures
11	0.817101E-01	0.156416E-03	Bottom reflector structures
12	0.850790E-01	0.209092E-03	Bottom reflector structures
13	0.819167E-01	0.358529E-04	Bottom reflector structures
14	0.541118E-01	0.577456E-04	Bottom reflector structures
15	0.332110E-01	0.178309E-06	Bottom reflector structures
16	0.881811E-01	0.358866E-04	Bottom reflector structures
17,55,72,74, 75,76,78, 79	0.765984E-01	0.346349E-02	Boronated carbon bricks
18,56,73	0.797184E-01	0.000000E+00	Carbon bricks
19	0.761157E-01	0.344166E-02	Boronated carbon bricks
20	0.878374E-01	0.471597E-06	Graphite reflector structure
21	0.579696E-01	0.311238E-06	Graphite reflector structure
22,23,25,49, 50,52,54,66, 67,69,71, 80	0.882418E-01	0.473769E-06	Graphite reflector structure
24,51,68	0.879541E-01	0.168369E-03	Graphite reflector structure
26	0.846754E-01	0.454621E-06	Graphite reflector structure
27	0.589319E-01	0.266468E-02	Boronated carbon bricks
28,82	0.678899E-01	1.400000E-05	Graphite reflector structure
29	0.403794E-01	1.400000E-05	Graphite reflector structure
30,41	0.678899E-01	0.364500E-06	Graphite reflector structure
31-40	0.634459E-01	0.340640E-06	Graphite reflector, control rod borings region
42	0.676758E-01	0.125331E-03	Graphite reflector structure
43,45	0.861476E-01	0.462525E-06	Graphite reflector structure
44	0.829066E-01	0.445124E-06	Graphite reflector structure
46	0.747805E-01	0.338129E-02	Boronated carbon bricks
47	0.778265E-01	0.000000E+00	Carbon bricks
48	0.582699E-01	0.312850E-06	Graphite reflector structure
53	0.855860E-01	0.459510E-06	Graphite reflector structure
57	0.728262E-01	0.391003E-06	Graphite reflector structure
58,59,61,63	0.760368E-01	0.408240E-06	Graphite reflector, cold helium flow region
60	0.757889E-01	0.145082E-03	Graphite reflector, cold helium flow region
62	0.737484E-01	0.395954E-06	Graphite reflector, cold helium flow region
64	0.660039E-01	0.298444E-02	Boronated carbon bricks
65	0.686924E-01	0.000000E+00	Carbon bricks
70	0.861500E-01	0.462538E-06	Graphite reflector structure
77	0.749927E-01	0.339088E-02	Boronated carbon bricks
81	0.797184E-01	0.000000E+00	Dummy balls, but artificially taken as carbon bricks

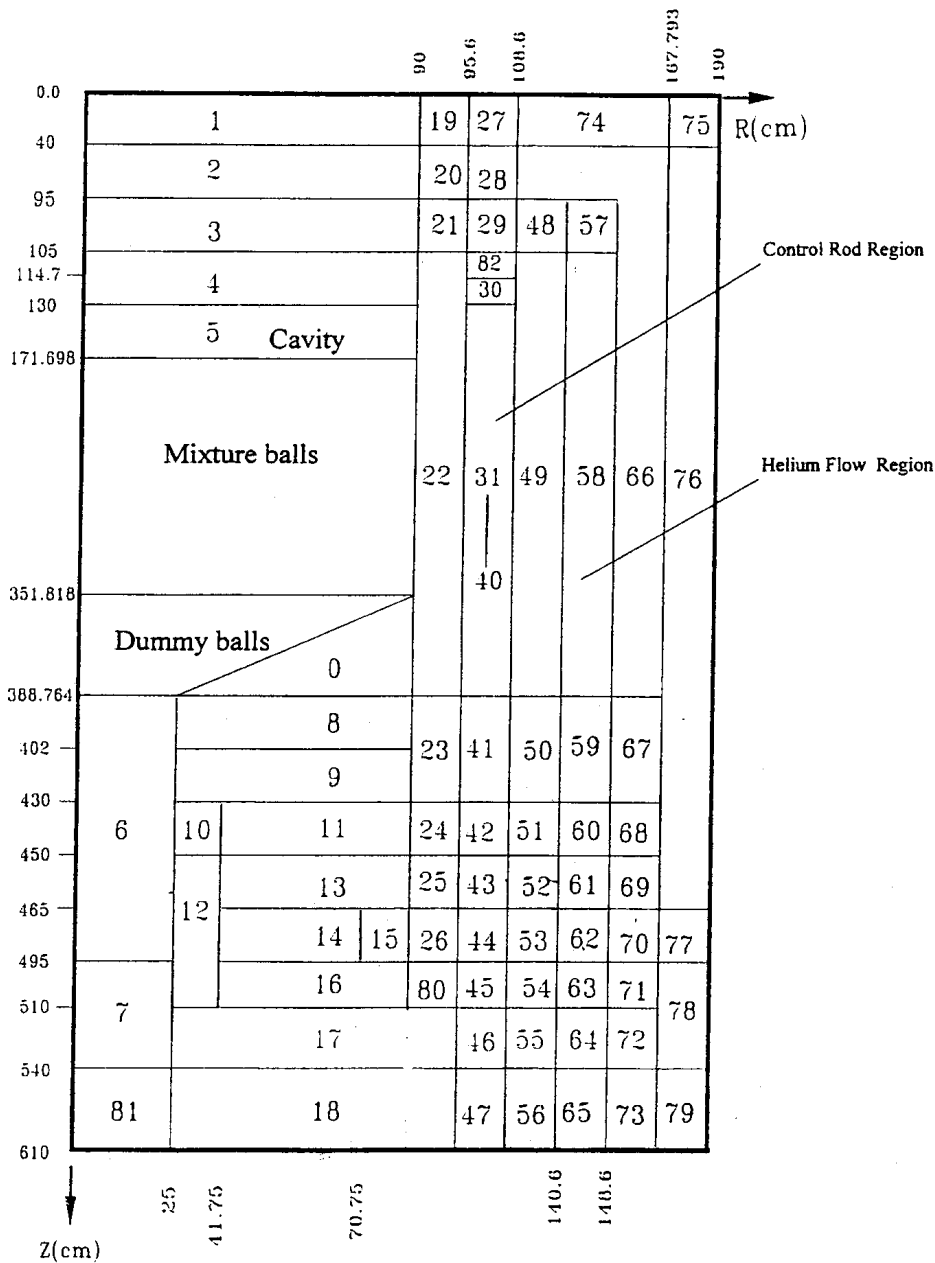


FIG. 4.10. HTR-10 core physics calculation model (see Table 4-3).

The reactor model described in the HTR-10 facility description and Figure 4.10 and Table 4.3, above is directed more generally for diffusion calculations, where homogenized atom densities are given. For Monte Carlo calculation, reactor geometries could be simulated in a more accurate manner. Therefore, following notes are provided for the modeling of Monte Carlo calculation.

The position and dimension of borings in graphite structures (refer to Figures 4.6 and 4.7) are provided below.

1. Twenty helium flow channels

- Channel diameter/Radial coordinate of channel center: 80/1446 mm
- Channel height (z coordinate): 1050-6100 mm

2. Ten control rod channels and three Irradiation channels  
 Channel diameter/Radial coordinate of channel center: 130/1021 mm  
 Channel height (z coordinate): 0-4500 mm
3. Seven small absorber ball channels  
 Location in z-coordinate: 0-1300 mm and 3887.64-6100 mm  
 Round channel, diameter/radial coordinate of center: 60/986 mm  
 Location in z-coordinate: 1300-3887.64 mm  
 Channel cross-sectional shape and dimension: see Figure 4.7
4. Hot gas duct (refer to Figures 4.1 and 4.10)  
 Duct diameter: 300 mm  
 Position of duct axis: z = 4800 mm  
 Duct length in R-direction: 900-1900 mm
5. Fuel discharge tube  
 Fuel discharge tube:  $0 < R < 250 \text{ mm}, 3887.64 \text{ mm} < Z < 6100 \text{ mm}$

If the above borings are to be modeled in the Monte Carlo calculation, the following corrections are to be made in the atom densities:

- Atom densities of 23, 25-26, 28, 30-41, 43-45, 49-50, 52-54, 58-59, 61-63, 66-67, 69-71, 80, 82 shall be the same as atom densities of 22.
- Atom densities of 27, 46, 55, 64, 72, 74-79 shall be the same as atom densities of 17.
- Atom densities of 47, 56, 65, 73 shall be the same as atom densities of 18.
- Atom densities of 29 and 42 are to be multiplied by 1.29978.
- Atom densities of 60 are to be multiplied by 1.16051.
- Region No. 6 shall be filled with graphite balls [4-7].

#### 4.1.2.1. Initial Criticality (Benchmark Problem B1)

This benchmark problem involves calculating the amount of loading (given in loading height, starting from the upper surface of the conus region) for the first criticality:  $K_{\text{eff}} = 1.0$  under the atmosphere of helium and core temperature of 20 °C, without any control rod being inserted.

#### 4.1.2.2. Temperature Coefficient (Benchmark Problem B2)

Calculation of the effective multiplication factor  $K_{\text{eff}}$  of the full core ( $5\text{m}^3$ ) under helium atmosphere and core temperatures as follows: 20°C(B21), 120°C(B22) and 250°C(B23) respectively, without any control rods being inserted.

#### 4.1.2.3. Control Rod Worth for Full Core (Benchmark Problem B3)

This problem includes calculating the reactivity worth of the ten fully inserted control rods (B31), and of one fully inserted control rod (B32, the other rods are in withdrawn position) under helium atmosphere and core temperature of 20 °C for full core.

#### *4.1.2.4. Control Rod Worth for the Initial Core (Benchmark Problem B4)*

Calculation of the reactivity worth of the ten fully inserted control rods (B41) under helium atmosphere and core temperature of 20 °C for a loading height of 126cm, and the differential worth of one control rod (B42, with the other rods in the withdrawn position). The differential reactivity worth is proposed to be calculated when the lower end of the rod is at the following axial positions: 394.2cm, 383.618cm, 334.918cm, 331.318cm, 282.618cm, 279.018cm, 230.318cm.) under helium atmosphere and core temperature of 20 °C for a loading height of 126cm.

Core temperature is defined as the temperature of the balls and all the surrounding structures included in the core physics model as described above in the HTR-10 reactor model and core configuration. Full core volume of 5m<sup>3</sup> is defined as the total volume of the mixed balls and the graphite balls in the conus region. Loading height is the height of the mixed balls starting from the upper surface of the conus region.

## 4.2 HTR-10 BENCHMARK PROBLEM ANALYSIS/RESULTS

The benchmark problems associated with the HTR-10 addressed within this CRP focus on core physics calculations. Chief Scientific Investigators from China, France, Germany, Indonesia, Japan, the Netherlands, Russia, Turkey, South Africa and the USA participated in these benchmarks. The methodologies, calculations and results are provided in the following sections.

### 4.2.1. China

#### 4.2.1.1. Calculation methodology

The following methodologies were utilized by INET in the analysis of the HTR-10 benchmark problems:

#### ***Diffusion approach for criticality calculation***

The VSOP code system has been used for the calculation. The code system includes GAM for the calculation of fast and epithermal spectrums and THERMOS for the calculation of thermal spectrum. The finite mesh diffusion code CITATION in the code system calculates the eigenvalue problem in four energy groups and in two or three dimensional reactor geometry. Cross-sections of the resolved and unresolved resonances are generated by the ZUT-DGL code. The code system takes into accounts the following basic features of pebble bed reactors (Ref.: Jül-2897, E. Teuchert et al., *V.S.O.P ('94) Computer Code System for Reactor Physics and Fuel Cycle Simulation*, 1994):

- the unique heterogeneity features of the coated particle fuel elements,
- streaming correction of the diffusion constant in the pebble bed,
- buckling feedback in the spectrum calculation,
- anisotropic diffusion constants correction for the top cavity.

The overall core physics model has been previously presented in Section 4.1. (refer to Figure 4.10). The identification numbers in this figure represent the material features of the reactor. For spectrum calculations, the pebble bed core and its surrounding graphite and carbon structures are also divided into spectrum zones based on material features and eventually the temperatures levels in the materials. Each spectrum zone covers an area that usually is identified by several material identification numbers.

The VSOP code system based on diffusion approach contains the GAM-Library and THERMOS-Library which are extracted from the basic nuclear data sets ENDF/B-V and JEF-I. The GAM-Library covers the fast and epithermal spectrums from 10MeV down to 0.414eV in a 68 energy group structure, and the THERMOS-Library covers the thermal spectrum from 0.0eV up to 2.05eV in a 30 energy group structure.

For the fast and epithermal spectrum calculation with the GAM code, P1-approximation is used based on a zero-dimensional cell of each spectrum zone. The materials in the cell were homogenized. The neutron leakage between neighboring spectrum zones is considered by buckling which is calculated by the diffusion of the whole reactor. The 68 fine group cross-sections are finally merged into 3 broad group cross-sections for the diffusion calculation.

The THERMOS code for the thermal spectrum calculation with a 30 group structure uses a one-dimensional spherical cell model. The structure of the coated particles is taken into account. The neutron exchange between spectrum zones is considered by the albedo out of the leakage term. Finally, the THERMOS calculation provides the one-group constant for the thermal spectrum.

In the one-dimensional spherical cell model of the THERMOS calculation, the mixture of fuel elements and graphite balls in the pebble bed is represented. The spherical cell is divided into three regions (Figure 4.11). The outer radius of each region in the cell is 2.5cm, 3.0cm and 3.61823cm, respectively. The material from the inner region to the outer region is fuel matrix, graphite shell and graphite moderator layer (corresponding to the graphite ball) respectively. A spherical cell model with a radius of 3 cm is used in the calculation for the core bottom region which contains only graphite balls.

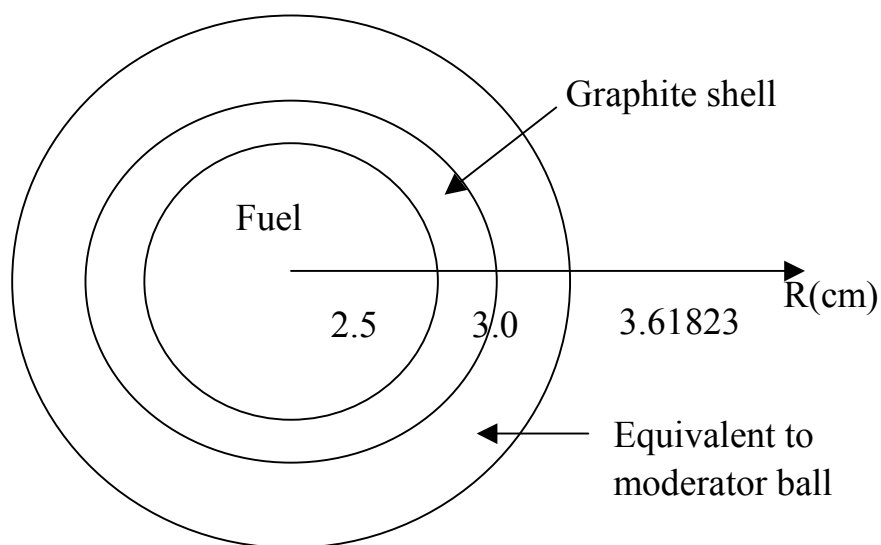


FIG. 4.11. Spherical cell model for calculation of thermal spectrum.

With the cut-off energy being 1.86 eV, four group constants are generated for the CITATION diffusion calculation in R-Z geometry based on the finite differential method and the calculation provides the multiplication factor for the given reactor.

### **Monte Carlo (MCNP) approach for the criticality calculation**

For the Monte Carlo Calculation, the code version of MCNP-4A has been used in the criticality calculation. Nuclear data are based on ENDF/B-V. The code allows for fine simulation of the reactor geometry. A three-dimensional model is established for the MCNP calculation. In the model, the following heterogeneity elements in the graphite structures are included: twenty helium flow channels, ten control rod channels, seven absorber ball channels, and the hot gas duct. The fuel discharge tube is not explicitly modeled. In the simulation of one fuel element, 8,335 coated particles are arranged in the graphite matrix on a hexahedron lattice with an edge dimension of 0.19876cm. The arrangement of the fuel elements and dummy balls is done aiming at the simulation of the given fuel/dummy ball

ratio. The arrangement of balls is top-to-top in z-direction and hexagonal prism lattice on the x-y plane.

In the MCNP calculation, continuous energy neutron cross-section data are used. The number of cycles is 140. The number of source neutrons is 10,000 per cycle. The number of cycles skipped is 5 for collecting  $K_{\text{eff}}$ .

#### ***Methodology for control rod worth calculation***

For the control rod worth calculation, the VSOP code system and the MCNP-4A code are both used. For the VSOP calculation, a homogenization treatment of the control rods is made: first, the GAM and THERMOS codes are run to prepare the microscopic cross-sections of the materials of the control rod assemblies. Then, a separate  $S_N$  code is run in two-dimensional R- $\theta$  geometry to account for the detailed geometries of the control rods. Based on this, group constants are generated for homogenized control rods. Finally, the CITATION diffusion calculation is made in order to determine the worth values of the control rods.

For the Monte Carlo calculation of the control rod worth, the methodology is the same as for the criticality calculation. Detailed modeling of the control rods is integrated into the overall three dimensional model of the reactor.

#### *4.2.1.2. Calculation results of HTR-10 core physics benchmark problems*

##### ***Benchmark Problem B1 (initial criticality)***

This benchmark problem is to determine the amount of loading (given in loading height, starting from the upper surface of the conus region) for the first criticality  $K_{\text{eff}} = 1.0$  under the atmosphere of helium and core temperature of 20°C, without any control rod being inserted.

Calculation of the multiplication factors ( $K_{\text{eff}}$ ) for different core loading heights was performed using the VOSP code and the MCNP code. The results are presented in Tables 4-4 and 4-5.

Table 4-4.  $K_{\text{eff}}$  calculation with VSOP for HTR-10 initial criticality

Loading height (cm)	Number of fuel balls	Number of dummy balls	$K_{\text{eff}}$ (27°C)	$K_{\text{eff}}$ (20°C)
190	14864	11214	1.135005	1.135195
180.114	14091	10630	1.119559	1.119747
170	13300	10033	1.102303	1.102486
160	12517	9443	1.083329	1.083508
150	11735	8853	1.062702	1.062873
140	10953	8262	1.039203	1.039394
130	10170	7673	1.012327	1.012486
126	9857	7437	1.000448	1.000602
120	9388	7082	0.982018	0.982162
110	8606	6492	0.947881	0.948021
100	7823	5902	0.908632	0.908767
90	7041	5312	0.863683	0.863796

Based on the data in the above table which are calculated through the diffusion approach, the core with an effective multiplication factor  $K_{\text{eff}}$  equal to 1 under 20°C helium should be achieved when the loading height is 125.804cm, which corresponds to 9842 loaded fuel balls and 7425 loaded graphite dummy balls, or a total number of 17267 mixed balls.

Table 4-5.  $K_{\text{eff}}$  calculation with MCNP for HTR-10 initial criticality

Loading height (cm)	$K_{\text{eff}}$ (27°C)	Standard deviation	99 % confidence intervals	VSOP-MCNP Difference(%)
180	1.12192	0.00082	1.11976-1.12408	-0.236
150	1.06201	0.00081	1.05988-1.06414	0.0692
126	0.99965	0.00091	0.99725-1.00206	0.0798
120	0.98148	0.00088	0.97917-0.98379	0.0538
90	0.86062	0.00083	0.85843-0.86281	0.306

Based on the data in the above table which are calculated through the Monte Carlo approach, the core with an effective multiplication factor  $K_{\text{eff}}$  equal to 1 under 27°C helium should be achieved when the loading height is 126.116cm, which corresponds to 9866 loaded fuel balls and 7443 loaded graphite dummy balls, or a total number of 17109 mixed balls.

It can be seen that the results of problem B1 obtained from the diffusion approach and the Monte Carlo approach agree with each other very well.

#### ***Benchmark Problem B2 (temperature coefficient)***

The scope of this problem is to calculate the effective multiplication factor ( $K_{\text{eff}}$ ) of the full core ( $5\text{m}^3$ ) under helium atmosphere and core temperatures of 20°C(**B21**), 120°C(**B22**) and 250°C(**B23**), respectively, without any control rod being inserted.

The VSOP calculation with the diffusion approach was utilized in analyzing this problem.  $K_{\text{eff}}$  values of full core under helium atmosphere and core temperature of 20°C, 120°C and 250°C are given in Table 4-6.

Table 4-6. VSOP calculation results of problem B2

Problem	B21	B22	B23
Temperature (°C)	20	120	250
$K_{\text{eff}}$	1.119747	1.110435	1.095961

#### ***Benchmark Problem B3 (control rod worth for the full core)***

The reactivity worth of the ten fully inserted control rods (**B31**), and of one fully inserted control rod (**B32**, the other rods are in withdrawn position) for full core under helium atmosphere and core temperature of 20°C are calculated in this benchmark problem.

The reactivity worth of ten fully inserted control rods was calculated with VSOP and MCNP, while the reactivity worth of one fully inserted rod was calculated only with MCNP. All calculations were performed for a 27°C helium atmosphere. The calculation results are given in Table 4-7.

Table 4-7. Reactivity worth of control rods for full core

Problem	B31 (ten rods, 27°C helium)	B32 (one rod, 27°C helium)
VSOP	15.24%	-
MCNP	16.56%	1.413%

**Benchmark Problem B4 (control rod worth for the initial core)**

This problem includes calculating the reactivity worth of the ten fully inserted control rods (**B41**) under helium atmosphere and core temperature of 20°C for a loading height of 126cm, and the differential worth of one control rod (**B42**, the other rods are in withdrawn position. The differential reactivity worth is to be calculated when the lower end of the rod is at the following axial positions: 394.2cm, 383.618cm, 334.918cm, 331.318cm, 282.618cm, 279.018cm, 230.318cm.) in a helium atmosphere and core temperature of 20 °C for a loading height of 126cm.

Calculations of control rod worth were made with VSOP and MCNP for the initial core (loading height is 126cm) in a 27°C helium atmosphere. The calculation results are presented in Tables 4-8 and 4-9.

Table 4-8. Reactivity worth of control rods for initial core

Problem	B41	Integral worth of one rod
VSOP	18.27%	1.619%
MCNP	19.36%	1.793%

Table 4-9. Differential reactivity worth of one control rod for initial core (B42)  
(Calculation with VSOP)

Axial position (cm)	230.318	279.018	282.618	331.318	334.918	383.618	394.200
Rod worth (%)	0.2564	0.6103	0.6489	1.266	1.302	1.609	1.619

*4.2.1.3. Deviations in the benchmark definition*

After the HTR-10 core physics benchmark problems were defined and before the initial core loading, two conditions changed from the benchmark definition regarding the initial core loading and the first criticality experiment.

- First, the dummy balls that were to be loaded into the initial core were not the same as defined in the benchmark definition. Graphite balls of another kind were prepared. The differences of the prepared graphite balls from the defined ones lie, in terms of physics calculation, in two aspects: density and impurity. The density of the prepared graphite balls is 1.84 g/cm<sup>3</sup> in comparison to the defined value of 1.73 g/cm<sup>3</sup>. Boron equivalent of impurities in the prepared dummy balls is 0.125 ppm instead of 1.3 ppm which as the defined value.
- Second, the first criticality experiment would be made under atmospheric air instead of helium which was the case in the benchmark definition. The following list summarizes the above deviations:

- Density of dummy balls: 1.73 → 1.84 g/cm<sup>3</sup>
- Boron equivalent of impurities in dummy ball: 1.3 → 0.125 ppm
- Core atmosphere at initial criticality: Helium → Air

**Calculated results of the deviated benchmarks**

When the above deviations became known, some calculations based on the new conditions were made to provide prediction for the criticality experiment. The changes in the graphite ball properties were placed in the physics model. To account for the air condition, atmospheric humid air (0.1013MPa) was filled in the upper cavity above the pebble bed and in the spaces between the pebbles. The density of water vapor was taken as 2.57E-5 g/cm<sup>3</sup> and the density of air was taken as 1.149E-3 g/cm<sup>3</sup>. Oxygen and nitrogen compositions in air are 23.14% and 75.53%, respectively. In the VSOP calculation, the influence of humid air was taken into account in the cell model of the spectrum calculation.

**Problem B1 (initial criticality)**

Initial criticality calculations with VSOP and MCNP are made and the results are given in Tables 4-10 and 4-11.

Table 4-10. VSOP calculation for HTR-10 initial criticality under air

Loading height (cm)	Number of fuel balls	Number of dummy balls	K <sub>eff</sub> (27°C)
126	9858	7436	1.010562
120	9388	7082	0.992149

By linear interpolation of the calculated values, the critical loading height predicted by VSOP is 122.558 cm, which corresponds to a total loading of 16821 balls.

Table 4-11. MCNP calculation for HTR-10 initial criticality under air

Loading height (cm)	Number of fuel balls	Number of dummy balls	K <sub>eff</sub> (27°C)	Standard deviation	99% confidence intervals
126	9858	7436	1.01002	0.00087	1.00772-1.01232
120	9388	7082	0.99079	0.00080	0.98869-0.99290

By linear interpolation of the calculated values, the critical loading height predicted by MCNP is 122.874 cm, which corresponds to the loading of 16864 balls in total and agrees well with the VSOP calculation.

**Problem B2 (temperature coefficient)**

For this problem, it was defined that the core atmosphere be completely helium. Therefore, the calculation was performed for helium condition with the results provided below in Table 4-12.

Table 4-12. VSOP and MCNP calculation for full core criticality, real dummy balls

	$K_{\text{eff}}$ at 27°C	$K_{\text{eff}}$ at 120°C	$K_{\text{eff}}$ at 250°C
VSOP	1.135779	1.126158	1.111115
MCNP	1.13813	-	-

**Problem B3 (control rod worth for the full core)**

For the calculation of control rod worth for the full core, the influence of humid air was again not considered. The VSOP and MCNP calculation results are provided in Table 4-13.

Table 4-13. Reactivity worth of the control rods for a full core and real dummy balls

Problem	B31 (ten rods, 27°C helium)	B32 (one rod, 27°C helium)
VSOP	14.46%	1.277%
MCNP	15.31%	1.343%

**Problem B4 (control rod worth for the initial core)**

In the calculation of the control rod worth for the initial core the influence of humid air was not included, as it was studied and determined that the effect of humid air on rod worth was negligible. The VSOP and MCNP calculation results are provided in Tables 4-14 and 4-15.

Table 4-14. Reactivity worth of control rods for the initial core and real dummy balls

Problem	B41	Integral worth of one rod
VSOP	17.23%	1.540%
MCNP	18.28%	1.572%

Table 4-15. Differential reactivity worth of one control rod for the initial core (B42) and real dummy balls (calculation with VSOP)

Axial position (cm)	230.318	279.018	282.618	331.318	334.918	383.618	394.200
Rod worth (%)	0.2395	0.5765	0.6167	1.201	1.236	1.528	1.540

**4.2.1.4. Summary of calculation results**

An overall summary of the calculation results obtained by INET for the HTR-10 core physics benchmark problems are presented in Table 4-16.

Table 4-16. Summary of calculation results of HTR-10 core physics benchmark

Benchmark Problems		Original Benchmark		Deviated Benchmark	
		VSOP	MCNP	VSOP	MCNP
B1		125.804 cm	126.116 cm	122.558 cm	122.874 cm
B2	B21	1.119747	-	1.135779	1.13813
	B22	1.110435	-	1.126158	-
	B23	1.095961	-	1.111115	-
B3	B31	15.24%	16.56%	14.46%	15.31%
	B32	-	1.413%	1.277%	1.343%
B4	B41	18.27%	19.36%	17.23%	18.28%
	B42	1.619%	1.793%	1.540%	1.572%

From the summary table, it can be concluded that VSOP and MCNP calculations for problems of B1 and B2 agree very well, but only relatively well for problems of B3 and B4 (results difference between the two approaches is less than 10%). The control rod worth calculated with VSOP tends to be less than that with MCNP.

#### 4.2.1.5. Experimental results

##### *Initial criticality*

The first criticality experiment on the HTR-10 was performed in December 2000, with the extrapolation approach. The loading process was the same as described in the benchmark definition. There were three neutron counters in the side reflector which were used to predict the number of balls still to be loaded to reach criticality. The neutron source for start-up was an Am-Be source placed in the side reflector. With an intensity of 20 Curies, it emits  $4.4 \times 10^7$  neutrons per second.

The extrapolation curves are shown in Figure 4.12. In the experiment, the first criticality was reached when a total number of 16,890 balls were loaded into the reactor core, of which 9,627 were fuel balls and 7,263 were dummy graphite balls, for a ratio of 57:43. This loading corresponded to a loading height of 123.06cm. The core atmosphere temperature was 15°C air when first criticality was achieved.

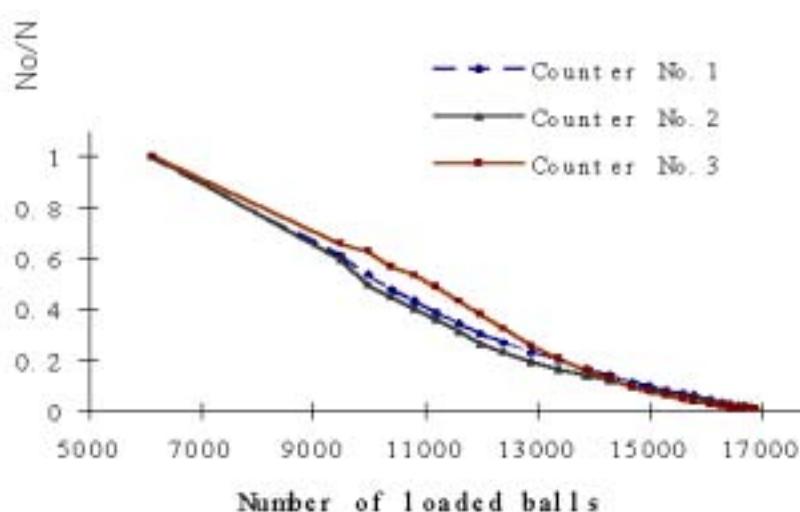


FIG 4.12. Extrapolation curve of the initial criticality approach

### ***Control rod worth***

The control rod worth calibration experiment was made for some control rods when the reactor core was loaded with 17,000 balls. This corresponded to a loading height of 123.86cm. The integral worth of one typical rod (rod S3, see Figure 4.7) was 1.4693%. In the calibration experiment, the control rod lower end position was moved from  $z = 1712\text{mm}$  to  $z = 3942\text{mm}$ . The experimental rod worth curve is shown in Figure 4.13.

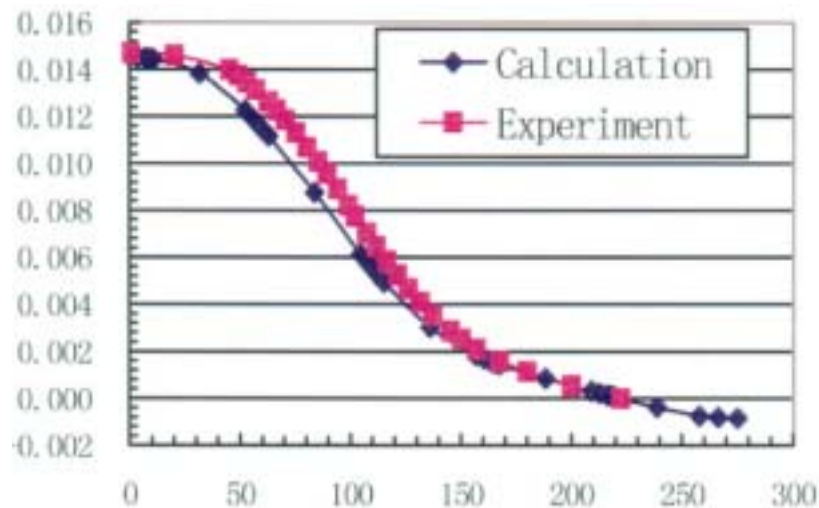


FIG. 4.13. Reactivity worth curve of one control rod.

#### *4.2.1.6. Comparison between the calculated and experimental results*

### ***Initial criticality***

Calculation with VSOP and MCNP predicted first criticality at a loading of mixed balls of 16,821 and 16,864 at 27°C, respectively. The actual air temperature was 15°C while initial criticality was achieved. After temperature coefficient correction, VSOP predicted a critical loading of 16,759 mixed balls which corresponds to a loading height of 122.11cm. The experimental critical loading was 16,890 mixed balls or 123.06cm in terms of loading height. The calculation error was less than one percent.

For the initial criticality (Problem B1), the calculation and experimental results agreed with each other very well. Also, the two calculation approaches (VSOP and MCNP) agree very well.

### ***Control rod worth***

The experimental conditions were not the same as specified in the benchmark definition of Problem B4. The main differences were in the control rod elevation height and the amount of loading in the reactor core. In the calculation, the control rod lower end position was changed from  $z = 1192\text{mm}$  to  $z = 3942\text{mm}$ , while in the experiment, the control rod lower end position moved from  $z = 1712\text{mm}$  to  $z = 3942\text{mm}$ . In the calculation, the specified loading condition was 126cm loading height which was equivalent to between 17,293 and 17,294 balls, while the experimental condition was 17,000 balls. As previously mentioned, within the calculation, the core atmosphere was helium instead of air as was in the experimental case.

In spite of these differences between the calculation and experiment conditions, the data could still be put together and compared. The integral worth of one control rod was determined to be 1.4369% by experiment (control rod elevation was  $z = 3942 \rightarrow 1712\text{mm}$ ) and 1.540% (VSOP) or 1.572% (MCNP) by calculation (control rod elevation is  $z = 3942 \rightarrow 1192\text{mm}$ ). According to the calculation, the control rod worth for the case of “control rod elevation is  $z = 3942 \rightarrow 1712\text{mm}$ ” was 1.448%. The calculated differential worth curve is presented together with the measured one in Figure 4.13. In this figure, the “control rod elevation” means the elevated height of the rod lower end from the lowest position of  $z = 3942\text{mm}$ . To obtain a better illustration in the figure, rod worth is defined as zero when the control rod lower end is at  $z = 1712\text{mm}$ .

It is believed that the different loading condition (about 293 balls) and air atmosphere should have a minor effect on control rod worth. Therefore, it can be considered that the calculated integral and differential worth of one control rod agrees well with the experimental results.

#### 4.2.2. Indonesia [4-15]

Herein are the results of the benchmark calculation on HTR-10 first core performed by BATAN. The calculations were performed using the WIMS/D4 code [4-9] and SRAC code system [4-16]. Other calculations were also performed in collaboration between Indonesia and Japan using the DELIGHT code.

The core under study, HTR-10, is a graphite-moderated and helium gas-cooled pebble bed reactor with an average helium outlet temperature of 700°C and thermal output of 10 MW. Details of the core and its associated components are provided in Section 4.1. The nuclear fuel is UO<sub>2</sub> with <sup>235</sup>U enrichment of 17% and a core fuel to moderator ball ratio of 57/43.

##### 4.2.2.1. Calculation model and methodology

Calculations for the evaluation of HTR-10 first criticality were carried out using WIMS/D4 nuclear design code system. In addition to that, a code system consisting of DELIGHT [4-10], TWOTRAN-II [4-11] and CITATION-1000VP [4-12] codes were also used in collaboration between Indonesia and Japan.

The average group constants for fuel mixtures, moderator ball and reflectors were carried out as follows:

##### *Fuel mixture cell*

Fuel mixture group constants were calculated using a spherical fuel cell model as shown in Figure 4.14. The fuel mixture cell consists of fuel and moderator balls homogenized in a cell placed inside the active core region. The materials for this model from the inner to outer regions are, fuel matrix, graphite shell, and coolant.

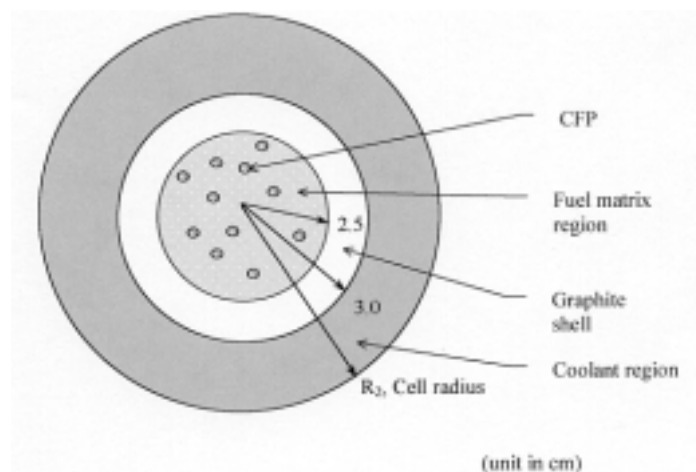


FIG. 4.14. The model of fuel cell used in WIMS/D4 and SRAC.

The radius of the fuel mixtures cell was determined from the following geometrical relationship.

The volume of a unit cell of fuel mixture centered on one fuel ball is,

$$V_c = V_p (1+m)/f$$

where,  $m$  is moderator to fuel ball ratio.

In the HTR-10, the values of  $m$  and  $f$  were given to be 43/57 and 0.61, respectively [4-13]. Therefore, the equivalent cell radius,  $R_2$ , of fuel mixtures cell can be calculated using the relation,

$$V_c = 4\pi/3 \times R_2^3,$$

which yields  $R_2$  equals to 4.2663 cm.

Table 4-17. HTR-10 core design parameters

Fuel	
Fuel element	
Diameter of ball	6.0 cm
Diameter of fueled zone	5.0 cm
Density of graphite in fueled zone and outer shell	1.73 g/cc
Heavy metal (uranium) loading per ball	5.0 g
Enrichment of $^{235}\text{U}$	17%
Natural boron impurities in uranium	4 ppm
Natural boron impurities in graphite	1.3 ppm
Volumetric filling fraction of balls in core ( $f$ )	0.61
Coated particles	
Fuel kernel	
Radius of fuel kernel	0.025 cm
UO <sub>2</sub> density	10.4 g/cm <sup>3</sup>
Coatings	
Coating layer material(starting from kernel)	PyC/PyC/SiC/PyC
Coating layer thickness (cm)	0.009/0.004/0.0035/0.004
Coating layer density (g/cm <sup>3</sup> )	1.1/1.9/3.18/1.9
Moderator Balls	
Diameter of ball	6.0 cm
Density of graphite	1.73 g/cm <sup>3</sup>
Natural boron impurities in graphite	1.3 ppm

Table 4-18. Calculated atomic densities in fuel balls

Nuclide	<i>Atomic Density [nuclei/(barn-cm)]</i>				
	UO <sub>2</sub> fuel particles (500 μ dia.)	Homogenous fuel region (5 cm dia.)	Graphite shell (0.5 cm thick)	Homogenous fuel ball (6 cm dia.)	Homogenous core region
$^{10}\text{B}$	1.8495E-8	2.2221E-8	2.2439E-8	2.2331E-8	1.3650E-8
$^{11}\text{B}$	7.4445E-8	8.9441E-8	9.0321E-8	8.9884E-8	5.4943E-8
Carbon	0.0	8.6015E-2	8.6738E-2	8.6319E-2	5.2764E-2
Oxygen	4.6472E-2	3.8732E-4	0.0	2.2414E-4	7.7933E-5
Silicon	0.0	4.2293E-4	0.0	2.4475E-4	8.5099E-5
$^{235}\text{U}$	3.9500E-3	3.2927E-5	0.0	1.9055E-5	6.6254E-6
$^{238}\text{U}$	1.9286E-2	1.6074E-4	0.0	9.3021E-5	3.2343E-5

Using the above geometric relationship and the HTR-10 data given in Table 4-17, the atomic densities for fuel balls in the HTR-10 core can be calculated, and the results of this calculation are depicted in Table 4-18.

### ***Moderator cell***

The moderator cell group constants were calculated using the same model as that of the fuel mixture. The moderator consists of graphite balls with the same radius as the fuel ball. The group constants of the moderator ball are needed for the evaluation of the cone region at the bottom of the core, which, in the initial core, is filled only with graphite balls.

The volume of the unit cell associated with one moderator ball equals to  $V_p/f$ , where,  $V_p$  is the volume of a ball and  $f$  is filling fraction.

The volume of void space associated with one ball of any type =  $V_p(1-f)/f$ .

In the calculation of group constant for moderator balls (dummy balls), the CFP volume fraction in the moderator ball was taken as very small, such that almost all fuel matrix volume is occupied by graphite. The filling fraction ( $f$ ) of the moderator ball was assumed the same as that of the core region, i.e. 0.61.

The cell volume of the moderator ball is therefore,  $V_c = V_p/f$ . The equivalent cell radius,  $R_2$ , is 3.5373 cm.

### ***Reflector cell***

To generate the cross-section for the reflector and other structural material, a cell model based on the moderator ball was adopted. In this case, the value of  $f$  was taken to be exactly equal to 1.0. Therefore, the radius of the equivalent reflector cell is the same with that of the ball, i.e. 3.0 cm. In all cell calculations, the natural boron concentration,  $N_B$ , in the graphite matrix region was calculated directly from the given values of impurities in the graphite.

$$N_B = \text{impurities (ppm)} \times \rho \times A/M,$$

where,

$\rho$ , density of graphite,

$A$ , Avogadro number ( $0.6022045 \times 10^{24}$ /mol).

$M$ , molecular weight of graphite (12.011 gr./mol).

As for the fuel matrix region, natural boron from both uranium and graphite must be taken into account. The natural boron concentration,  $N_B$ , becomes,

$$N_B = f_{UM} \times N_{BU} + (1 - f_{UM}) \times N_{BG}$$

where,

$f_{UM}$  is volume fraction occupied by all uranium kernels in fuel matrix region,

$N_{BU}$  and  $N_{BG}$  are boron number densities in uranium and graphite, respectively.

In the DELIGHT code, the natural boron must be rewritten in its constituents,  $^{10}\text{B}$  and  $^{11}\text{B}$ . In this calculation the atomic percentage of 19.9 and 80.1 were taken for  $^{10}\text{B}$  and  $^{11}\text{B}$ , respectively.

1	19	27	74		75												
2	20	28	66		76												
3	21	29	48	57													
4	22	82	49	58		66											
		30															
5 (upper cavity)		86 ~ 90 (pebble bed fuel mixtures of fuel balls and moderator balls)					31 ~ 40	49	58	66							
Cone (dummy balls)											91	bt. ref 83					
													8	23	41	50	59
6		9					24	42	51	60	68						
		10										11	25	43	52	61	69
		12										13	26	44	53	62	70
					14							15					
7		16			80		46	55	64	72							
	17	47	56	65		73					79						
81	18	47	56	65	73	79											

FIG. 4.15. HTR-10 Core calculation model in R-Z geometry.

In the calculation, a white-reflective boundary condition was used in the model as the outer boundary condition. The neutron spectrum in the fuel cell was calculated in all 68 fast and 50 thermal energy groups in the DELIGHT code. For the calculation of neutron flux distribution in the fuel cell, the energy groups were collapsed into 40 energy groups, i.e. 20 in fast and 20 in thermal regions. The flux distribution was used for averaging the group constants in fuel cell.

In the calculation with the WIMS/D4 code, the energy groups were condensed to 4 (3 fast and 1 thermal group). The SRAC cell calculation used 6 groups (3 fast and 3 thermal).

The core eigenvalue calculation was performed using the diffusion code CITATION that analyzed the reactor core in R-Z geometry. The XEDIT routine in DELIGHT-7 was used to generate the microscopic group constants for core calculation input.

The cross-sections resulted in this step were then used in the CITATION-1000VP code that calculates the core eigenvalues, reaction rates and neutron flux distributions in the whole core. The core physics model used in CITATION code is shown in Figure 4.15.

In order to speed up convergence in the core calculation, special treatment must be applied to the upper cavity region in pebble bed reactor. For the treatment of this region, a diffusion theory approach was used [4-14], where a cavity is treated as a diffusion region with zero reaction cross sections. Suitable diffusion constants in this region were obtained by introducing an appropriate amount of graphite diluted into the helium atmosphere.

#### 4.2.2.2. Results of loading at first criticality (benchmark problem B1)

The results of the HTR-10 criticality search for several heights of fuel loading are shown in Table 4-19. It can be seen that, according to the results of DELIGHT code calculation, criticality is expected at the height of ~ 110 cm of fuel mixtures loading with the value of effective multiplication factor,  $k_{eff}$ , 1.0134. A more precise loading height at first criticality can be deduced from the graph of multiplication factors vs. loading height as shown on Figure 4.16. The just criticality loading height according to this graph is approximately at 107 cm from the top of the cone at the bottom of the core.

Table 4-19. Results of HTR-10 core criticality calculation.

Loading heights (cm)	Effective Multiplication Factor ( $k_{eff}$ )		
	DELIGHT	WIMS/D4*	SRAC
90	0.9125	-	-
100	0.9612	-	0.9261
110	1.0134	-	0.9643
120	1.0388	0.923	0.9973
130	1.0700	0.971	1.0262
140	-	0.984	1.0516
150	-	0.999	-
160	-	1.020	-
170	-	1.027	-

\* Results from WIMS/D4 were obtained with model parameters that were not correct and are provided herein as a historical record of analyses by BATAN. The figures given in DELIGHT and SRAC reflect the correct model parameters.

According to WIMS/D4 calculation, the first criticality was expected at loading height of ~150 cm. While the SRAC calculation expected the initial criticality at a loading height of ~ 120 cm.

The calculated core loading characteristics at 110 cm loading height, is depicted in Table 4-20. The amount of fuel loaded in this calculation equals 43.0 kg heavy metal (uranium), which occupies a volume of 2.8 m<sup>3</sup>. The equivalent amount of <sup>235</sup>U at this loading is 7.2 kg, and that of <sup>238</sup>U is 35.8 kg.

Table 4-20. HTR-10 loading characteristics near criticality.

$k_{eff}$	1.0134
Loading heights	110 cm
Number of fuel balls	8604.5
Number of moderator balls	6536.7
Volume of ball mixture in core	2.8x10 <sup>6</sup> cm <sup>3</sup>
Equivalent uranium (heavy metal) mass	43.0 kg

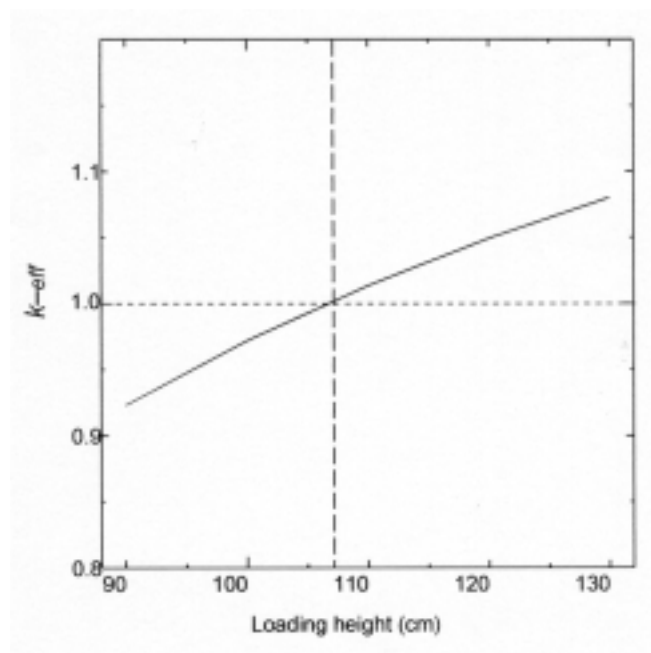


FIG. 4.16. Calculated  $K_{eff}$  vs. loading height for the HTR-10

Table 4-21. HTR-10 full core (5 m<sup>3</sup> volume) multiplication factor at different temperatures.

Core temperatures	Effective Multiplication Factor ( $k_{eff}$ )		
	DELIGHT	WIMS/D4	SRAC
20°C	1.2193	1.1197	1.1381
120°C	1.1983	1.1104	1.1149
250°C	1.1748	1.0956	1.0844

#### 4.2.2.3. Results of full core $k_{eff}$ at different coolant temperatures (benchmark B2)

The effective multiplication factors for the HTR-10 at fully loaded core with a volume of 5 m<sup>3</sup>, at 20 °C, 120 °C and 250 °C are shown in Table 4-21. It can be seen that the reactor shows a negative temperature coefficient of reactivity, and an increase in core temperature results in lower values of effective multiplication factors, i.e. from  $k_{eff}$  of 1.2193 at 20°C to 1.1748 at 250°C for the DELIGHT calculation.

### 4.2.3. Japan [4-17, 4-18]

#### 4.2.3.1. Introduction

In the calculation associated with the HTR-10 core physics benchmarks presented at the 2<sup>nd</sup> RCM in Beijing, the diffusion results showed a large discrepancy when compared to the experimental results. To improve the calculation accuracy, some improvements have been applied to the calculation model.

#### 4.2.3.2. Analysis and model methodology

Calculations for the benchmark problems were carried out using HTTR nuclear evaluation code system. The code system consists of DELIGHT, TWOTRAN-II and CITATION-1000VP codes. The DELIGHT code is a one dimensional cell burnup code. Nuclear data is based on ENDF-IV, and III. TWOTRAN-II code is used for control rod cell calculation. CITATION-1000VP code is used for two-dimensional core calculation. The outline of each model is summarized in the OHP entitled “Code, model and nuclear data library”[4-18]. Table 4.22 is a summary of the codes and model utilized in calculating the core physics benchmark problems for the HTR-10 [4-17].

Table 4.22. Code, model and nuclear data library

Nuclear Data File	ENDF/B-III,IV
Fuel cell code	DELIGHT
Theory	Collision probability
Model	Ball cell
Cut off energy	2.38 eV
Number of Groups	40
CR cell code	TWOTRAN-II
Theory	Transport
Model	2-D (r- $\theta$ )
Number of Groups	6
Core calculation code	CITATION
Model	2-D (r-Z)
Number of Groups	6
(Fast + Thermal)	3+3

#### **Revised Areas of Calculation [4-18]**

The revised points of calculations are streaming effects in the pebble bed, streaming effects in the upper cavity and consideration of control rods.

In the previous calculation, streaming effects in the pebble bed were not considered. The pebble bed was considered to be a homogeneous mixture of uranium and graphite. The streaming effect in the pebble bed was then considered in the revised calculation. Diffusion coefficients in the pebble bed were calculated by the method of referred to in reference [4-19].

The upper cavity was considered as a mixture of helium and diluted graphite to have similar diffusion coefficients of helium void region as in the previous calculation. In the revised calculation, the region was treated as helium region which have effective diffusion coefficients which were calculated by the method of reference [4-20].

The control rods of the HTR-10 remain in the upper reflector region when fully withdrawn. However, the control rods were neglected in the previous calculation. To consider the control rods, group constants of control rod were generated using the TWOTRAN-II code using the flux-weighted method. The homogenized region is shown in Figure 4.17, "CR cell model by TWOTRAN-II. The revised calculations were investigated in the following manner (Table 4-23).

Table 4-23. Comparison with previous calculations

	Previous Calculation	Present Calculation
Streaming in Pebble Bed	Not Considered	Considered (Core mixture, Dummy ball)
Streaming in Upper Cavity	Considered in Z Direction	3D $= \Sigma D_t$
Control Rod	Not Considered	Considered $\Sigma_a$ by TWOTRAN-II

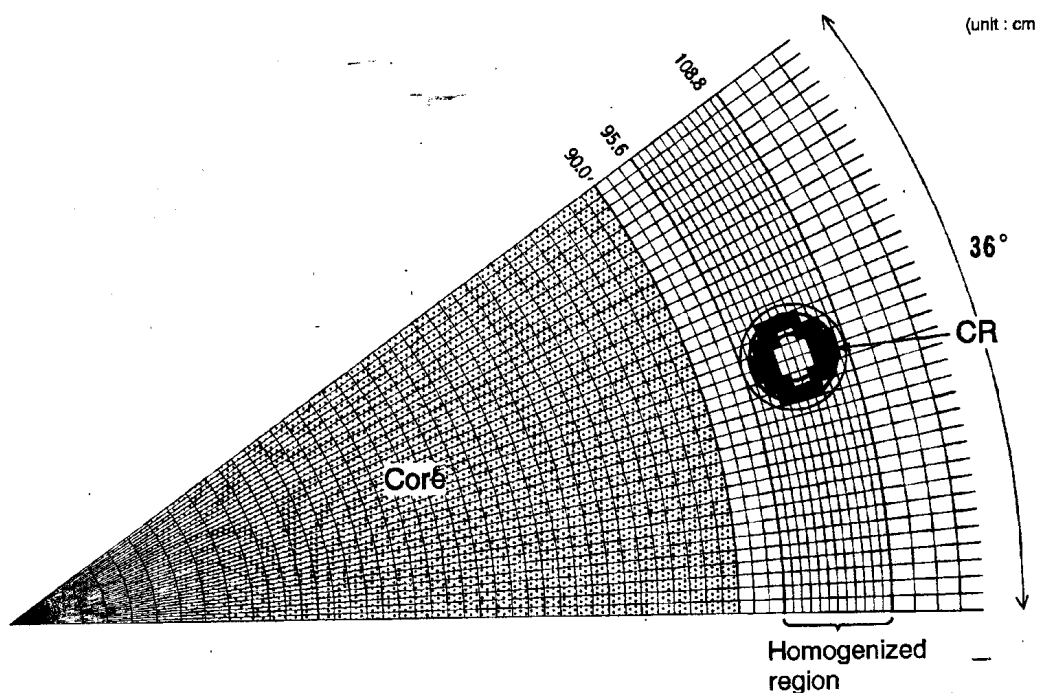


FIG. 4.17. CR cell model by TWOTRAN-II.

#### 4.2.3.3. Calculation [4-17, 4-18]

Core calculations were carried out by two-dimensional r-Z model. The model is the same as the model used in previous calculation. In the calculation of the first criticality, the control rods were fully withdrawn. The position of lower end of control rods was 144.7 cm. Cone and discharge tube were filled by dummy ball. The diffusion coefficients considering streaming effect of pebble bed were used in the cone and discharge tube region.

The calculations were carried out by changes in the core fuel mixture height. Within the fuel mixture, the ratio of fuel ball to dummy ball was kept constant as 57:43.

It was reported that the first criticality of the HTR-10 was achieved in air atmosphere. Therefore, calculations under helium atmosphere and air atmosphere were

calculated. The results show that the loading height of the first criticality under helium atmosphere and air atmosphere are 113 cm and 116 cm, respectively. The effect of air is about 3 cm in loading height. The China's results by VSOP code are also shown in Figure 4.18. These results are higher than those obtained by China.

Table 4.24. Calculated results for B1 and B3 for air and helium

Atmosphere	Helium	Air
B1 Loading height	113 cm	116 cm
B1 Number of fuel balls	14,500	14,880
B3	18% $\Delta k/k$	

\* Effect of air in upper cavity and pebble bed is about 0.8% $\Delta k/k$

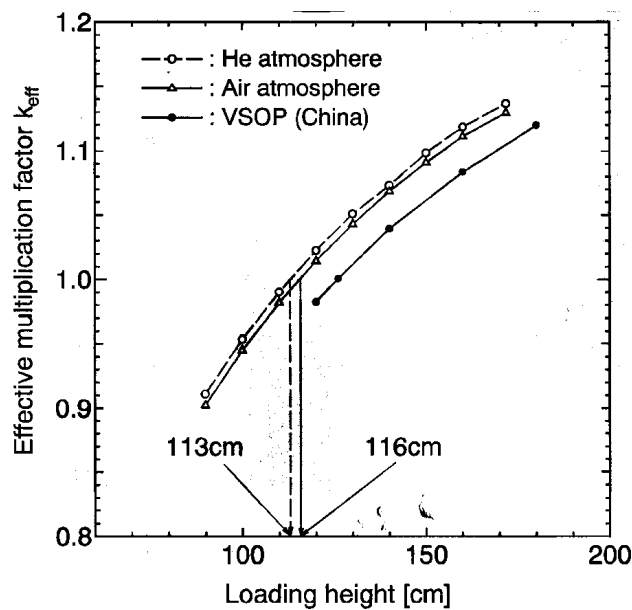


FIG. 4.18. Comparison with results from INET using VSOP.

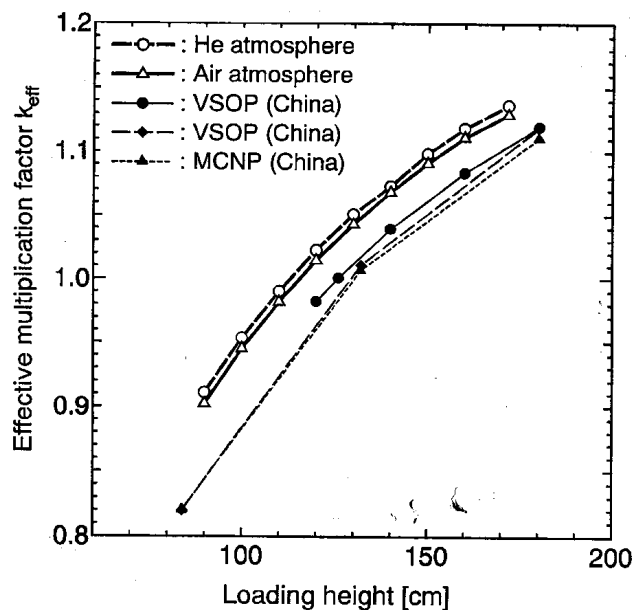


FIG. 4.19. Comparison with INET for  $K_{eff}$  vs. loading height (MCNP and VSOP).

There are calculation results by the Monte Carlo code MCNP carried out by China which were presented at the 2<sup>nd</sup> RCM in Beijing. The comparison with China's results by VSOP and MCNP are provided herein as Figure 4.19. China's results of VSOP show good agreement with the results by MCNP. In the calculation by MCNP, holes for control rods, etc are considered. Therefore, it is necessary to consider the effects of streaming not only in the pebble bed but also in holes for control rods. The effects of holes of control rods and coolant holes in the reflector region are not considered in our calculation. To improve the calculation accuracy, it is necessary to consider the streaming effects at holes for control rods and coolant channels. Also, three-dimensional calculation is necessary to consider the streaming effects.

The summary of JAERI's revised calculation includes the loading height at first criticality under helium and air atmospheres to be 113 cm and 116 cm, respectively (Table 4.24). The control rod worth is calculated as  $18\% \Delta k/k$ . Also, the effect of air in upper cavity and pebble bed is evaluated to be  $\sim 0.8\% \Delta k/k$ .

### ***Streaming Effects [4-18]***

The benchmark calculation results for the loading height of the first criticality show higher results than experimental results. From various calculation results, it is considered that streaming effect of voids is one of the reasons. Streaming effect of control rod holes, coolant channels is reported about  $1.2\% \Delta k/k$  from China's calculation. Considering the streaming effect of control rod holes, coolant channels, core height at the first criticality will be about 120 cm. The results will be closer to the experimental result. Therefore, the streaming effect of control rod holes, coolant channels should be considered. A three-dimensional core calculation is necessary when considering the streaming effect. Also, it should be clear that the atmosphere is either helium or air.

#### ***4.2.3.4. Conclusions [4-18]***

Benchmark problems of B1 and B3 are re-calculated by revised calculation model. The revised core calculation model is a two-dimensional model which considers the streaming effects of the pebble bed and upper cavity. Control rods are also considered. The revised calculation results show lower core height at the first criticality than the experimental results. It is considered that streaming effects of control rod holes, coolant channels should be considered. To consider the streaming effects, three-dimensional calculation should be utilized.

## 4.2.4. Russia Federation

### 4.2.4.1. General analysis method and model description

For HTR-10 reactor the critical number of spherical elements of the active core (critical height) formed from fuel elements and graphite spheres in the ratio 57 and 43 % at the temperature 300 K, was estimated. Also multiplication coefficients of the reactor with fully loaded core were calculated at the temperatures of 300, 400 and 500 K on condition that the control rods in the side reflector are fully withdrawn. Besides, 10 fully inserted side reflector control rods were weighted at normal temperature and atmospheric helium pressure.

A configuration of both structures of the active core and components of HTR-10 reflector were submitted in the specification [4-21].

### ***Diffusion calculation model***

The *WIMS-D/4 code* was used to calculate few group macrosections characterizing fuel cells and reflector blocks. The main results of diffusion approximation were obtained in two-group with thermal cut-off energy of 0,625 eV.

The *JAR-code* of 3D reactor calculation was used for estimation of multiplication coefficients.

The cylindrical active core was approximated by the finite number of hexagonal prisms with the across flats size selected from a condition of simulation of cylindrical surface. The calculational model in axial direction has some layers including the active core, cavity, top and bottom reflectors. The channels for the control rods in the side reflector were described by separate geometrical zones (Figure 4.20).

The *unit cell calculations* were performed to obtain few-group cross-sections of the fuel composition. The parameters of the cell for preparation of few-group cross sections of the fuel cell are the following:

- The volume fraction of the fuel region in the cell centered on one fuel pebble is  $\left(\frac{f}{1+m}\right) \cdot \left(\frac{r_1^3}{r_2^3}\right)$ , where  $r_1$  is the radius of fuel region inside the fuel pebble (2.5 cm), and  $r_2$  is other radius of the fuel pebble (3.0 cm);
- The volume fraction of the unfluenced graphite shell region in the unit cell centered on one fuel pebble is  $\left(\frac{f}{1+m}\right) \cdot \left(\frac{r_2^3 - r_1^3}{r_2^3}\right)$ ;
- The volume fraction of the void region in the unit cell centered on one fuel pebble is  $(1-f) = 0.39$ ;

- The volume fraction of the moderator pebble is  $\frac{f \cdot m}{1 + m}$ , where m is the moderator-to-fuel pebble ratio (m = 0.47);
- Total volume of the unit cell centered on one fuel pebble is  $V_{\text{cell}} = \frac{113.097 \cdot (1 + m)}{f} \text{ (cm}^3\text{)}$ .

Dancoff correction factor including double heterogeneity effects associated with coated fuel particles was calculated with using of Segev algorithm, described in Section 2.2.6 of this report.

The upper cavity was treated according to the procedure developed by Gerwin and Scherer [4-20], where practically zero reaction cross sections and special diffusion coefficients are used.

The reflector region cross sections were evaluated for an infinite graphite reflector neutron spectrum. The cross section of the channels for control rods (with and without absorber) were obtained from calculations of the cell centered on one control rod, surrounded by a graphite layer and by a layer with homogenized content of the active core. So the cross sections of control rods were obtained for core leakage neutron spectrum.

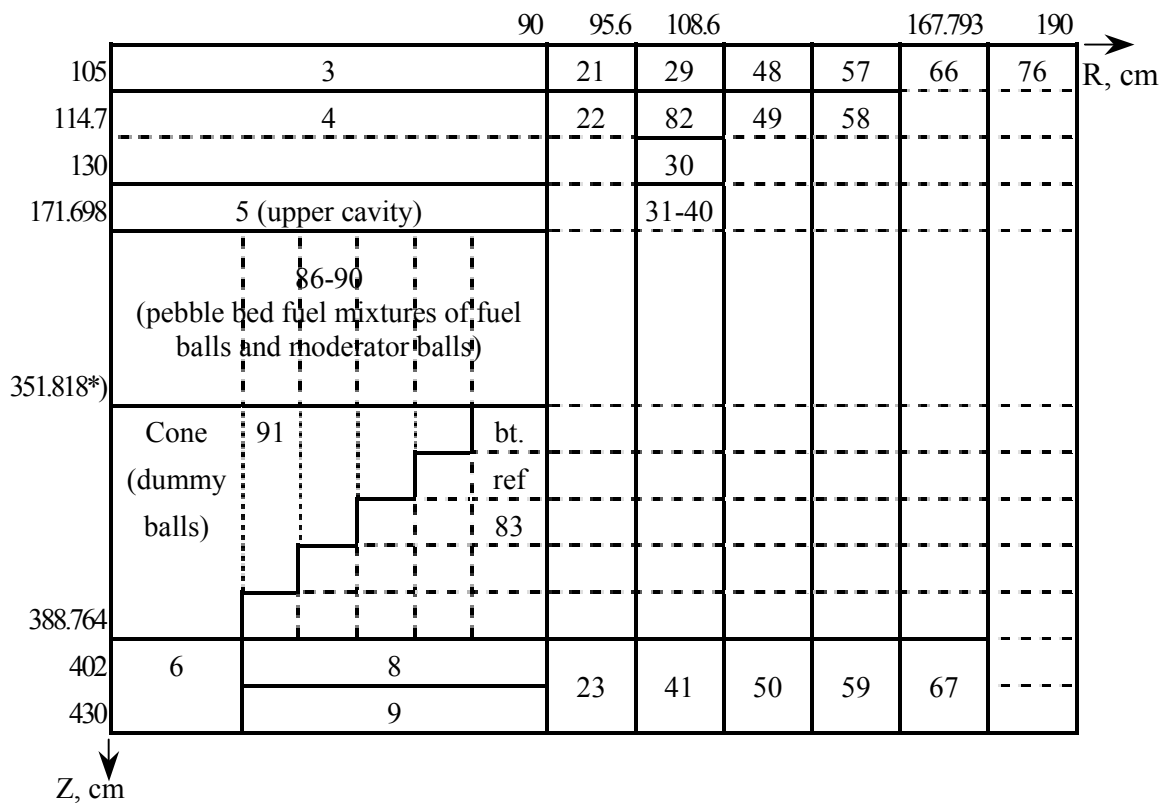
#### ***Method and model of Monte Carlo calculations***

MCNP code was used for precise calculations. For these calculations the detail composition of the reactor, as presented in [4-21], was considered. The opportunity of MCNP code application for HTGR calculation characterized by fuel arrangement with double heterogeneity is illustrated in paper [4-23] on the basis of comparison with other codes.

General analysis method and model description are presented in tables 4-25 and 4-26.

Table 4-25. Codes, model and library of nuclear data for diffusion calculations

Items	Name of Country	Russia
	Name of Institute	OKBM
Nuc. data file	ENDF/B6	
Fuel cell code	WIMS-D/4	
Theory	S4	
Model	Cylindrical cell	
Cut - off energy	0,625 eV	
No. of groups	69	
Control rod cell cal.	WIMS-D/4	
The theory	S4	
Model	Cylindrical cell with the central absorbing zone	
Number of groups	69	
Core cal. Code	JAR-3D	
Model	Triangular lattice	
No. of groups (Fast + Thermal)	1+1	



\*) All sizes and number of materials are given accordingly [4-21].  
 Position 351.818 cm (on Z direction) is corresponded to "0" in calculations of core height.

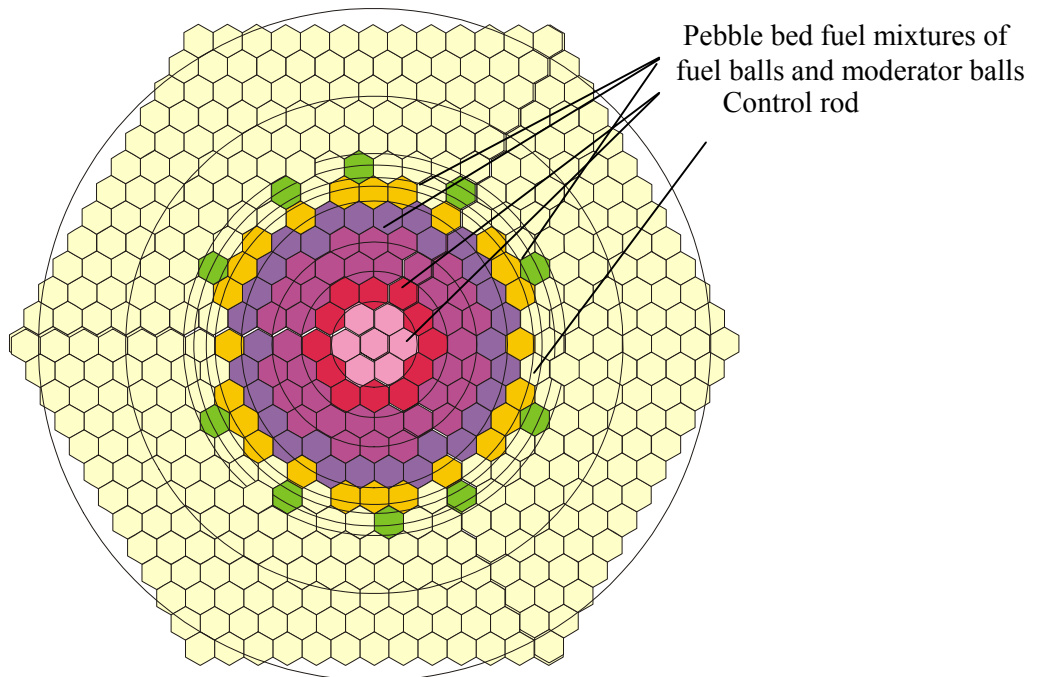


FIG. 4.20. HTR-10 Core Diffusion Calculation Model in R-Z geometry.

Table 4-26. Codes, models and nuclear data library for Monte-Carlo calculations

Items	Name of Country: Russia
	Name of Institute: IBRAE
Nuc. data file	ENDF/B6 NJOY
Energy structure	Continuous
Code	MCNP 4A
Coated fuel particles	Detailed account
History	2000
Batches	1000
Skipped batches	10

The main results of HTR-10 calculations were presented in [4-24] and are illustrated below.

#### 4.2.4.2. Initial Criticality [B1]

Table 4-27. Calculated Values Associated with the Benchmark HTR-10 FC

Items	Calculated values	
	Diffusion results	Monte-Carlo results
Organization	OKBM	IBRAE
Critical pebble bed height* at temperature 300 K, cm	136	137.3±0.4 130.8±0.2 <sup>a)</sup>

\*Core height is determined from the top of the dummy balls zone.

#### 4.2.4.3 Isothermal Temperature Coefficient [B21, B22, B23]

Table 4-28. Calculated Values Associated with the Benchmark HTR-10 TC

Items	Calculated values	
	Diffusion results	Monte-Carlo results
Organization	OKBM	IBRAE
Multiplication coefficient of fully loaded core at various temperatures (K) (H <sub>core</sub> = 180,12 cm, homogenized side reflector)		
k <sub>300</sub> [B21]	1.1182	1.1076 ± 0.0005 1.1284 ± 0.0004 <sup>a)</sup>
k <sub>400</sub> [B22]	1.1079	1.0933 ± 0.0006 1.1169 ± 0.0003 <sup>a)</sup>
k <sub>523</sub> [B23]	1.0927	1.0794 ± 0.0008 1.1016 ± 0.0004 <sup>a)</sup>

<sup>a)</sup> Critical height, reflector control rods and multiplication factors were recalculated with taken into account of corrected ppm of boron (1.3 → 0.125), helium replacement with air, changing of temperature (15 °C → 20 °C) and density of dummy balls (1.73 → 1.84 g/cm<sup>3</sup>). Result was obtained by MCNP-4C code with library ENDF/B-6, Rev. 8.

#### 4.2.4.4. Control Rod Worth [B31]

Table 4-29. Calculated Values Associated with the Benchmark HTR-10 CR

Items	Calculated values	
	Diffusion results	Monte-Carlo results
Organization	OKBM	IBRAE
Worth of fully inserted 10 control rod at temperature 300 K		
$\rho$ ( $\Delta k/k$ )	0.1550	$0.179 \pm 0.0012$ $0.161 \pm 0.001$ <sup>a)</sup>

<sup>a)</sup> Critical height, reflector control rods and multiplication factors were recalculated with taken into account of corrected ppm of boron (1.3 → 0.125), helium replacement with air, changing of temperature (15 °C → 20 °C) and density of dummy balls (1.73 → 1.84 g/cm<sup>3</sup>). Result was obtained by MCNP-4C code with library ENDF/B-6, Rev. 8.

#### 4.2.4.5. Accuracy analysis

Accuracy analysis of obtained results is presented below in Tables 4-30, 4-31 and 4-32.

Table 4-30. Core critical height [B1]

Diffusion calculations	
Average value (in accordance with RCM4 results), cm	123.6
Average calculated value / experimental value, %	-0.3
WIMS-JAR value / average calculated value, %	+ 10
WIMS-JAR value / experimental value, %	+ 9.8
Monte - Carlo calculations	
Average value (in accordance with RCM4 results), cm	130.6
Average calculated value / experimental value, %	+ 5.4
MCNP value / average calculated value, %	+ 5.1
MCNP value / experimental value, %	+ 11
MCNP value / experimental value, % <sup>a)</sup>	+ 5.6

Table 4-31. Multiplication coefficient versus temperature [B21, B22, B23]

	B21	B22	B23
Diffusion calculations			
Average value (in accordance with RCM4 results)	1.1262	1.1132	1.0954
WIMS-JAR value / average calculated value, %	- 0.7	- 0.5	- 0.3
Monte - Carlo calculations			
Average value (in accordance with RCM4 results)	1.1089	1.0848	1.0686
MCNP value / average calculated value, %	- 0.7	+ 0.8	+ 1.0

Table 4-32. Reflector control rods worth [B31]

Diffusion calculations	
Average value (in accordance with RCM4 results), cm	15.4
Average calculated value / experimental value, %	+ 7.2
WIMS-JAR value / average calculated value, %	+ 0.6
WIMS-JAR value / experimental value, %	+ 7.6
Monte - Carlo calculations	
Average value (in accordance with RCM4 results)	18.0
Average calculated value / experimental value, %	+ 25
MCNP value / average calculated value, %	- 0.6
MCNP value / experimental value, %	+ 24
MCNP value / experimental value, % <sup>a)</sup>	+ 12

<sup>a)</sup> Recalculated results

Analysis of HTR-10 benchmark calculation results demonstrates that difference in critical height from average calculated and experimental values for diffusion calculation is about 10 % and in Monte-Carlo calculations is less by half.

Initial data correction relatively experimental conditions (helium replacement with air, ppm of boron, density of dummy blocks) provides decrease difference from experimental value down to 5.6 % (instead of 11 %).

Dependence of multiplication factor versus temperature (problems B2, B22, B23) both by diffusion codes and Monte-Carlo codes well coincide between themselves and with average values.

Side reflector control rods worth calculation by Monte-Carlo (MCNP) is characterized by significant error 24 % (12 % - with corrected initial data) that determines necessity to specify initial data on moisture content in reflector graphite, on the one hand, and graphite thermalization constants, on the other hand.

## 4.2.5. Netherlands

### 4.2.5.1. Introduction

Calculations have been performed by NRG-Petten within the framework of the HTR-10 initial core benchmark [4-21]. The HTR-10 is the Chinese prototype pebble bed gas cooled reactor. For a description and the main data of the reactor, reference is made to the Benchmark Description [4-21].

### 4.2.5.2. Codes and Methodology

The HTR-10 has been modelled in the PANTHERMIX code [4-22], a combination of the 3-D diffusion reactor code PANTHER 5.1 [4-25] coupled to the 2-D thermal hydraulics code THERMIX./DIREKT [4-26] The nuclear data necessary for the PANTHER code has been generated by means of the WIMS8 [4-27] code system.

### *Cell calculations*

#### Library

The calculations with WIMS8 has been performed with an adapted version of the standard 172 groups 1997 WIMS library based on JEF-2.2. Adaptations has been made for Pu, Am and Cm isotopes to extend the range of temperatures and of the potential scattering to improve the resonance treatment.

#### Calculational Method

The method followed to overcome the impossibility of modelling the pebbles on coated fuel particle (CFP) scale is to model a cylindrical cell with an equivalent radius. This method has been proved adequate in the PROTEUS benchmark.

The spherical pebble is transformed into an infinite long cylinder but with the same mean chord length. The mean chord length of a concave body is given by the simple relation: 4 times the ration of volume over surface.

So the fuelled part of the pebble (radius 2.5cm) is translated into a cylinder of 1.667 cm radius and contains the fuel kernels, coatings and matrix graphite. This cylinder is surrounded by an annulus of radius 2.191 cm to accommodate the unfuelled shell of 0.5 cm based on conservation of volume ratio. Finally the outer cylinder which contains the admixed moderator pebbles and the void between the pebbles this radius amounts to 3.716 cm in our model. These dimensions and densities are fed into the WIMS module WPROCOL to produce collision probabilities for use in the resonance treatment, for U235, U238 and Pu239 in WRES after an approximate resonance treatment in WHEAD for all other resonant isotopes not treated explicitly in WPROCOL/WRES. This treatment is based on equivalence theory with calculated potential scatter cross section applied on slabs with thickness according to mean chord lengths of the fuel kernel, coatings and matrix graphite belonging to the kernel. In this approximation a Dancoff factor has been used which is derived analytically to account for the double heterogeneity of kernels and pebbles [4-28]. After smearing and condensation of the pebble and kernel materials to one material and in 16 neutron energy groups, a pseudo reactor calculation has been started in as well the axial direction (infinite radius) as in the

radial direction (infinite length) in the real reactor dimensions. This has been done for the case without control rods (unrodded) and with control rods inserted (rodded).

Three kinds of control rod banks have been used:

- a): the normal control rods to govern the power level,
- b): the KLAK system for cold shut-down of the reactor and
- c): a ‘gas’ control rod bank. This is a control rod bank, which comprises all core channels in the PANTHER model. This bank in the unrodded state returns the nuclear data of the fuel in the unrodded axial meshes of the core, in the rodded state it returns the nuclear data of the Helium void on top of the pebble-bed in the rodded axial intervals. By moving in and out this “gas” rod one can simulate the level of the pebble-bed height in the core. The gas space above the pebble bed has ‘artificial’ and anisotropic diffusion coefficients obtained according to the Gerwin-Scherrer method [4-20].

KLAK system and control rod calculations have been performed for the radial pseudo reactor calculations by means of the WIMS CACTUS-module (Figure 4.21). After these pseudo reactor calculations, the materials comprised in the reactor were smeared and condensed into 2 neutron groups, one thermal and one fast neutron group, for the PANTHER full core calculations. The division between the thermal and the fast energy group was 2.1 eV.

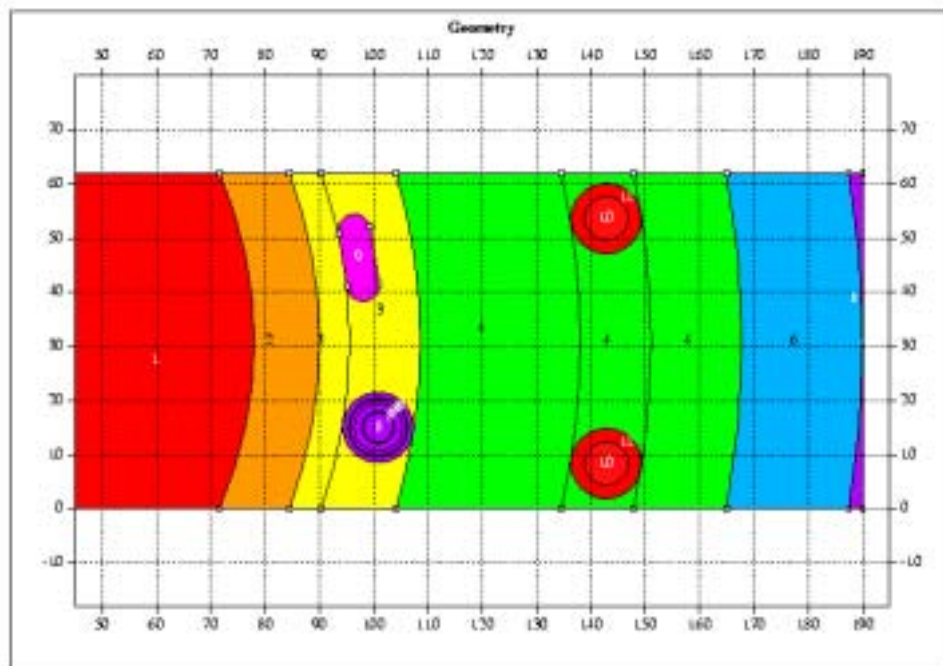


FIG. 4.21. CACTUS model of control rod holes, KLAK holes and coolant channels. The red and orange areas on the right are part of the core.

These pseudo reactor calculations were done for different depletion levels and at different temperatures. This way a database has been constructed, which is temperature, burn-up, control rod and Xenon dependent, in which PANTHER can perform a multidimensional interpolation in the nuclear data, according to the local condition in the reactor.

## Core calculations

### PANTHER

The HTR-10 has been approximated in the diffusion code PANTHER in the 3-D X-Y-Z mode with radial 861 square meshes (channels) of 11.48 cm by 11.48 cm and 52 axial intervals of different height but over the core height all 11.10 cm high. The full model comprised 193 core channels, 668 reflector channels, 20 core layers (plus 8 layers to model the bottom cone) 14 bottom reflector layers and 10 top reflector layers. The size of the square mesh has been chosen such that concentric ‘rings’ can be composed from these meshes in a manner that those rings fit snugly with the main radial dimensions of the reactor structures (Figures 4.22, 4.23 and 4.24).

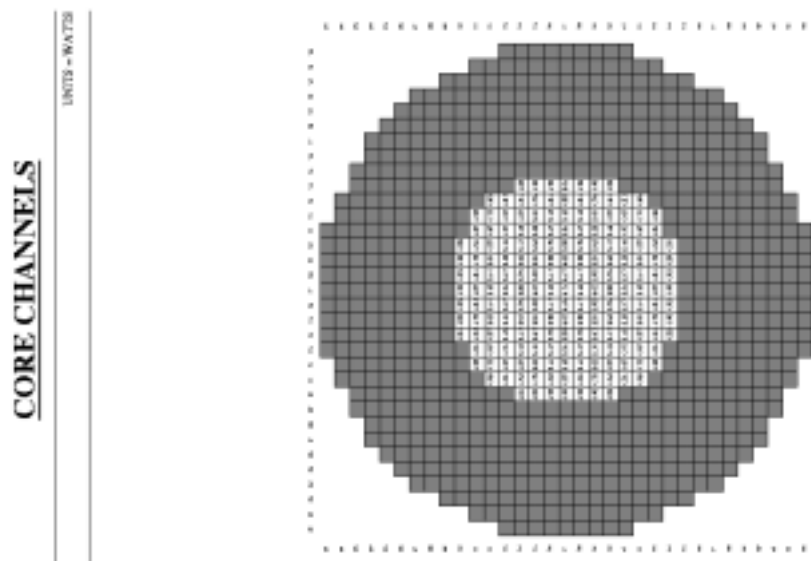


FIG. 4.22. Layout of the core and reflector channels in PANTHER.

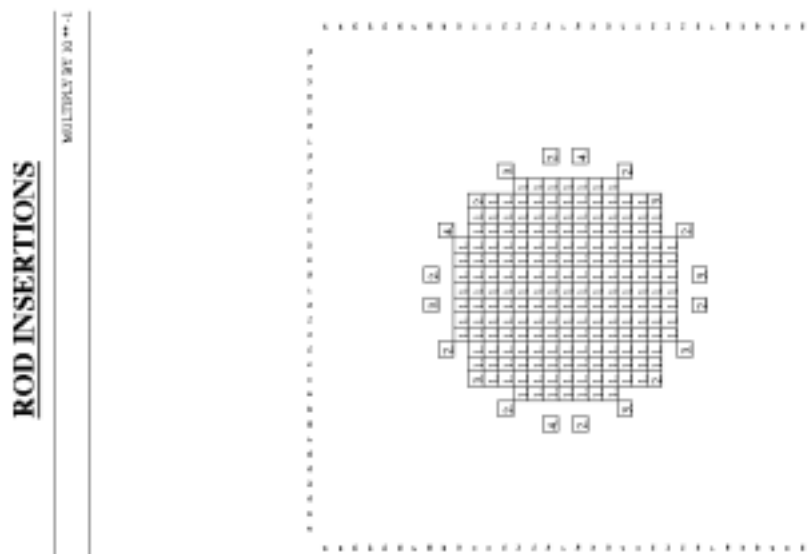


FIG. 4.23. Layout of the rod types. The “gas” rod bank, which insertion determines the core height, is indicated by a 1, the normal control rods in the reflector are numbered with a 2, the KLAKE system by a 3 and the instrumentation channels are designated by a 4.

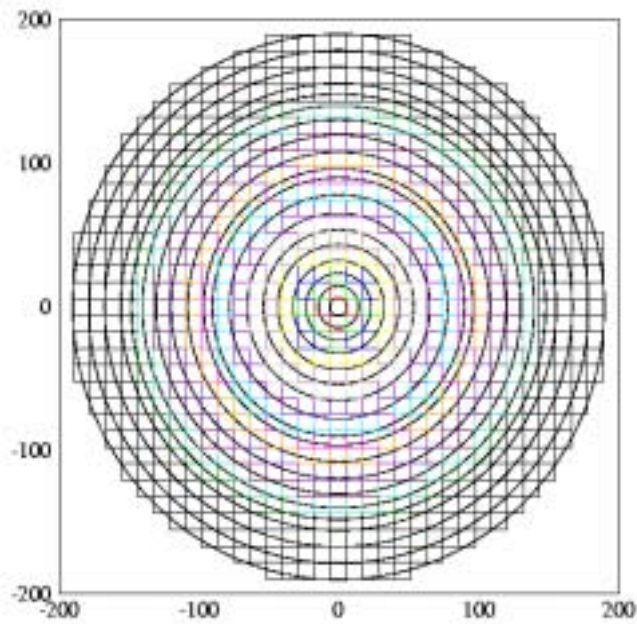


FIG. 4.24. Reactor channels and assigned rings to correspond with the 2D R-Z THERMIX model.

Each mesh in the PANTHER model contains a distinct material with a corresponding set of nuclear data. In each mesh the nuclear data will be generated according to the local burn-up, temperature, etc. from the nuclear database to perform a new time step. An algorithm has been added to PANTHER to simulate the flow of the pebbles through the reactor after each time step by means of transfer of basic parameters (local burn-up) to the neighbouring meshes and keeps track of the classes of the local burn-up distribution.

The aforementioned rings do coincide with the radial meshing of the thermal hydraulic code THERMIX part of the PAN(THER THER)MIX code package. They are used to transfer the power distribution from PANTHER to THERMIX and receive back the temperature field from THERMIX.

## THERMIX

THERMIX or better the THERMIX/DIREKT code is a 2-D R-Z thermal hydraulics code to calculate the temperature distribution for the solid and gaseous materials in the reactor from a given power distribution (by PANTHER). For the mapping of the 3-D power profile on the 2-D grid of THERMIX the power in the squares which form a 'ring' in PANTHER are radially averaged and transferred to the mesh in THERMIX. For the temperature profile from THERMIX the values for a R-Z set are unfolded to a PANTHER ring. There are 19 radial rings composed in the PANTHER model and 22 radial meshes in the THERMIX model of which the extra meshes do form the boundary conditions. The THERMIX part of the code solves the (time-dependent) equations for the conductive and radiative heat transfer whereas DIREKT solves the (time-dependent) equations for the heat transfer from solid material to the gaseous coolant and the continuity equation of the gas flow. Contrary to the thermal hydraulic options in PANTHER, THERMIX allows for cross channel flows necessary to simulate natural convection in a situation without mass flow.

The complex heat transfer and heat conductivity in the pebble bed is chosen as modelled in THERMIX according to the Zehner-Schlünder method [4-29].

Thermal data like heat conductivity and heat capacity of the different materials are calculated as function of temperature and pressure according build-in equations. For the graphite the properties of un-irradiated A3 grade have been used.

#### 4.2.5.3. HTR-10 Benchmark Problem Results

##### ***HTR-10 critical core level***

Under benchmark conditions, so with an isothermal reactor temperature of 20 °C, the control rods at 114.7 cm and atmospheric Helium in the coolant spaces, a critical search on the core level ('gas'rod insertion) has been performed by PANTHER. The critical core level was found to be:

$$H_{\text{crit}} = 125.3 \text{ cm,}$$

above the bottom cone filled with moderator balls.

##### ***HTR-10 isothermal temperature coefficient***

With the reactor at isothermal temperatures of 20, 120, 200 and 250 °C and a core height of 180 cm (full core), PANTHER calculated the corresponding multiplication factor.

According to the definition of  $\rho(T) = (k_{T1} - k_{T2}) / ((k_{T1} * k_{T2}) * (T_1 - T_2))$  we found the following values, listed together with the values as obtained by VSOP at INET (Table 4-33).

Table 4-33: Isothermal Temperature Coefficient Values for NRG and INET (VSOP)

Temp(C)	k <sub>eff</sub> INET	k <sub>eff</sub> NRG	ρ(T) NRG	ρ(T) INET
20	1.119747	1.11759		
120	1.110435	1.10846	-7.37E-05	-7.49E-05
200		1.10115	-7.49E-05	
250	1.095961	1.09629	-8.05E-05	-9.15E-05
		average	-7.64E-05	-8.32E-05

##### ***HTR-10 scram reactivity***

With the core level at 180.0 cm (full core) and a uniform reactor temperature of 20 °C, The insertion of the control rods from 119.2 cm to 394.2 cm gave rise to a reactivity effect of:

$$\rho_{\text{scram}} = 0.1186.$$

And with the core level at 125.3 cm (critical level) and a uniform reactor at 20 °C, the insertion of the control rods from 119.2 cm to 394.2 cm gave rise to a reactivity effect of:

$$\rho_{\text{scram}} = 0.1367.$$

This is rather low compared with the measured data of 0.18 (INET) and can probably be explained by strong steaming in the holes to accommodate the control rods and the KLAK system. Recalculations will be done later with modified anisotropic diffusion coefficients according to the Behrens method.

### HTR-10 control rod worth

With the reactor at 20 °C and the core level at 125.3 cm a series of calculations has been done for different insertion fractions of all control rods (Table 4-34). Fraction 0 is at the top of the reactor and fraction 1 is at the bottom of the reactor: 610 cm (Figure 4.25).

Table 4-34: Rod Worth Relative to CR Insertion Fraction

rod fract.	rod (cm)	$k_{\text{eff}}$
0.00	0.0	1.00233
0.05	30.5	1.00234
0.10	61.0	1.00219
0.15	91.5	1.00156
0.20	122.0	1.00005
0.25	152.5	0.99342
0.30	183.0	0.98584
0.35	213.5	0.97838
0.40	244.0	0.96887
0.45	274.5	0.94921
0.50	305.0	0.91803
0.55	335.5	0.89298
0.60	366.0	0.88344
0.65	396.5	0.88153

Calculation of the worth for a single control rod is not sensible because in our model, as can be seen from Figure 4.23, the control rods are on three distinct positions with only the average midpoint radius equal to the stated radius.

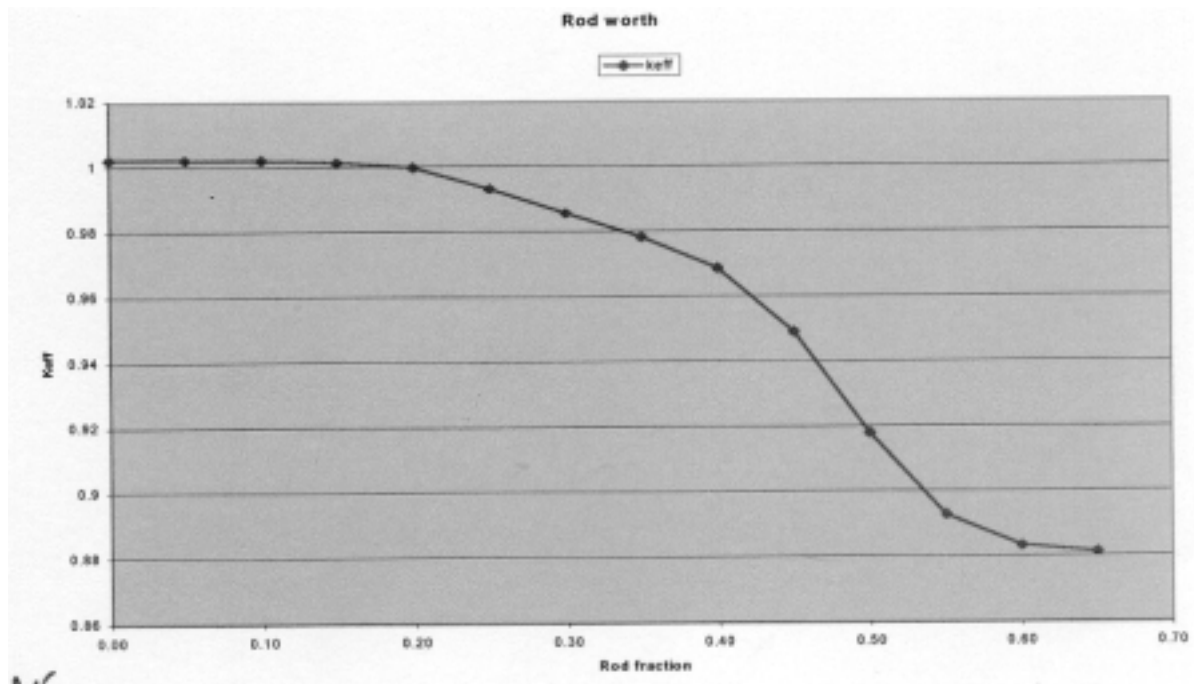


FIG. 4.25. Reactivity of the reactor as function of the control rod bank insertion for the critical core (core level at: 125.3 cm).

### Full Power Calculations

A thermal hydraulics model has been built to be able to calculate the full power (10 MW) conditions as, flux distributions, power distribution, solid structure temperatures and coolant temperature and mass flow over the reactor. Results for the hot critical initial core (core level at 155 cm) can be seen in Figures 4.26 to 4.31.

Some key values are:

Maximum pebble temperature	867 °C.
Maximum coolant temperature	804 °C.
Maximum power density	3.41 MW/m <sup>3</sup> .
Pressure difference inlet/outlet	0.017 bar.

### Planned activities

A re-evaluation of the control rod model with anisotropic diffusion coefficients, as well as transient calculations are foreseen. After installation of the flow pattern for the pebbles burn-up calculations can be done and an equilibrium core can be investigated.

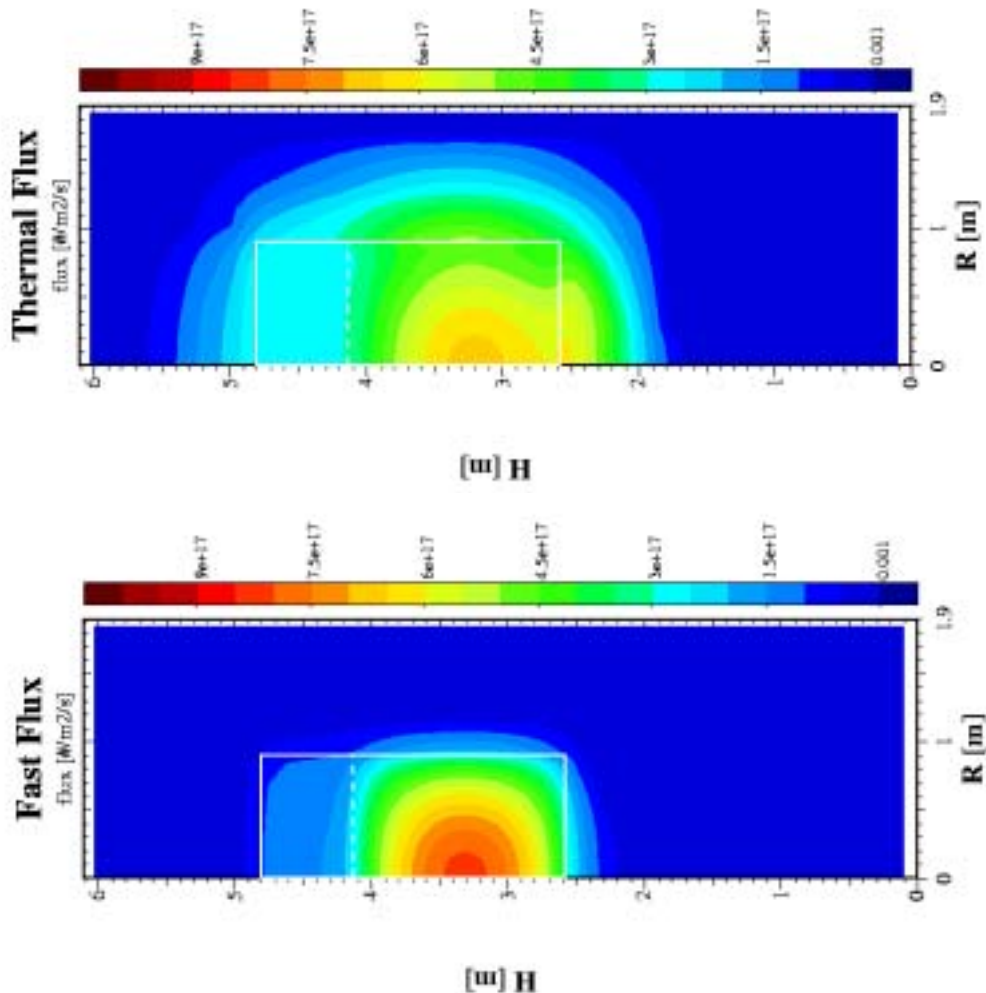


FIG. 4.26. and 4.27. Thermal and fast flux (fluence rate) over the reactor, white lines indicate the core boundaries whereas the dashed line gives the core level.

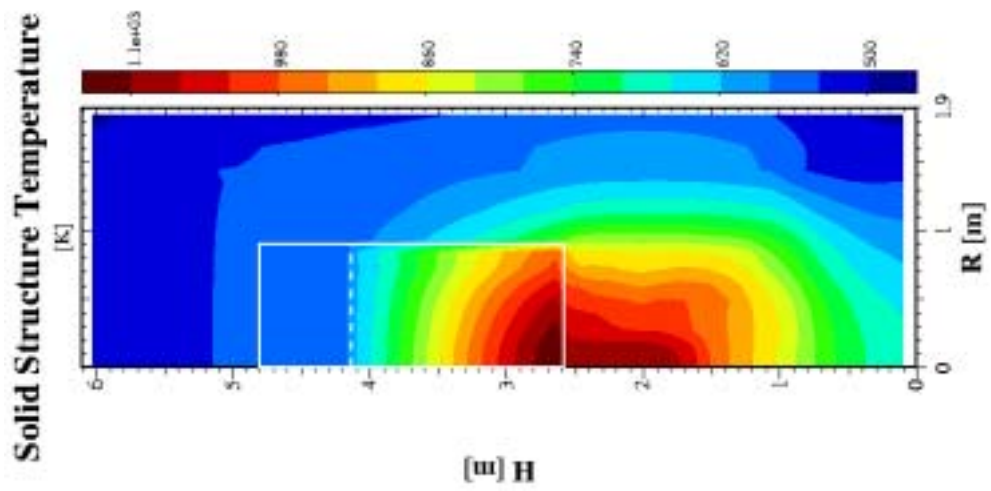
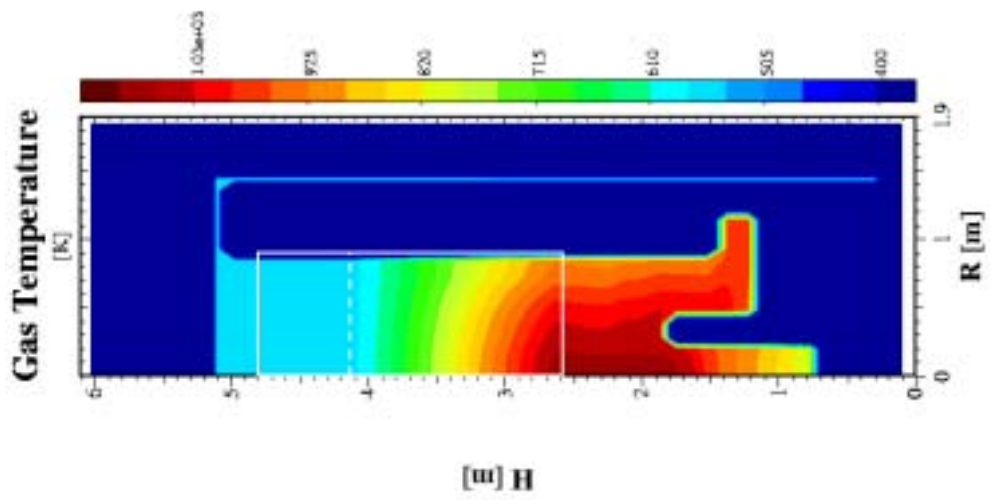
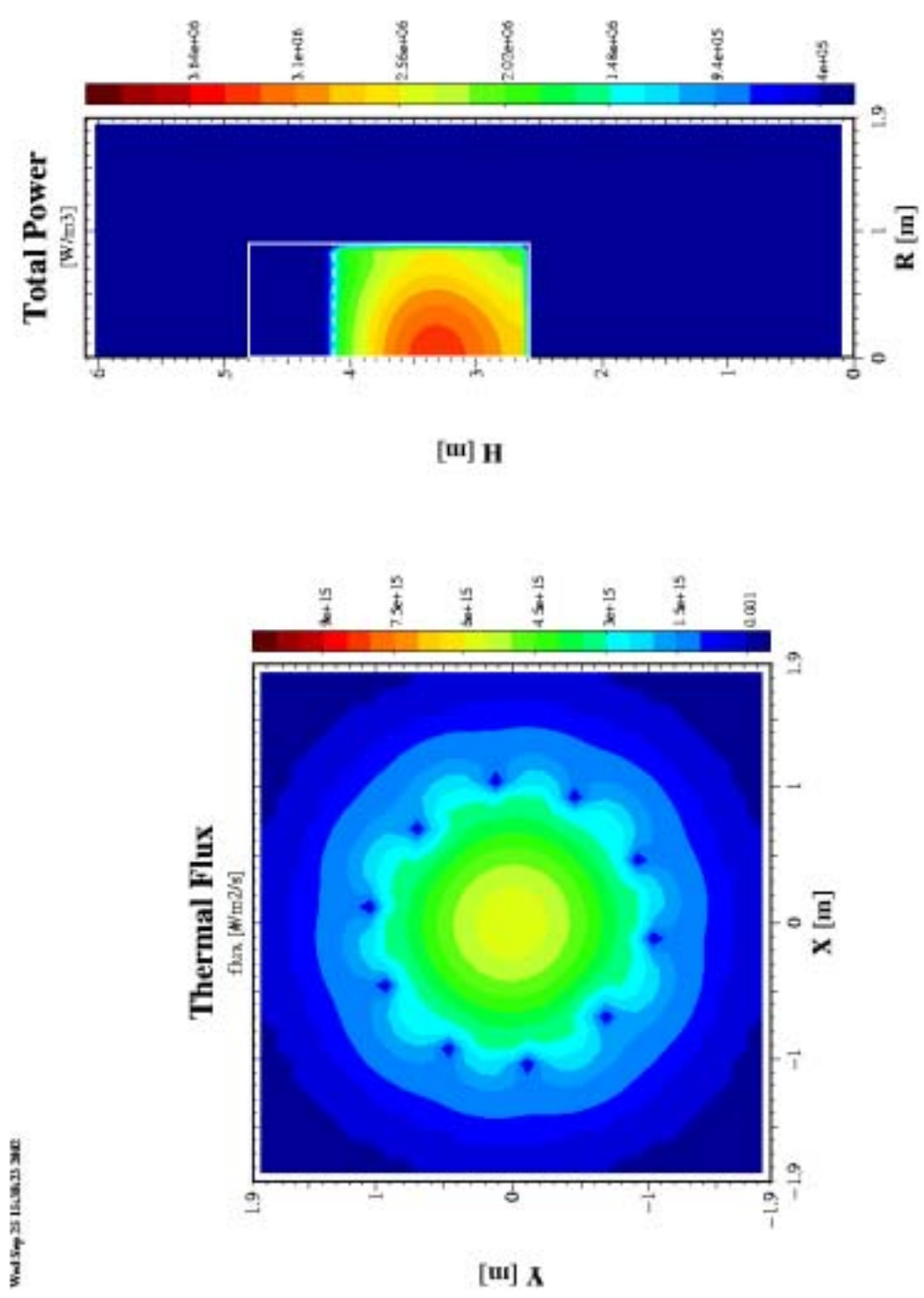


FIG. 4.28. and 4.29. Temperature distribution for the coolant and reactor structure in degrees Kelvin.



Wed Sep 25 15:38:23 2002

FIG. 4.30. Power density distribution at full power. FIG. 4.31. Radial plot of the thermal flux over the reactor with inserted control rods (arbitrary units).

#### 4.2.6. United States of America

A benchmark criticality analysis was performed of the HTR-10 pebble-bed reactor by the Nuclear Engineering Department of the Massachusetts Institute of Technology (MIT) using the continuous-energy Monte Carlo code MCNP (Version 4B).

The physics benchmark problem consisted of three parts:

- a) Prediction of the initial, cold, critical core loading with the control absorbers completely withdrawn at 20°C and a helium coolant pressure 3.0 MPa.
- b) Calculation of the effective multiplication constant of a completely filled core with the control absorbers completely withdrawn. The analysis is performed for a uniform core temperature of 20°C, 120°C and 250°C; the helium coolant pressure is 3.0 MPa.
- c) Calculation of the total reactivity worth of the control absorbers at a core temperature of 20°C and a helium coolant pressure of 3.0 MPa.

##### 4.2.6.1. Computational methods [4-30]

The detailed MCNP4B model of the reactor included the double heterogeneity of the coated fuel particles and the graphite pebbles, and an explicit representation of the graphite reflector. However, the specified fuel-to-moderator pebble ratio of 57% to 43% cannot be modeled exactly using the repeated geometry feature of MCNP4B. A BCC lattice was used to approximate the packing of pebbles in the core, with the size of the moderator pebble reduced in a manner that reproduces the specified fuel-to-moderator pebble ratio while preserving the 0.39 void fraction. An additional approximation, required because insufficient geometry data was provided in the benchmark problem specification, involved the homogenization of the control rod interiors.

The MCNP4B criticality analysis was performed using ENDF/B-VI cross-section data evaluated at 300 K, and the University of Texas at Austin cross-section library for the temperature-dependent calculations. All cases were run for 1 million starting neutron histories, resulting in a 1- $\sigma$  statistical error in the effective multiplication constant of 0.1%.

Table 4-35. Control Rod Geometry and Material Specifications

Description	Value	Units
Control rod channel radius	6.5	cm
Radial position of channel center	102.1	cm
Length of B <sub>4</sub> C segment	48.7	cm
Length of bottom metallic end	4.5	cm
Length of metallic joints	3.6	cm
Length of top metallic end	2.3	cm
Inside radius of inner stainless-steel sleeve	2.75	cm
Thickness of stainless-steel sleeve	0.2	cm
Thickness of gap between sleeve and B <sub>4</sub> C	0.05	cm
Thickness of B <sub>4</sub> C annulus	2.25	cm
Density of B <sub>4</sub> C	1.7	g/cm <sup>3</sup>
Length of control rod	264.7	cm

To provide a common starting point for the modeling of the HTR-10 with a variety of codes, a simplified reactor description was utilized for the physics benchmark specification (see Sections 4.1.1. and 4.1.2).

Benchmark problem B3 (CR reactivity worth) requires the explicit modeling of the control rods. The design of the control rod is depicted in Section 4.1.1 and its geometry and material specifications are summarized in the following Table 4-35. Boron carbide ( $B_4C$ ) is used as the neutron absorber. Each control rod contains five  $B_4C$  annular segments with outer stainless-steel sleeves, and which are joined together using stainless steel joints. As specified in the benchmark problem, the metallic structures are modeled as iron with 64% the density of stainless steel ( $5 \text{ g/cm}^3$ ).

### ***MCNP***

MCNP (Monte Carlo N-Particle) is a general-purpose, continuous-energy, generalized-geometry, time-dependent, coupled neutron-photon-electron, Monte-Carlo transport code system [4-32]. The analysis at MIT was performed using version 4B of the code (MCNP4B).

MCNP can treat any three-dimensional configuration of materials, and uses point-wise continuous-energy cross section data. Multi-group data may also be used, especially for fixed-source adjoint calculations.

All neutron reactions in any given cross-section evaluation are accounted for. Both free-gas and  $S(\alpha,\beta)$  thermal treatments are used. Criticality sources, as well as fixed and surface sources, are available. For photons the code takes into account coherent and incoherent scattering with and without electron binding effects, the possibility of fluorescent emission following photoelectric absorption, and absorption in pair production with local emission of annihilation radiation.

A very general source and tally structure is available. The tallies have extensive statistical analysis of convergence, and rapid convergence is achieved by a wide variety of variance reduction methods. Energy ranges are 0-20 MeV for neutrons, and 1 keV – 1 GeV for photons and electrons. The capability to calculate the effective multiplication constant ( $k_{\text{eff}}$ ) for fissile systems is a standard feature.

The general geometry modeling capability of MCNP and its use of continuous-energy cross sections make it possible to model nuclear reactors very accurately, especially zero-power critical assemblies. Such critical experiments are particularly well suited for the validation of MCNP, because the composition of fresh fuel is known exactly and room-temperature cross-section libraries are readily available. There are two aspects to the validation of MCNP: the validation of physical models and data used by the code itself, and the determination of the systematic bias introduced by the approximate modeling of the experiment. Although MCNP has been shown to simulate physical processes correctly (*e.g.*, Reference [4-33]), it must still be validated for specific reactor applications.

The HTR-10 physics benchmark problem was specified in a manner suitable for both diffusion-theory and Monte Carlo codes. The resultant simplification of the reactor model reduces the accuracy with which MCNP can reproduce experimental measurements. Moreover, the specification of a fuel-to-moderator pebble ratio of 57% to 43% further reduces the accuracy of the repeated geometry feature in MCNP, since all regular packings of mono-

sized spheres have even coordination numbers [4-34]. This fuel-to-moderator pebble ratio was selected by INET to ensure criticality of the full core.

### Reactor Structure

The MCNP model consists of the reactor structure, which includes the graphite reflector and the borated carbon bricks that surround the reflector, and the pebble-bed core. A vertical cross-sectional view of the modeled structure is shown in Figure 4.32. This model is identical to the core physics calculation model provided in Section 4.1.2. (including the zone numbers) except for the presence of control, irradiation and coolant channels. These channels are shown in the horizontal cross-sectional view of the reactor (Figure 4.33).

### Control Absorbers

Details regarding the stainless-steel joints between the control absorber were not included in the benchmark problem definition. Thus, the interior of the control rods was spatially homogenized using a mixture of carbon, natural boron, iron and helium (see Table 4-36). The model was prepared assuming that the joints preserve the annular geometry of the absorber segments to allow coolant flow. The geometry of the control-rod channels is otherwise modeled as specified in Table 4-35. An advantage of this modeling approach is that it permits the vertical positions of the control rods to be changed easily.

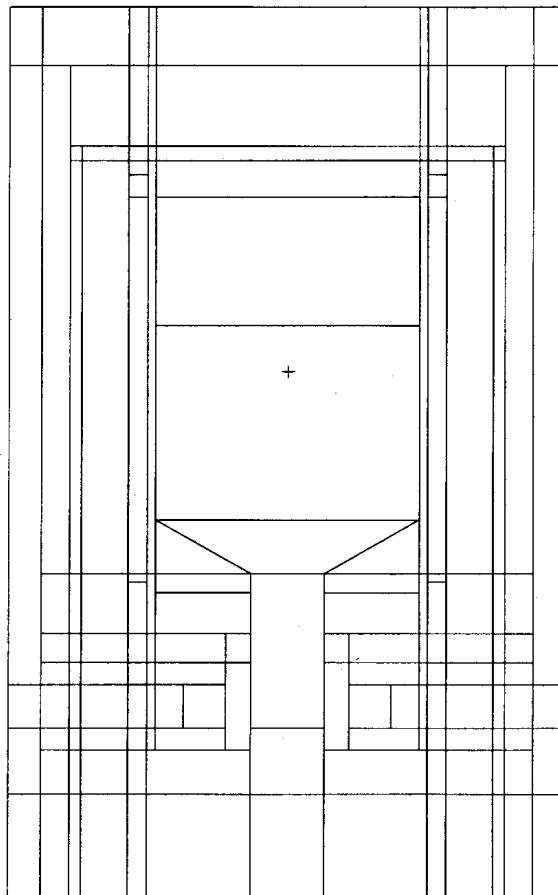


*FIG. 4.32. Vertical Cross-sectional View of the MCNP Model of HTR-10.*

Table 4-36. Homogenized Control Rod Composition

isotope	atom density (1/b-cm)
C	$1.04589 \times 10^{-2}$
$^{11}\text{B}$	$3.35103 \times 10^{-2}$
$^{10}\text{B}$	$8.32529 \times 10^{-3}$
Fe	$8.64966 \times 10^{-3}$
He	$1.99240 \times 10^{-4}$
total	$6.11434 \times 10^{-2}$

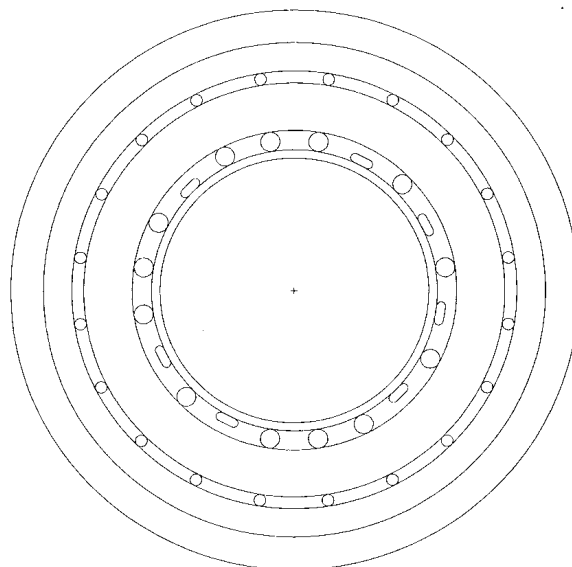


FIG. 4.33. Horizontal Cross-sectional View of the MCNP Model of HTR-10.

Since information about the control-rod drive shafts was also not provided, the control rods were modeled without such components. The absorber-ball and irradiation channels were assumed to be empty (helium filled). The atom densities of the spatially homogenized zones that contain the various channels were corrected for the presence of these holes.

#### Core

Since a random packing of pebbles cannot be modeled using the standard version of MCNP,<sup>1</sup> the pebble-bed core must be idealized as a regular lattice of spherical pebbles. However, the specification of a 57:43 fuel-to-moderator pebble percent ratio for the initial HTR-10 core loading complicates the modeling of the core using the repeated geometry feature of MCNP. Regular lattices composed of equal-sized spheres, which are characterized by even coordination numbers, cannot be used to model an uneven fuel-to-moderator ratio while preserving the original geometry of the pebbles.

<sup>1</sup> A modified version of the code, MCNP-BALL, has been developed in the Department of Nuclear Engineering at Osaka University, Japan, which statistically generates the positions of fuel pebbles and coated fuel particles (CFPs). Packing fractions of fuel pebbles, moderator pebbles and CFPs are reproduced to within a 2% relative error. [4-35]

Instead, the core zone was approximated using a body-centered cubic (BCC) lattice with moderator pebbles of reduced diameter, which reproduces the specified fuel-to-moderator pebble ratio. The BCC lattice was chosen because the two-pebble content of the unit cell minimizes the size adjustment for the moderator pebbles. The original size of the fuel pebble was maintained to preserve the effect of the single heterogeneity on the  $^{238}\text{U}$  resonance escape probability, which is expected to dominate reactivity effects, while minimizing the perturbation due to the double heterogeneity of the lattice. The size of the unit cell was also varied to achieve the specified volumetric packing fraction of 0.61 (or a void fraction of 0.39) in the pebble bed. This procedure assures that the fuel loading, the mass of heavy metal per unit core volume, is the same as for the 57:43 percent random packing.

The individual TRISO coated fuel particles, which were modeled explicitly, were distributed in the fueled region of the fuel pebbles using a simple-cubic (SC) lattice. The dimensions of the SC unit cell were chosen to reproduce the specified uranium loading of 5 g per fuel pebble. Table 4-37 summarizes the geometry specifications of the pebble-bed core as modeled with MCNP.

Table 4-37. Model Pebble-Bed Geometry Specifications

Parameter	Value	Units
Fuel-to-moderator pebble volume ratio	1.3256	–
Radius of fuel pebble	3.0	cm
Radius of fueled region	2.5	cm
Packing fraction	0.61	–
Moderator pebble radius	2.7310	cm
BCC unit cell size	6.8773	cm
SC unit cell size	0.19876	cm

Figures 4.34 through 4.36 show horizontal cross sections of the CFP, fuel pebble and pebble bed, respectively. The material compositions of the fuel kernels and the graphite moderator that were used in the MCNP model are given in Table 4-38. The compositions of the pyrolytic carbon and silicon-carbide layers in the TRISO coating of the fuel kernels are as specified in the benchmark problem specification.

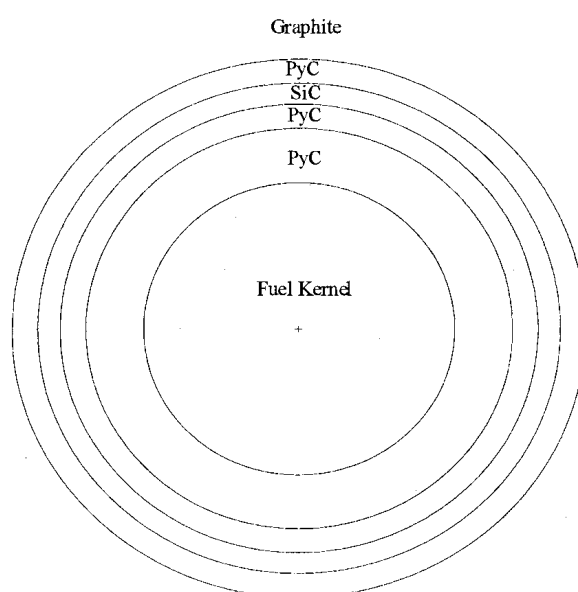


FIG. 4.34. MCNP Model of Coated Fuel Particle.

## Boron Content

Impurities in graphite and uranium are specified in the benchmark problem definition in terms of equivalent concentrations of natural boron. The absolute isotopic abundance of  $^{10}\text{B}$  is not given and the nominal value of 19.9% was used. This is a significant source of modeling uncertainty, since a natural variation in  $^{10}\text{B}$  from 19.1% to 20.3% has been measured [4-36].

Table 4-38. Material Compositions of Pebble-Bed Core

Isotope	Atom Density (1/b-cm)
<i>Graphite moderator:</i>	
C	8.674169E-02
$^{10}\text{B}$	2.244010E-08
$^{11}\text{B}$	9.032424E-08
total	8.674180E-02
<i>Fuel kernel:</i>	
$^{235}\text{U}$	3.992067E-03
$^{238}\text{U}$	1.924449E-02
O	4.647329E-02
$^{10}\text{B}$	1.849637E-08
$^{11}\text{B}$	7.445022E-08
total	6.970994E-02

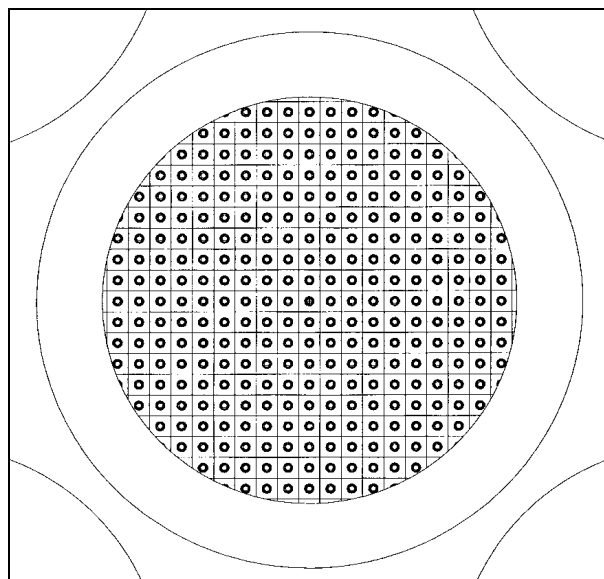
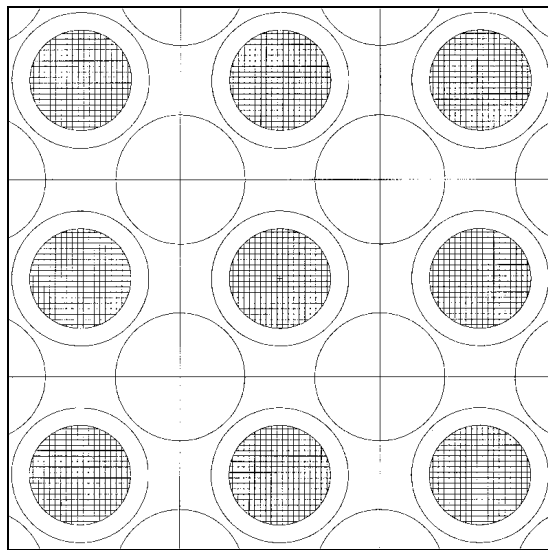


FIG. 4.35. MCNP Model of Fuel Pebble.

### 4.2.6.2. Results of MCNP Calculations

The HTR-10 physics benchmark problems comprise a set of criticality calculations, in which the effective multiplication factor ( $k_{\text{eff}}$ ) is determined for several core configurations. These configurations are achieved by varying the height of the pebble bed, adjusting the position of the control rods, or changing isothermally the temperature of the core. The total reactivity worth of all ten control rods is derived from  $k_{\text{eff}}$  values with the control rods first

fully inserted and then fully withdrawn. The temperature-dependent MCNP calculations in this study (benchmark problems B21 and B22) did not include the reactivity effect due to the isothermal expansion of the reflector.



*FIG. 4.36. A Horizontal Cross-section through the MCNP Model of the Pebble-Bed Core.*

Benchmark problems B1, B21 and B3 were analyzed using the standard ENDF/B-VI cross-section data processed at 300 K. Benchmark problems B22 and B23, which correspond to 393.15 K (120°C) and 523.15 K (250°C) respectively, were estimated using temperature-dependent cross sections evaluated at the University of Texas at Austin. All the cross-section libraries were originally evaluated using the NJOY nuclear data processing system [4-37].

#### ***Benchmark problem B1 (initial criticality) [4-31]***

Problem B1 calls for the prediction of the initial, cold, critical core loading with the control and shutdown absorbers completely withdrawn at 20°C and a helium pressure of 3.0 MPa.

The detailed MCNP4B model of the reactor included the double heterogeneity of the CFPs and the graphite spheres, and an explicit representation of the graphite reflector. However, an F/M ratio of 57/43 cannot be modeled exactly using MCNP4B. A body-centered-cubic (BCC) lattice was used to approximate the packing of spheres in the core, with the size of the moderator sphere reduced in a manner that reproduces the specified F/M ratio while preserving the 0.39 void fraction and the mass fraction of all constituents.

An additional approximation, which is required because of the repeated geometry feature of MCNP4B, involves the addition of a 1.71 cm exclusion zone around the periphery of the pebble bed. The exclusion zone compensates for fuel spheres that overlap the boundary of the core [4-35]. This method was validated using the HTR-PROTEUS critical experiments [4-41], in particular ‘stochastic’ cores 4.1 to 4.3 [4-42]. These randomly packed cores, which utilized an F/M ratio of one, were modeled using a 1.5 cm sphere exclusion zone. The use of a CFP exclusion zone in the fuel spheres was also investigated.

Results of the MCNP4B analysis, which appear in Table 4-39 together with the experimental results and the predictions of a Monte Carlo code that utilizes a statistical geometry model [4-42], demonstrated that it is possible to model accurately a randomly packed pebble-bed core with a regular sphere lattice. Therefore, the same methodology was applied to the prediction of the initial critical loading of the HTR-10.

Table 4-39. HTR-PROTEUS Criticality Analysis

Core	Critical Height (cm)	Packing Fraction	Effective Multiplication Constant		
			Experiment	MCNP4B <sup>†</sup>	MCNP-BALL <sup>[6]</sup>
4.1	158	0.600	1.0134±0.0011	1.0208±0.0011	1.0206±0.0011
4.2	152	0.615	1.0129±0.0008	1.0172±0.0010	1.0168±0.0011
4.3	150	0.618	1.0132±0.0007	1.0176±0.0011	1.0172±0.0011

<sup>†</sup> Using ENDF/B-VI cross-section data evaluated at 300 K; 0.5 million neutron histories.

The MCNP4 criticality analysis of the HTR-10 startup core was performed using both the ENDF/B-VI and the University of Texas at Austin (UTXS) cross-section libraries at 300K. The UTXS cross-section library was used for the temperature-dependent portions of the physics benchmark problem. The predicted initial critical height, and the corresponding number of spheres, is shown in Table 4-40. The largest sources of epistemic error are the specified packing fraction in the core and nominal uranium loading of the fuel spheres [4-13]. The critical loading predicted with the ENDF/B-VI nuclear data exceeds the actual value by 16 total spheres (approximately 9 fuel spheres). The results given in Table 4-40 are based on 1 million neutron histories, reducing the 1- $\sigma$  statistical errors to 0.1%.

Table 4-40. MCNP4B Criticality Predictions for HTR-10  
(Total critical loading = 16,890 spheres)

Cross-section Library	Effective Multiplication Constant	Critical Height (cm) <sup>‡</sup>	Number of Spheres	Percent Error
ENDF/B-VI	0.99980 ± 0.00090	128.0	16,906	0.09
UTXS	0.99961 ± 0.00094	127.5	16,840	-0.30

<sup>‡</sup> Measured above the conus region of the core.

### **Benchmarks B2 and B3 (temperature coefficient and control rod worth)[4-30]**

The University of Texas cross-section libraries (UTXS) are only available at 300 K, 450 K and 558 K in the temperature range of interest. The predictions for benchmark problems B22 and B23 were therefore obtained by interpolation using a polynomial fit of the  $k_{\text{eff}}$  values determined at the UTXS temperatures. The results for these cases are presented in Table 4-41. The calculations were performed using both ENDF/B-VI and UTXS cross-section libraries to determine the systematic bias between the two data sets. The results are based on 1 million (active) neutron histories per case, which reduced the estimated 1- $\sigma$  statistical errors to ~ 0.1%. Twenty non-active cycles, with 5000 neutrons per cycle, were used to establish a uniform source distribution.

Table 4-41. MCNP Simulation Results

Case	Critical Height (h) / $k_{\text{eff}}$ (k)	Cross Sections	Comments
B21	$k = 1.12976 \pm 0.00086$	ENDF/B-VI	300 K
	$k = 1.13185 \pm 0.00087$	UTXS	300 K
	$k = 1.13220$	UTXS	293.15 K; polynomial fit <sup>†</sup>
B22	$k = 1.12790$	UTXS	393.15 K; polynomial fit
B23	$k = 1.12452$	UTXS	523.15 K; polynomial fit
B3	$k = 0.95172 \pm 0.00096$	ENDF/B-VI	$\Delta\rho_{\text{rods}} = 165.6$ mk; 300 K
	$k = 0.95376 \pm 0.00101$	UTXS	$\Delta\rho_{\text{rods}} = 165.0$ mk; 300 K

<sup>†</sup>  $k(T) = 1.15328 - 9.35208E-05*T + 7.36721E-08*T^2$ , (T in °K); error not calculated.

### Discussion of results [4-30]

Tables 4-42 and 4-43 summarize the preliminary HTR-10 physics benchmark results reported at the IAEA Research Coordination Meeting for the Coordinated Research Project on the "Evaluation of High Temperature Gas-Cooled Reactor Performance," held October 18-22, 1999, in Beijing [4-39]. Both diffusion-code and MCNP results calculated by several international organizations are shown.

Table 4-42. Diffusion Code Benchmark Results by Other Participants

Case	China <sup>1</sup>	Indonesia/Japan <sup>2</sup>	Russia <sup>3</sup>	Comments
B1	125.81 cm	107.0 cm	179.6 cm	critical height
B21	1.1197	1.2193	1.0290	k-eff
B22	1.1104	1.1983	1.0112	k-eff
B23	1.0956	1.1748	0.9938	k-eff
B3	152.0 mk	–	146.6 mk	control worth

<sup>1</sup>VSOP [4-39]; <sup>2</sup>DELIGHT/CITATION-1000VP [4-10, 4-12]; <sup>3</sup>WIMS-D4/JAR [4-40]

Table 4-43. MCNP Benchmark Results for Other Participants and MIT

Case	China <sup>1</sup>	Russia <sup>2</sup>	MIT <sup>3</sup>	Comments
B1	~137 cm	164.6 cm	123.5 cm	critical height
B21	–	$1.0364 \pm 0.0008$	$1.1319 \pm 0.0009$	k-eff
B22	–	$1.0198 \pm 0.0008$		k-eff
B23	–	$1.0005 \pm 0.0009$		k-eff
B3	–	167.1 mk	165.0 mk	control worth

<sup>1</sup>MCNP4A and ENDF/B-V; <sup>2</sup>MCNP4A and ENDF/B-VI; <sup>3</sup>MCNP4B and UTXS.

There is clearly large variation in the results. However, there is good agreement between the MIT calculations using MCNP4B in two instances: the INET (China) prediction for the initial critical height, and the OKBM (Russia) estimate for the total control-rod reactivity worth. A high-fidelity MCNP model of a fresh core is expected to predict criticality within 2-3 mk. It is for this reason that MCNP models are often used to benchmark other codes. However, such an accurate model cannot be readily developed for the HTR-10 startup core because of the proposed 57:43 fuel-to-moderator pebble percent ratio.

The analysis of the HTR-10 initial core using MCNP has identified several deficiencies in the definition of the physics benchmark problem:

- a) The isotopic composition of natural boron in the graphite moderator and reflector has not been specified. Similar uncertainty is believed to be the main reason for the inaccurate prediction of initial criticality in the Japanese HTTR reactor.
- b) The reference core physics model is expressed in terms of an approximate R-Z geometry, which does not take full advantage of the generalized geometry features of MCNP.
- c) Insufficient information is provided on the design of the control rods, specifically the stainless-steel joints and the drive shaft. The presence of the control rods is completely ignored in the reference model, *i.e.*, the all-rods-out case is simulated using a region with low density (homogenized graphite plus void).

An increase in the temperature of the reflector is expected to reduce the reactivity of the core, because the decrease in the graphite density would reduce the number of thermal neutrons scattered back into the core. This effect was investigated at MIT for benchmark problem B23 by assuming a uniform expansion of the graphite reflector corresponding to an increase in temperature from 27°C to 285°C. The resulting decrease in reactivity of approximately 1 mk is inconsequential.

Finally, criticality calculations using the University of Texas at Austin cross-section library (UTXS) was found to match closely the corresponding results obtained with ENDF/B-VI data. The UTXS results are approximately 1-2 mk more reactive, with the worst agreement (2.2 mk) observed for benchmark problem B23 in which all ten control rods were fully inserted.

## 4.2.7. Turkey [4-45]

### 4.2.7.1. Introduction

This study was performed by the Hacettepe University Nuclear Engineering Department at Ankara, Turkey, and deals with the core physics benchmark problems proposed for HTR-10 reactor initial core. Both Monte Carlo and diffusion approach have been considered. Monte Carlo calculations have been carried out by KENOVA module of SCALE4.4 code system. Diffusion calculations have been performed by VSOP'94.

### 4.2.7.2. HTR-10 Reactor and Initial Core Loading

The HTR-10 is a working example of gas cooled pebble bed reactors. Reactor core is located at the internal cavity which is consisted of a cylindrical body at the top and cone region at the bottom. Fuel spheres as well as graphite moderator spheres are placed in the core region. Core region is surrounded by a 1 m thick cylindrical graphite side reflector. Reflector region has openings for absorber balls made of B<sub>4</sub>C. There are also 10 control rods in the reflector region. Helium coolant is circulated from top to bottom. Helium flow is not only through the core region but also through the coolant channels located at side reflector. It has been reported that graphite components of the reactor contains different amount of boron impurities [4-43]. These impurities are considered during the evaluation of cross sections. Typical characteristics of HTR-10 are given in Table 4-44.

Table 4-44. Characteristics of HTR-10 reactor [4-43]

Reactor thermal power	10	MW
Reactor core diameter	180	mm
Reactor core height	197	mm
Average helium inlet temperature	250	C
Average helium outlet temperature	700	C
Number of control rods at side reflector	10	
Number of absorber ball unit at side reflector	7	
Fuel Material	UO <sub>2</sub>	
Heavy metal loading per fuel element	5	Gram
Fresh fuel enrichment	17	%

### 4.2.7.3. HTR-10 Model with SCALE4.4 and VSOP'94

The SCALE4.4 code system is a collection of program modules for various purposes such as criticality and shielding calculations and cross section evaluation. Criticality calculations are performed by KENOVA module of SCALE4.4 code package. Monte Carlo technique is utilized in these calculations. Spherical fuel elements are assembled with 8335 TRISO particles in graphite matrix. Homogenized cross sections of fuel are evaluated by CSAS module. 27 group ENDF/B IV and 44 group ENDF/B V cross section sets are used throughout the study. Normally, spherical elements make hexagonal lattice in the core. However, cubical cells are constructed in this study due to the limitation of SCALE4.4. These cubical cells are repeated to form the core region. In the reflector region, twenty helium flow channels are placed vertically having equal angular rotation in polar coordinates. In addition to helium flow channels, ten control rod channels, seven small absorber ball channels, and

three irradiation channels are placed in the side reflector. Hot gas duct is also included in the model. Due to the complexity of the model and geometry limitations imposed by SCALE4.4 certain simplifications are applied in the geometry construction. For instance, absorber ball channel cross section is rectangular in the middle and semicircles at the ends. This geometry is represented by equivalent circular cross sections. Conus region located at the bottom of the core initially contain only graphite ball and this is considered in the model. Geometrical model used in SCALE4.4 calculations is shown in Figures 4.37 and 4.38.

Criticality calculations are performed based on diffusion approach using VSOP'94 code. During these calculations fast and epithermal spectrums are evaluated GAM code whereas the thermal spectrum is evaluated with THERMOS code. Two dimensional reactor geometry is considered. CITATION with four energy groups is used. Resonance cross sections are obtained by ZUT-DGL code.

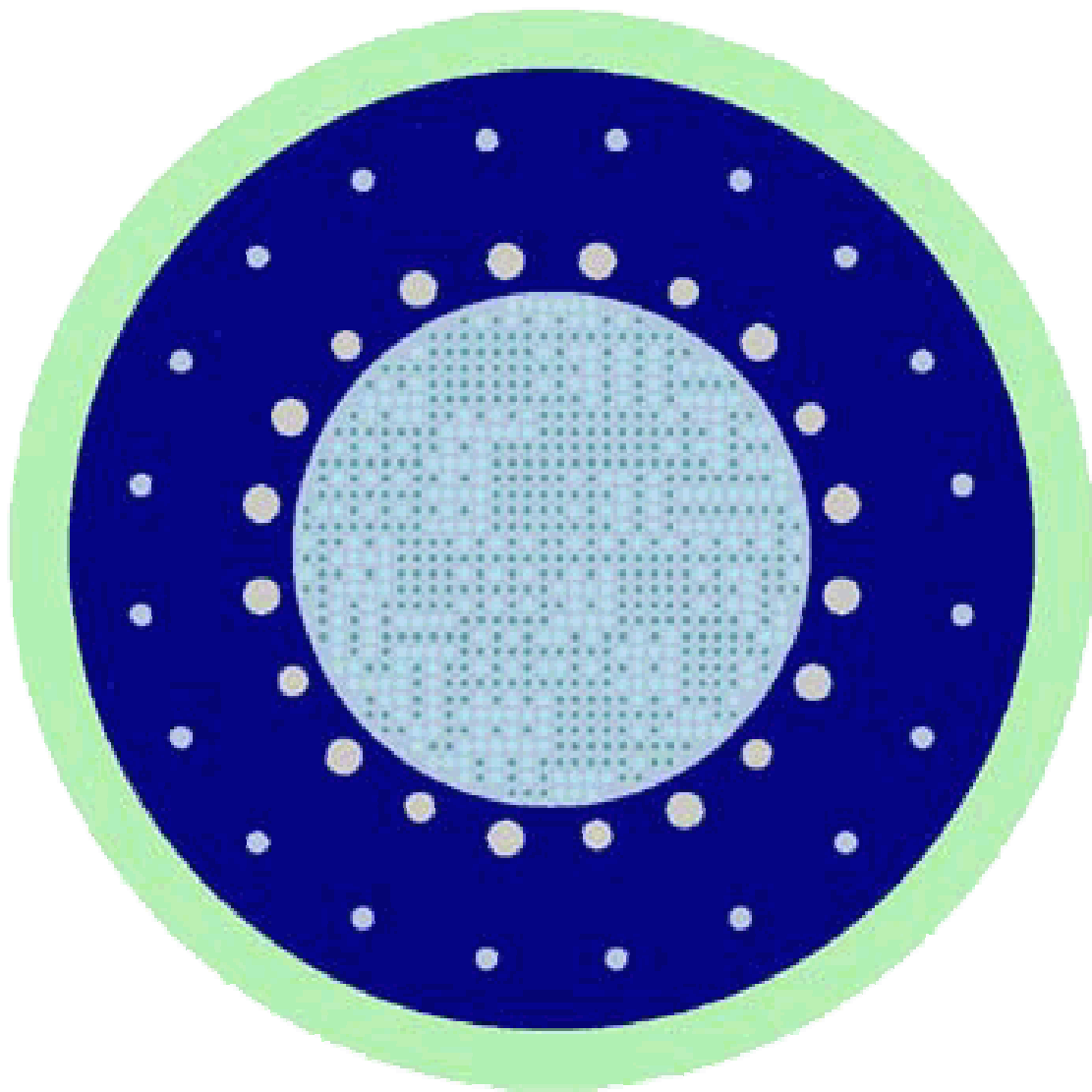


*FIG. 4.37. Horizontal cross sectional view of HTR-10 in SCALE4.4 model*

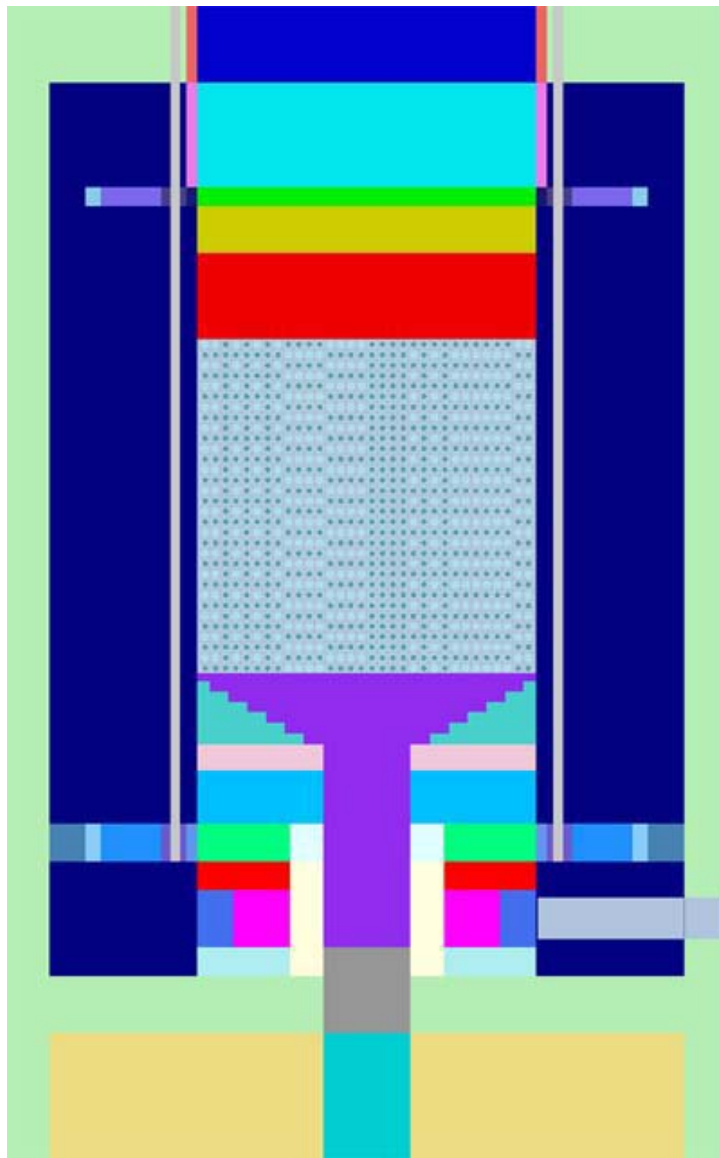


FIG. 4.38. Vertical cross section of HTR-10 reactor in SCALE4.4 model

#### 4.2.7.4. Results of Benchmark Problems

##### **Problem B1**

This problem deals with the determination of the core height for criticality. Initial criticality calculation is performed for a height of 99 cm. Then, calculations are repeated by increasing the core height each time by 11 cm.

Table 4-45. Effective multiplication factor as a function of initial core height by SCALE 4.4

	99 cm	110 cm	121 cm	132 cm	143 cm	154 cm	165 cm	176 cm	180 cm
27 Group	0.9130	0.9480	0.9774	1.0059	1.0287	1.0497	1.0698	1.0876	1.0941
44 Group	0.8998	0.9339	0.9653	0.9922	1.0179	1.0382	1.0584	1.0749	1.0809

Based on the calculations critical core height is found to be 129.7228 cm with 27 group ENDF- B IV cross sections and 135.3385 cm with 44 group ENDF-B V cross sections. Experimental observations show that critical height of the initial core is 123.06 cm which is less than both calculations.

Table 4-46. Effective multiplication factor as a function of initial core height calculated by VSOP'94

100cm	110cm	120cm	130cm	140cm	150cm	160cm	170cm	180cm
0.946145	0.975977	1.00188	1.02479	1.04569	1.06646	1.08529	1.10269	1.11844

Based on the calculations critical core height is found to be 119.274 cm with GAM and THERMOS library. Experimental observations show that critical height of the initial core is 123.06 cm which is higher than calculation results.

### **Problem B2**

The effective multiplication factor k-eff of the full core at various temperatures under helium atmosphere are calculated in this problem. Calculations are performed by SCALE4.4 with 27 group ENDF/B-IV and 44 group ENDF/B-V cross section sets. Results are given in Table 4-47.

Table 4-47. Effective multiplication factors and associated standard deviations for the full core at different temperatures

Temperature (C)	27-group ENDF/B-IV	44-group ENDF/B-V
20	1.0941±0.0008	1.0809±0.0007
120	1.0802±0.0006	1.0380±0.0006
250	1.0671±0.0007	1.0035±0.0006

### **Problem B3**

Reactivity worth of ten and one fully inserted control rods are calculated with SCALE 4.4. Results of this benchmark problem are given in Table 4-48.

Table 4-48. Control rod reactivity worths

	27-group ENDF/B-IV	44-group ENDF-B-V
Ten control rods	18.73%	21.88%
One control rod	2.53%	4.60%

### **Problem B4**

This benchmark problem deals with the calculation of reactivity worths of 10 control rods for the initial core loading which corresponds to 126 cm fuel loading. Reactivity worths for this case are evaluated by SCALE4.4 and results are 20.02% and 23.65% for 27 group ENDF/B-IV and 44 group ENDF/B-V cross section libraries. This problem also deals with the calculation of differential rod worth of a single control rod while all the others are fully withdrawn.

Differential control rod worth is evaluated at axial positions starting from 230.318 cm and with 48.07 cm increments. Results are shown in Table 4-49.

Table 4-49. Differential control rod reactivity worth calculation results

Axial position (cm)	27-group ENDF/B-IV	44-group ENDF/B-V
230.318	0.49%	2.42%
279.018	0.97%	3.03%
282.618	1.01%	3.16%
331.318	1.68%	3.90%
334.918	1.82%	3.98%
383.618	1.96%	4.13%
394.200	2.09%	4.19%

### **Conclusions**

Results presented in this study are preliminary in nature. Although the geometry of HTR-10 reactor is well represented in SCALE4.4 model, there are some considerable deviations from expected results. Moreover, benchmark problem results deviate from one cross section set to another even if the same geometrical model is employed. Criticality calculations show better agreement with experimental observations. In this context, 27 group ENDF/B IV cross section set yields better estimates for effective multiplication factor as well as control rod reactivity worth estimates. Control rod reactivity worth estimates are much higher than expected values. Results show that there is a significant dependency on cross section sets. Apparently, cross sections provided by SCALE and used in this study are more relevant to LWR type reactors since they have been generated by using typical LWR lattices [4-44]. Furthermore, some irregularities have been reported in these libraries associated with certain nuclides [4-44]. Work is in progress to generate new cross section sets for gas cooled reactors through the evaluation of reduced group cross sections by NJOY 97 in AMPX format. Once this is done, necessary adjustments may be done in the model to improve the results.

## 4.2.8. France

### 4.2.8.1. General Analysis Method and Model Description

#### Codes and calculation scheme

In the following HTR-10 calculations, the French reactor physics code system SAPHYR has been used. SAPHYR gathers several codes developed at CEA like APOLLO2 [4-46] (transport) based on a database produced with THEMIS/NJOY, CRONOS2 (diffusion-transport), FLICA4 (3D-thermal hydraulics), which are interconnected. Besides, the Monte-Carlo code TRIPOLI4 [4-47] has also been used throughout the study.

All of the HTR-10 problems proposed in reference [4-43] have been treated considering a calculation scheme based on a Transport – Monte-Carlo method. Figure 4.39 illustrates the general procedure. The standard 172-group or point-wise cross sections library issued mainly from JEF-2.2 are used for the calculations.

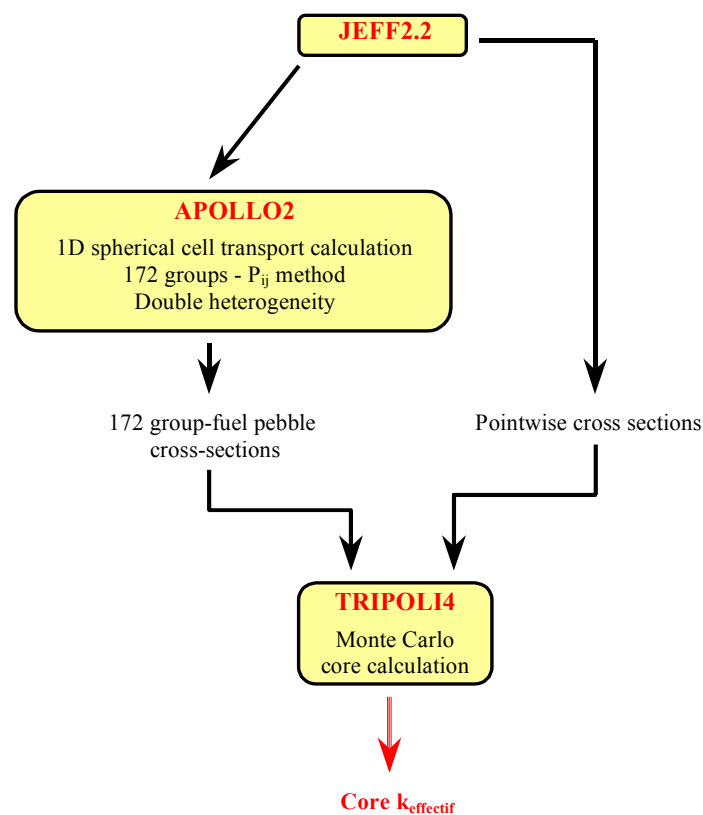


FIG. 4.39. Description of the Transport – Monte-Carlo calculation scheme.

#### Fuel pebble calculation (APOLLO2)

Knowing that the stochastic geometries calculations (coated fuel particles - CFP - randomly distributed in the inner zone of the fuel pebble) are not available in the Monte-Carlo code TRIPOLI4, a 1D-cell calculation has been performed as a first step (Figure 4.40). It takes into account a precise spherical description of the particles with their coatings, which themselves fill the spherical fuel zone of the pebble. The self-shielding of the uranium isotopes is calculated during this calculation step. A collision probability method is used to solve the transport equation with 172 energy groups. The critical buckling search allows taking into account the neutron leakage by the addition of a homogeneous leakage term in the

form of  $DB^2\Phi$ . The extra region of the spherical cell is representative of the helium coolant plus the moderator pebbles (dummy balls) loaded into the core with the fuel pebbles. The volume of the extra-region has been calculated by considering a volumetric filling fraction of pebbles (fuel and dummy balls) of 0.61 in the core and a 57:43 fuel-to-moderator pebble percent ratio.

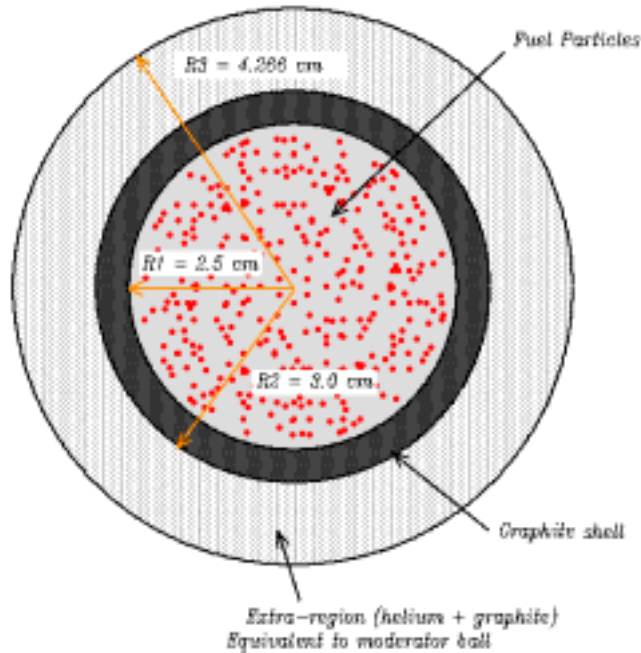


FIG.4.40. Spherical Fuel Pebble Model in APOLLO2.

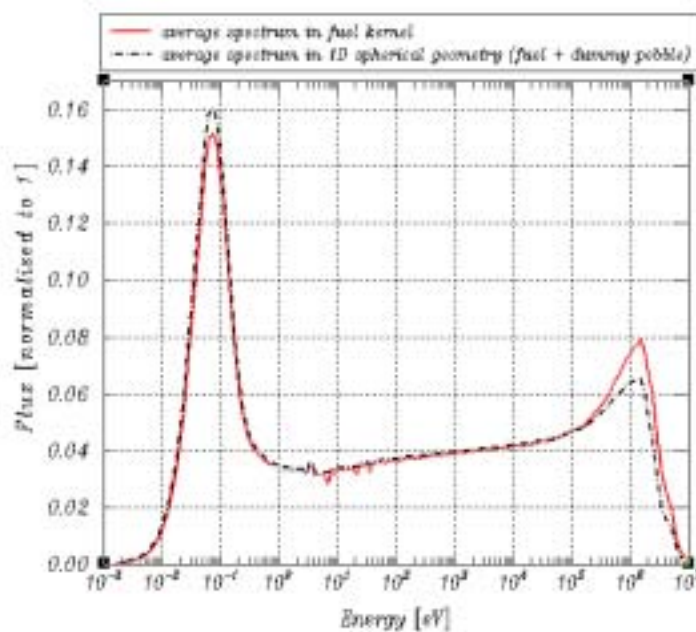


FIG. 4.41. Average neutron spectrum in fuel kernel and in fuel pebble surrounded by extra-region.

Table 4-50. 1D spherical – Transport calculation results in APOLLO2

	$k_{\infty}$	$M^2$ [cm <sup>2</sup> ]
Enrichment of U235 (weight) 17%	1.71926	1298.0

This first stage provides 172-group fuel region averaged cross sections for Monte-Carlo core calculations (TRIPOLI4). The fuel homogenization is performed with respect to the pebble bed description in the Monte-Carlo code TRIPOLI4. Indeed, for this benchmark, two types of pebble bed modeling have been analyzed. In the first one, the core calculations have been performed considering a homogenized pebble bed (mixture of fuel, moderator pebbles and coolant). In the second one, each pebble has been modeled in the core. In the last case, the fuel pebble calculation in APOLLO2 provided the homogenized cross sections for the fuel pebble inner zone (rad. = 2.5 cm).

Therefore, in the core calculations performed by TRIPOLI4, point-wise cross sections are used everywhere in the core except in the fuel pebble region where the multi-group cross sections have been generated with APOLLO2.

### ***Monte-Carlo core calculation (TRIPOLI4)***

#### **Pebble bed modeling**

Two sets of calculations have been performed on the core geometry. In both cases, all the core components are explicitly modeled (coolant and control rod channels...). The major difference concerns the pebble bed modeling (fuel and dummy balls modeling). In the first modeling, the pebble bed is represented with an homogeneous medium as shown on Figure 4.42. This homogeneous medium is a mixture of fuel, moderator pebbles and coolant. The equivalent pebble bed cross sections are homogeneous cross sections issued from APOLLO2 calculations (homogenization of the 1D-spherical geometry). This modeling will be called “Simplified Pebble Bed modeling”.

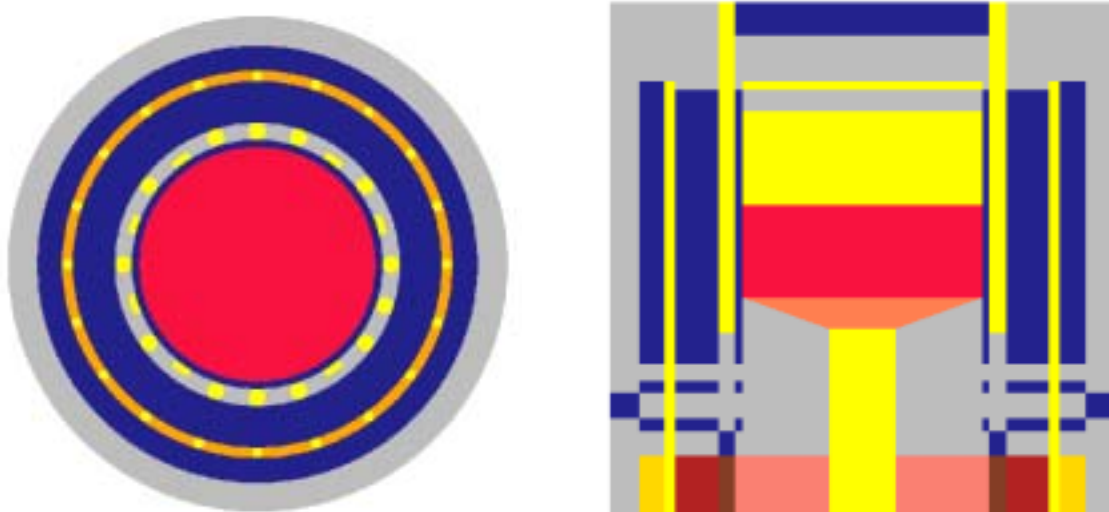


*FIG. 4.42. Core modeling in Monte-Carlo code TRIPOLI4 (“Simplified PB modeling”).*

In the second set of calculations, all the pebbles (fuel and moderator pebbles) loaded into the core have been described explicitly. Considering a Cubic-Face-Center lattice (theoretical filling fraction of 74%), the fuel and dummy pebbles have been randomly placed at lattice nodes to achieve an average filling fraction of 61% (Figure 4.43).

Besides, the specification of a 57:43 fuel-to-moderator pebble percent ratio for the initial HTR-10 core loading has been respected. For the calculations, the homogenized cross-sections for the fuel pebble inner-zone have been evaluated by APOLLO2. For the moderator pebble and the fuel pebble outer region, point-wise cross sections are used. This modeling will be called “Improved Pebble Bed modeling”.

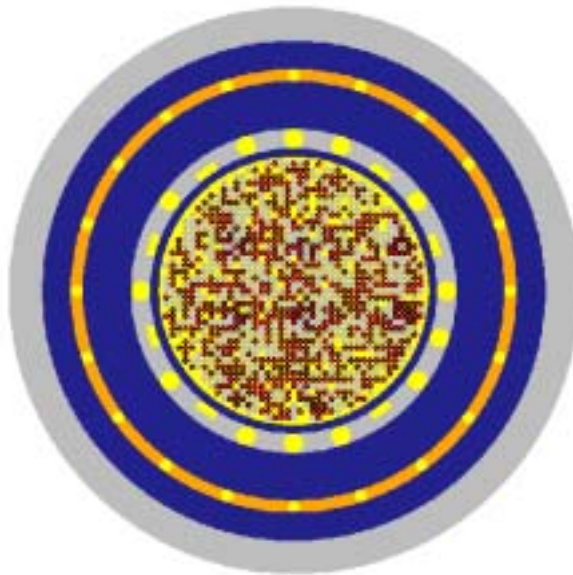


FIG. 4.43. Core modeling in Monte-Carlo code TRIPOLI4 (“Improved PB modeling”).

### Void channels modeling

In the preliminary results given by CEA, all the calculations were performed in TRIPOLI4 without modeling the void channels (control rods and coolant channels). The consequence was an over-estimation of the core reactivity during the criticality approach. For all the calculations presented in this paper, the void channels have been described exactly in the Monte-Carlo code TRIPOLI4. The cavities modeling impact on reactivity (streaming effect) has also been evaluated for an intermediate core configuration close to the critical core configuration.

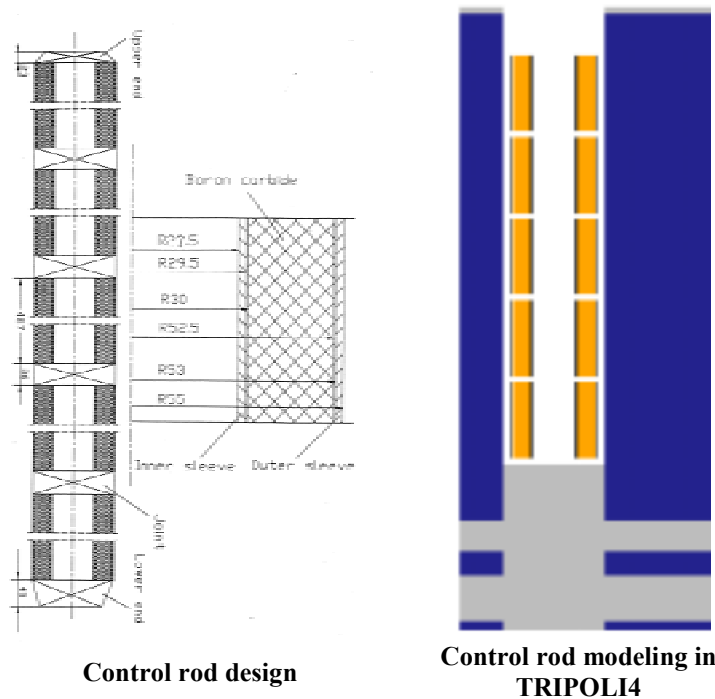


FIG. 4.44. Control Rods modeling in Monte-Carlo code TRIPOLI4.

## Control rods modeling

Ten control rods are designed in the side reflector of HTR-10. Each control rod contains five B4C ring segments, which are housed in the place between an inner and outer sleeve of stainless steel. In TRIPOLI4, the control rods have been modeled explicitly (Figure 4.44). It means that the annular geometry of the control rod has been modeled as well as the joints between the segments (3,6 cm height).

### 4.2.8.2. Benchmark Data and Void Channels Modeling Impact

#### *Void channels modelling impact (streaming effect)*

Some calculations have been performed with the Monte-Carlo code TRIPOLI4 in order to evaluate the impact of the void cavity modeling on the core neutron leakage. The results are presented in Table 4-51. In the first calculation (case a), the void channels (coolant and control rods channels) are homogenized with the surrounding graphite. In the second calculation, all the cavities have been described exactly in TRIPOLI4 (case b). In the selected configuration (the height of the pebble bed is approximately 123.0 cm), the streaming effect has been evaluated to 1.48% $\Delta k/k$ .

Table 4-51: Evaluation of the streaming effect in HTR-10

	TRIPOLI4 Case (a) Homogenized cavity	TRIPOLI4 Case (b) Exact modeling	$\Delta k$ [% $\Delta k/k$ ]
Core $k_{\text{eff}} \pm \sigma$ Pebble bed height = 123.06 cm	1.03586 $\pm$ 0.00034	1.01960 $\pm$ 0.00043	1.48

#### *Analysis of the benchmark data impact*

After the HTR-10 core physics benchmark problems were defined, two conditions changed and concerned the dummy balls loaded into the core and the core atmosphere at initial criticality. The following list summarizes the deviations [4-48]:

- Density of dummy balls: from 1.73 to 1.84 g/cm<sup>3</sup>
- Boron equivalent of impurities in dummy ball: from 1.3 to 0.125 ppm
- Core atmosphere at initial criticality: from Helium to Air

Considering the new benchmark data, some calculations have been performed with TRIPOLI4 in order to evaluate the impact on the core  $k_{\text{eff}}$ . The results that are presented in Table 4-52 are related to a core loading height of 123.06 cm. The decrease of the boron equivalent impurities in the dummy balls induces an increase of the core reactivity higher than the capture increase of air atmosphere. The impact on core reactivity amounts to 0.70%.

Table 4-52: Benchmark data impact

	TRIPOLI4 Helium	TRIPOLI4 Air + impurities + density	$\Delta k$ [% $\Delta k/k$ ]
Core $k_{\text{eff}} \pm \sigma$ Pebble bed height = 123.06 cm	1.01960 $\pm$ 0.00043	1.02669 $\pm$ 0.00048	0.70

#### 4.2.8.3. Benchmark Results

##### Initial criticality (problem B1)

The aim of the first benchmark problem was to evaluate the amount of loading (given in loading height, starting from the upper surface of the conus region) for the first criticality, under air atmosphere and core temperature of 20 °C, without any control rods being inserted. The core multiplication factor has been calculated for different core loading heights with TRIPOLI4 by using the two types of modeling described below. The results are summarized in Figure 4.45.

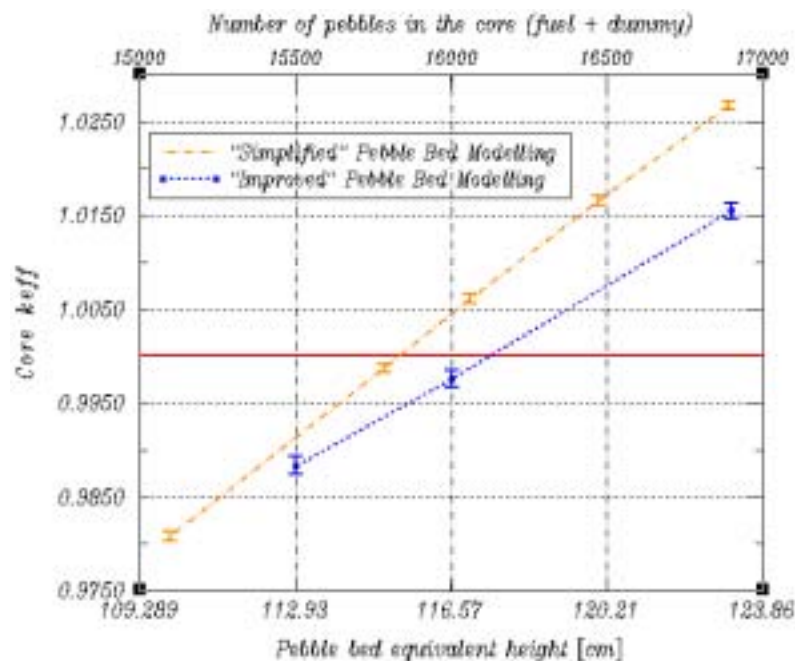


FIG. 4.45. Calculated  $k_{eff}$  vs loading height for HTR-10 initial criticality.

On the one hand, it should be noticed that for the core configuration close to the criticality, the core effective multiplication coefficient increases linearly with the number of pebbles loaded. On the other hand, the pebble bed modeling has a strong impact on the core  $k_{eff}$ . For example, the discrepancy between the simplified and the improved pebble bed modeling reaches 0.9%  $\Delta k/k$  for a core loading height of 123.133 cm. This discrepancy is lower when the number of pebbles loaded into the core decreases but in all cases, the core  $k_{eff}$  obtained with the improved PB modeling is lower than the one obtained with the simplified PB modeling.

In order to evaluate the impact of the pebble bed modeling on the results, calculations have been performed in a simplified configuration (infinite medium with white boundary condition). It allowed evaluating the impact of the pebble bed geometrical description without considering core physical effects such as streaming effect and spectrum transient at the interface between core and reflector. The results are gathered in Table 4-53. The  $k_{infinity}$  calculated with both modeling (homogenized pebble bed or randomly distributed pebble bed) are very closed. It shows that the two types of pebble bed modeling are equivalent in infinite medium.

Table 4-53. Pebble bed modelling impact in infinite medium

Pebble bed in infinite boundary conditions	TRIPOLI4		$\Delta k$ [% $\Delta k/k$ ]
	Simplified PB modeling	Improved PB modeling	
$k_{\infty} \pm \sigma$	$1.76431 \pm 0.00051$	$1.76155 \pm 0.00125$	0.15

After all, the discrepancies observed between the two modeling on the core geometry could be explained by:

- An underestimated streaming effect in the case of an homogenized pebble bed modeling,
- An over-estimation of the fission rates in the region close to the reflector in the case of the “*Simplified BP Modeling*”. The pebble bed geometrical modeling seems to have a strong impact in the regions where the neutron spectrum transients are important (at the interface between active core and reflector). Besides, this phenomenon increases when the size of the core decreases (the radius of the active core is 90 cm).

As far as the benchmark problem is concerned, the critical heights calculated with the two models are presented in Table 4-54. With the **simplified PB modeling**, the criticality is achieved with a loading height of **115.36 cm**. This loading height is equivalent to **15833 pebbles** (fuel and moderator pebbles) loaded into the core. With the **improved PB modeling**, the criticality is achieved with a loading height of **117.37 cm** that corresponds to **16108 pebbles** loaded.

Table 4-54. Critical height for the different HTR-10 modeling

B1	TRIPOLI4	
	Simplified PB modeling	Improved PB modeling
Critical height [cm]	<b>115.36</b>	<b>117.37</b>
Number of pebbles loaded		
Total	<b>15833</b>	<b>16108</b>
Fuel	~ 9025	~ 9182
Moderator	~ 6808	~ 6926

### Temperature coefficient (problem B2)

Only the calculations at 20 °C with an equivalent core loading height of 180,12 cm (24721 pebbles in the core) have been performed. The results are gathered in Table 4-55. The core  $k_{\text{eff}}$  reaches **1.15679** with the simplified PB modeling and **1.14737** with the improved PB modeling. The discrepancy observed between the two modeling is about 0.9% for the full core configuration.

Table 4-55.  $k_{\text{eff}}$  at full core

B21	TRIPOLI4	
	Simplified PB modeling	Improved PB modeling
Core $k_{\text{eff}} \pm \sigma$	$1.15679 \pm 0.00040$	$1.14737 \pm 0.00123$
Pebble bed height = 180.12 cm (full core)		

### Control rod worth for the full core (problem B3)

The reactivity worths of the ten fully inserted control rods (**B31**) and of one fully inserted control rod (**B32**, the other rods being withdrawn) have been calculated for the full core configuration. The results are presented in Table 4-56. The calculations have been performed with both pebble bed modeling and the reactivity worth is calculated by using the formulation:

$$\Delta\rho = \frac{k_{eff}(\text{rods in}) - k_{eff}(\text{rods fully withdrawn})}{k_{eff}(\text{rods fully withdrawn})} \quad (1)$$

The reactivity worth of ten control rods has been evaluated to **13.06%** with the **simplified PB** modelling and **13.44%** with the **improved PB** modelling. In addition, the reactivity worth of one control rod has been evaluated to **1.35 / 1.31%**. If the core  $k_{eff}$  depends on the pebble bed modelling, on the opposite, the reactivity worth of the control rod(s) calculated in both cases are similar.

Table 4-56.  $k_{eff}$  and reactivity worth of CRs for full core (core height = 180.12 cm)

	TRIPOLI4 Simplified PB modeling		TRIPOLI4 Improved PB modeling	
<b>Core <math>k_{eff} \pm \sigma</math> (rods fully withdrawn)</b>	1.15679 ± 0.00040		1.14737 ± 0.00123	
	<b>B31 (Ten rods fully inserted, 27 °C)</b>	<b>B32 (One rod fully inserted, 27 °C)</b>	<b>B31 (Ten rods fully inserted, 27 °C)</b>	<b>B32 (One rod fully inserted, 27 °C)</b>
<b>Core <math>k_{eff} \pm \sigma</math></b>	1.00562 ± 0.00030	1.14120 ± 0.00041	0.99297 ± 0.00099	1.13225 ± 0.00110
<b>Control rod(s) worth [%<math>\Delta k/k</math>]</b>	13.06 ± 0.07	1.35 ± 0.08	13.44 ± 0.26	1.31 ± 0.29

### Control rod worth for the initial core (problem B4)

As for the benchmark problem B31, the reactivity worth of the ten control rods has been calculated for an intermediate core loading height of 126 cm. All the results are gathered in Table 4-57. The reactivity worth of ten control rods has been evaluated to **13.66%** with the **simplified PB** modeling and **13.58%** with the **improved PB** modeling.

Table 4-57. Reactivity worth of ten CRs for intermediate core (core height = 126.0 cm)

	TRIPOLI4 Simplified PB modeling		TRIPOLI4 Improved PB modeling	
<b>Core <math>k_{eff} \pm \sigma</math> (rods fully withdrawn)</b>	1.03532 ± 0.00055		1.03211 ± 0.00085	
	<b>B41 (Ten rods fully inserted, 27 °C)</b>	<b>B41 (One rod fully inserted, 27 °C)</b>	<b>B41 (Ten rods fully inserted, 27 °C)</b>	<b>B41 (One rod fully inserted, 27 °C)</b>
<b>Core <math>k_{eff} \pm \sigma</math></b>	0.89390 ± 0.00038	0.88960 ± 0.00108	0.89390 ± 0.00038	0.88960 ± 0.00108
<b>Control rods worth [%<math>\Delta k/k</math>]</b>	13.66 ± 0.1		13.80 ± 0.20	

In the second part of the benchmark problem B4, the differential reactivity worth of one control rod for the initial core (loading height of 126.0 cm) has been calculated with the simplified PB modeling. The results are reported in Table 4-58. The integral worth of one control rod was determined to be **1.52%**. Even if the experimental conditions were not the same as specified in the benchmark (the main differences were in the control rod elevation height and the amount of loading in the reactor core), the calculation result can be compared to the experimental value. Thus, the experimental integral worth of one control rod was determined to be **1.437%**. The calculated value agrees well with the experimental results.

Table 4-58. Reactivity worth of one CR for intermediate core (core height = 126.0 cm)

TRIPOLI4 - Simplified PB modelling B42 (One rods, 27 °C)		
Axial position of the control rod [cm]	Core $k_{\text{eff}} \pm \sigma$	Differential control rod worth [% $\Delta k/k$ ]
Fully withdrawn	1.03532 $\pm$ 0.00055	*
<b>230.318</b>	1.03244 $\pm$ 0.00033	0.28 $\pm$ 0.10
<b>279.018</b>	1.02833 $\pm$ 0.00036	0.68 $\pm$ 0.10
<b>282.618</b>	1.02772 $\pm$ 0.00060	0.73 $\pm$ 0.12
<b>331.318</b>	1.02225 $\pm$ 0.00033	1.26 $\pm$ 0.10
<b>334.918</b>	1.02103 $\pm$ 0.00033	1.38 $\pm$ 0.10
<b>383.618</b>	1.01999 $\pm$ 0.00032	1.48 $\pm$ 0.10
<b>394.200</b>	1.01957 $\pm$ 0.00080	1.52 $\pm$ 0.13

#### 4.2.8.4. Concluding Remarks

The HTR-10's core physics benchmarks have been treated with a Transport – Monte-Carlo calculation scheme (APOLLO2 – TRIPOLI4 calculations) and by considering two different modeling for the pebble bed geometrical description. In the “*Simplified PB Modeling*”, the pebble bed has been represented by a homogeneous medium. In the “*Improved PB Modeling*”, each pebble has been represented in the core (moderator and fuel pebbles). In both case, the double heterogeneity (fuel particles in a graphite matrix) and the self-shielding of the heavy nuclides have been treated by APOLLO2.

Due to the streaming effect and the small size of the core (90 cm in radius), the “*Simplified PB modelling*” always overestimates the core  $k_{\text{effective}}$ . As a consequence, the critical pebble bed height calculated with the “*Simplified PB Modeling*” (**115.36 cm – 15833 pebbles in the core**) is much lower than the one calculated with the “*Improved PB Modeling*” (**117.37 cm – 16108 pebbles in the core**). These discrepancies between both models are also observed for the fully loaded (problem B2) core and for the intermediate core configuration close to the criticality (pebble bed height of 126 cm). Finally, the control rods worth evaluated with both modeling are very closed from each other (problem B31 & B32).

## 4.2.9 Germany [4-49]

### 4.2.9.1. Introduction

Within the frame of the IAEA Co-ordinated Research Programme (CRP-5) on "Evaluation of the High Temperature Gas Cooled Reactor Performance" a system of benchmark problems has been defined by the Institute of Nuclear Energy Technology (INET) [4-43], concerning the critical loading, control rod worth, and the isothermal temperature coefficients at zero power conditions of the HTR-10 reactor. The ISR of the Research Centre Jülich joined this CRP with the aim of validating its reactor code system VSOP [4-50]. This code system is being used as the main tool for design studies of high temperature reactors, and therefore, the validation of this code, specifically the accuracy in control and shutdown margins calculations, are of particular interest.

### 2.4.9.2. Calculational Methods and Nuclear Data

The benchmark problems are calculated using the following parts of the VSOP code system: the ZUT [4-51], GAM-1 [4-52], THERMOS [4-53], and the CITATION [4-54] code. The code system considers the following main features of pebble bed reactors:

- the double heterogeneous nature of the spherical fuel elements with the coated particles,
- the streaming correction of the diffusion constant in the pebble bed,
- detailed leakage feedback when using few group homogenised cross sections in the whole core diffusion calculation,
- the use of anisotropic diffusion constants in the upper cavity and in the channels of the control rods and of the small absorber balls.

Self-shielded cross sections in the resolved resonance region of  $U^{238}$  are generated by the ZUT code taking into account the double heterogeneity of the fuel elements. The resonance parameters processed by the ZUT code are taken from the JEF-1 data file [4-55].

Spectrum calculations are performed by a combination of the epithermal spectral code GAM-1 and the thermal cell code THERMOS using two fine group nuclear data libraries [4-56] based on JEF-1 and ENDF/B-V: an epithermal library with a 68 energy group structure ranging from 10 MeV to 0.414 eV, and a thermal library with 30 fine energy groups in the energy range from 2.05 eV to  $10^{-5}$  eV.

The 0-d spectrum code GAM-1 applies the  $P_1$ -approximation to homogenised spectrum zones. Neutron leakage between adjacent spectrum zones is considered by buckling terms determined from the fast and epithermal leakage values of the whole core diffusion calculation and transferred to the spectrum calculation. At the beginning all buckling terms are zero. Condensation of the fine energy groups is performed to three broad groups used in the diffusion calculation.

The thermal cell code THERMOS performs 1-d transport spectrum calculations using a heterogeneous cell model. The grain structure of the coated particles inside the fuel elements is taken into account. The neutron exchange between neighbouring spectrum zones is considered in the form of albedo terms at the cell surface. They are calculated from the thermal leakage value of the diffusion calculation and booked into the fine thermal energy groups. At the beginning of the leakage iteration a white boundary condition is assumed at the

outer surface of the cell. A cell-weighted condensation of the 30 fine group cross sections is performed to one broad energy group used in the diffusion calculation. The broad group structure is given in Table 4-59.

Table 4-59. Group Structure in the VSOP Diffusion Calculations

Group	Upper Energy Boundaries (eV)
1	$1.0 \cdot 10^7$
2	$1.111 \cdot 10^5$
3	29.0
4	1.86

The eigenvalues and flux distributions of the whole reactor are calculated by the diffusion code CITATION in 2-d r,z and 3-d r,φ,z geometry.

A streaming correction of the diffusion constants in the pebble bed is calculated according to Lieberoth [4-57]. In the upper void region the method of Gerwin and Scherer [4-20] is applied. For the boring holes of the control rods and of the small absorber balls a special transport calculation was performed in order to determine the corresponding diffusion constants.

The geometric dimensions of the fuel elements and core components and the atom number densities of the materials given in [4-43] are used.

#### 4.2.9.3. Unit Cell Models

According to the initial core loading of the HTR-10 - the inner cone region at the bottom of the core is filled with graphite balls, then, a mixture of fuel and graphite balls in the ratio of 0.57 to 0.43 is loaded gradually to approach first criticality- two kinds of spherical unit cell models are chosen: a fuel and a dummy (graphite) unit cell model.

1. The fuel unit cell model shown in Figure 4.46 consists of 4 zones: a fuel zone, containing the coated particles (cp) and the graphite matrix, the graphite shell, a helium or air gap as third zone corresponding to the packing fraction of 0.61, and a graphite/helium or air mixed zone as mock-up for the moderator pebbles and their corresponding void space. The coated particles grain structure inside the fuel zone is treated by effective macroscopic total cross sections replacing the homogenised macroscopic cross sections of the matrix and the coated particles.
2. The dummy unit cell model consists of two zones: a graphite zone with  $r = 3$  cm, and a void corresponding to the filling fraction  $f = 0.61$  of the dummy balls in the cone region.

The  $k_{\infty}$ -value of the fuel cell calculation is: 1.7475 at  $T = 293$  K using a white boundary condition.

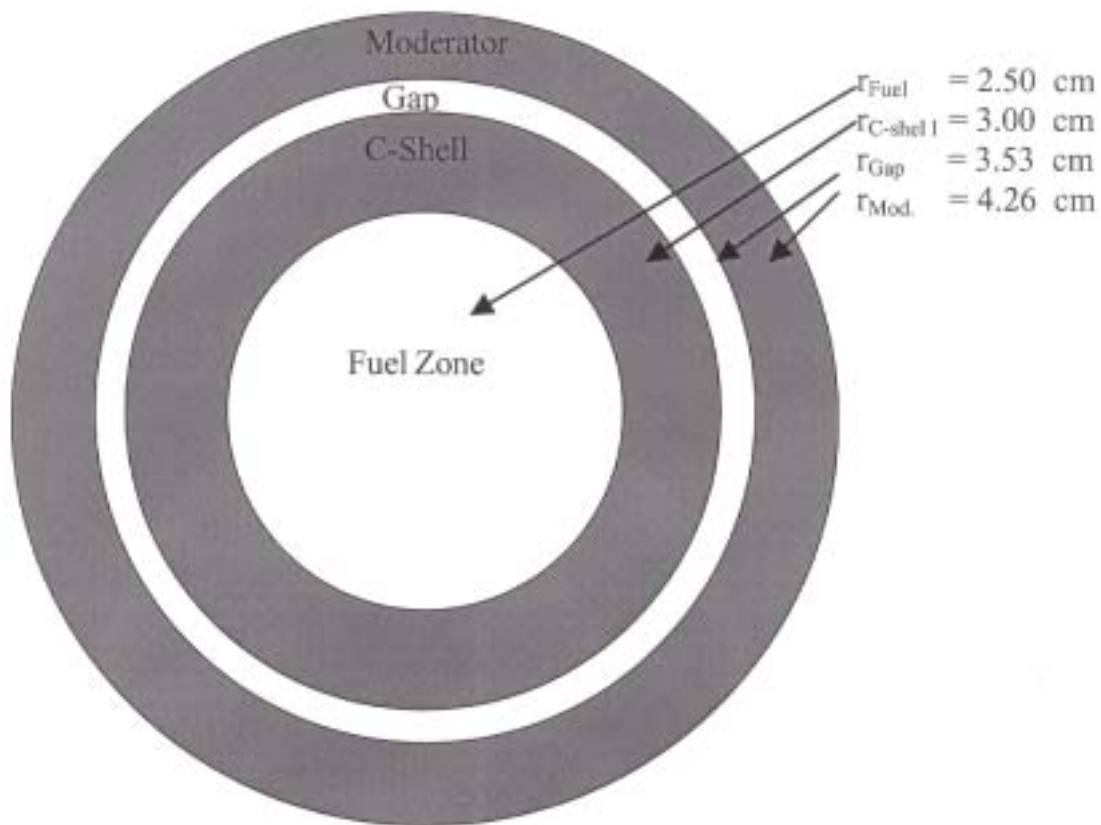


FIG. 4.46. 1-d Spherical Fuel Cell Model for THERMOS.

#### 4.2.9.4. Whole Reactor Calculations

Using the 4-group constants from the GAM-1 and THERMOS cell calculations the whole HTR-10 reactor is modelled with the CITATION diffusion code. Two geometric models are chosen in order to compare the results: a 2-d  $r,z$  model as presented in [4-43] and a 3-d  $r,\phi,z$  model. The assembly is modelled by dividing the volume into different spectrum zones each comprising several material compositions given in [4-43] (See Section 4.1.2 for details of the HTR-10 reactor physics benchmark problems). There are 16 different spectrum zones. The active core and the adjacent reflector regions are subdivided into smaller spectrum zones in order to take into account the core/reflector coupling accurately during the leakage iteration.

In the 3-d calculations the boring holes of the ten control rods and the seven channels for the small absorber balls are explicitly taken into account using anisotropic streaming coefficients in the remaining voids. All other channels or holes, as e.g. the helium flow channels, the hot gas duct, the three irradiation channels, are neglected. The control rods in the reflector in their withdrawn position (the lower end of the control rods is at the axial position of 114.7 cm) are also considered in the 3-d geometry.

#### 4.2.9.5. Control Rod Worth Calculations

As the diffusion method is generally not valid inside or in the vicinity of strong absorber regions, combined transport-diffusion methods have been developed in order to handle this problem. The basic idea is to model the absorber and its environment by transport

theory, in order to extract some macroscopic data from the transport solution and to use these data in a subsequent 3-d diffusion calculation for the whole core. One of these methods, the "Method of Equivalent Cross Sections", has been developed at the ISR [4-58]. When using this method, both the absorption in and the leakage into the absorber region are the same in diffusion and in the more accurate transport calculation. For this purpose the following steps have to be achieved:

- 1-d unit cell transport calculation for the heterogeneous absorber region using the 1-d integral spectrum code TOTMOS [4-59]. The cylindrical cell model for the control rod region is presented in Figure 4.47. It has to be pointed out that the mesh size in the absorber region and its immediate neighbours is prescribed by the mesh grid in the diffusion calculation.
- Calculation of the equivalent few group macroscopic cross sections and the equivalent diffusion constants by the code RODCIT [4-60].
- 3-d whole core calculation using diffusion theory and the equivalent macroscopic cross section data in the control rod region.

This method of equivalent cross sections is also applied here to the HTR-10 control rods and the equivalent diffusion parameters obtained are used to evaluate the reactivity worth for the whole core.

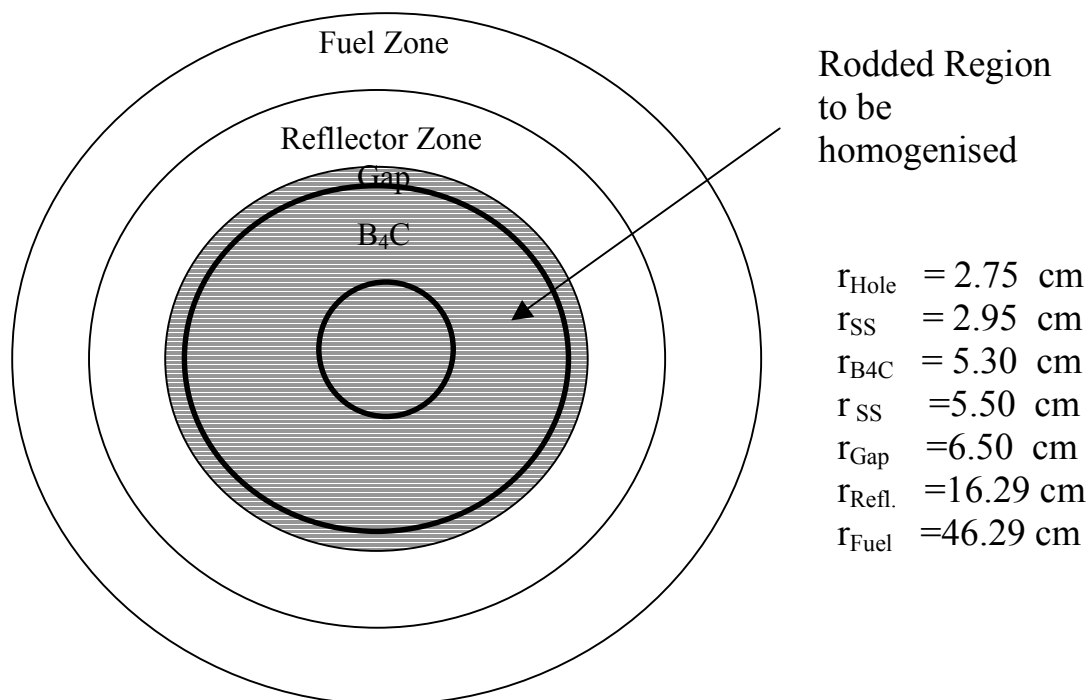


FIG. 4.47. 1-d Cylindrical Model of the CR-Cell for TOTMOS.

#### 4.2.9.6. Computational Results

##### **Benchmark problem B1**

As mentioned above, two series of diffusion calculations are performed for each of the different core loading heights, needed to determine the critical core height:

- one in 2-d geometry considering the empty CR- and KLAKE-channels by homogenised atom densities as given in [4-43],
- and a second one in 3-d geometry taking into account the neutron streaming in the channels of the CR's and KLAKE's and the CR insertion into the side reflector until an axial position of 114.7 cm.

Table 4-60. Diffusion Calculation Results for the Original Benchmark Problem B1

$H_{\text{core}}$ (cm)	$k_{\text{eff}}$ -Values at $T=20^{\circ}\text{C}$		
	2-d geometry	$\Delta k$	3-d geometry
180.12	1.13725	0.0106	1.12665
170.12	1.11870		
160.11	1.09836	0.0106	1.06483
150.10	1.07545		
140.09	1.04919	0.0087	1.01087
130.09	1.01961		
126	1.00639	0.0088	0.99736
120.08	0.98601	0.0089	0.97714
<b><math>H_{\text{crit}}</math> (cm)</b>	<b>124.2</b>		<b>126.8</b>

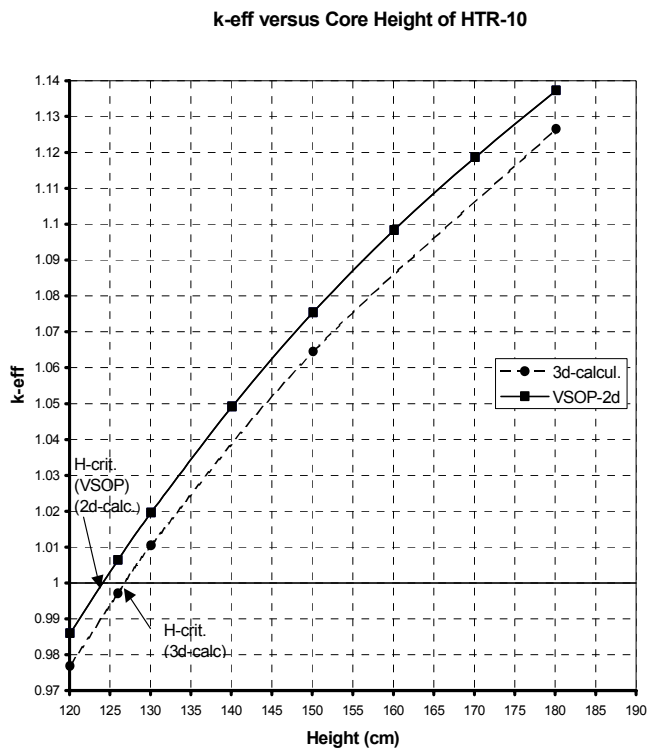


FIG. 4.48.  $k_{\text{eff}}$  versus Core Height of the HTR-10 (Original Benchmark Problem B1).

The results of both series, presented in Table 4-60 and Figure 4.48, differ considerably. The consideration of the large holes with their increased neutron streaming causes a difference in  $k_{\text{eff}}$  of about  $\Delta k \approx 0.01$ . Consequently, the corresponding critical core heights differ about 2.5 cm: when considering the CR-channels by homogenised atom densities in the 2-d diffusion calculation the critical loading height is:  $H_{\text{crit}} = 124.2 \text{ cm}$ , corresponding to 9716 fuel and 7330 dummy balls, but when considering the CR- and KLAK-boring holes explicitly in the 3-d diffusion calculation the critical height amounts to:  $H_{\text{crit}} = 126.8 \text{ cm}$ , corresponding to 9912 fuel and 7477 dummy balls. The latter result is in excellent agreement with the MCNP Monte Carlo result of the INET [4-61].

### ***Benchmark problem B2***

The temperature dependence of the  $k_{\text{eff}}$ -values is also determined with and without taking into account the boring holes of the CR's and KLAK's. The results are presented in Table 4-61. In both series, the difference between multiplication constants at different core temperatures remains constant, but the difference itself is considerably high compared to the INET/14/ results. The reason for this discrepancy could not yet be identified and further calculations will be made in order to clarify this point.

Table 4-61. Diffusion Calculations Results for the Original Benchmark Problem B2

Problem	B21	B22	B23
T (°C)	20	120	250
$k_{\text{eff}}$			
2-d geometry	1.13725	1.12404	1.10693
3-d geometry	1.12665	1.11331	1.09588
$\Delta k$			
2-d geometry		-0.0132	-0.0171
3-d geometry		-0.0133	-0.0174

### ***Benchmark problems B3 and B4***

The calculational results of the control rod worth are obtained by whole core diffusion calculations using the method of equivalent cross sections as described above. To determine the reactivity change associated with the insertion of ten or one control rods, respectively, the CITATION calculations are performed in 3-d geometry on the one hand for the unrodded core (all ten control rods are withdrawn, that means: the lower end is at  $z = 114.7 \text{ cm}$ ) and on the other hand for the rodded core (ten /one control rods are/is fully inserted with the lower end at the axial position of  $z = 389.7 \text{ cm}$ ). The lower and upper end cups of the control rods are not considered in the calculations. The neutron streaming effect in the void areas of the control rod channels is taken into account by anisotropic diffusion constants where  $D_z$  and  $D_r$  are obtained by comparing results of transport and diffusion solutions concerning identical void spaces and adjusting the diffusion constants by the results of the transport calculation.

All results for the control rods at fully loaded core (Benchmark problem B3) and at a core height of 126 cm are summarised in Tables 4-62, 4-63 and 4-64. The differential reactivity worth of one control rod at 126 cm core height (Benchmark Problem B42) is given in Table 4-65 and Figure 4.49. As can be noticed, the bank worth of the ten control rods agrees quite well with the result obtained by the Monte Carlo calculations of the INET [4-61]. It demonstrates that the difference between the two reactivity states is well reproduced by the CITATION calculation and the method of equivalent cross sections. In the case of one control rod, the reactivity worth calculated by this method is overestimated by about 10%, compared to the Monte Carlo result [4-61]. An explanation for this discrepancy could be that the boundary condition used in the rod cell model describes the situation better for the ten control rods than for one single rod.

Table 4-62. Reactivity Worth of One and of Ten Control Rod(s) at Different Core Heights together with the Corresponding  $k_{\text{eff}}$ -Values (Original Benchmark Problems B3 and B4)

Loading Height of the Core (cm)	Nr. of Fully Inserted Control Rods	$k_{\text{eff}}$ 10 Control Rods withdrawn	$k_{\text{eff}}$ Fully Inserted Control Rods	Worth ( $\Delta k/k\%$ )
180	10	1.1266	0.9490	16.60
	1		1.1071	1.56
126	10	0.9974	0.8277	20.5
	1		0.9782	1.97

Table 4-63. Reactivity Worth of the Control Rods at Full Core (Original Benchmark Problem B3)

Problem	B31 $\rho[\% \Delta k/k]$ 10 rods inserted, 20 <sup>0</sup> C	B32 $\rho[\% \Delta k/k]$ 1 rod inserted, 20 <sup>0</sup> C
VSOP-CITATION 3d-calculation	16.60 %	1.563 %

Table 4-64. Reactivity Worth of the Control Rods at 126 cm Core Height (Original Benchmark Problem B4)

Problem	B41 $\rho[\% \Delta k/k]$ 10 rods inserted, 20 <sup>0</sup> C	Integral Rod Worth $\rho[\% \Delta k/k]$ 1 rod inserted, 20 <sup>0</sup> C
VSOP-CITATION 3d-calculation	20.55 %	1.969 %

Table 4-65. Differential Worth of One Control Rod at 126 cm Core Height  
(Original Benchmark Problem B42)

Axial Position (cm)	Rod Worth $\rho$ [% $\Delta k/k$ ]
230.32	0.4207
279.02	0.9424
282.62	0.9976
331.32	1.679
334.92	1.716
383.62	1.968
394.20	1.969

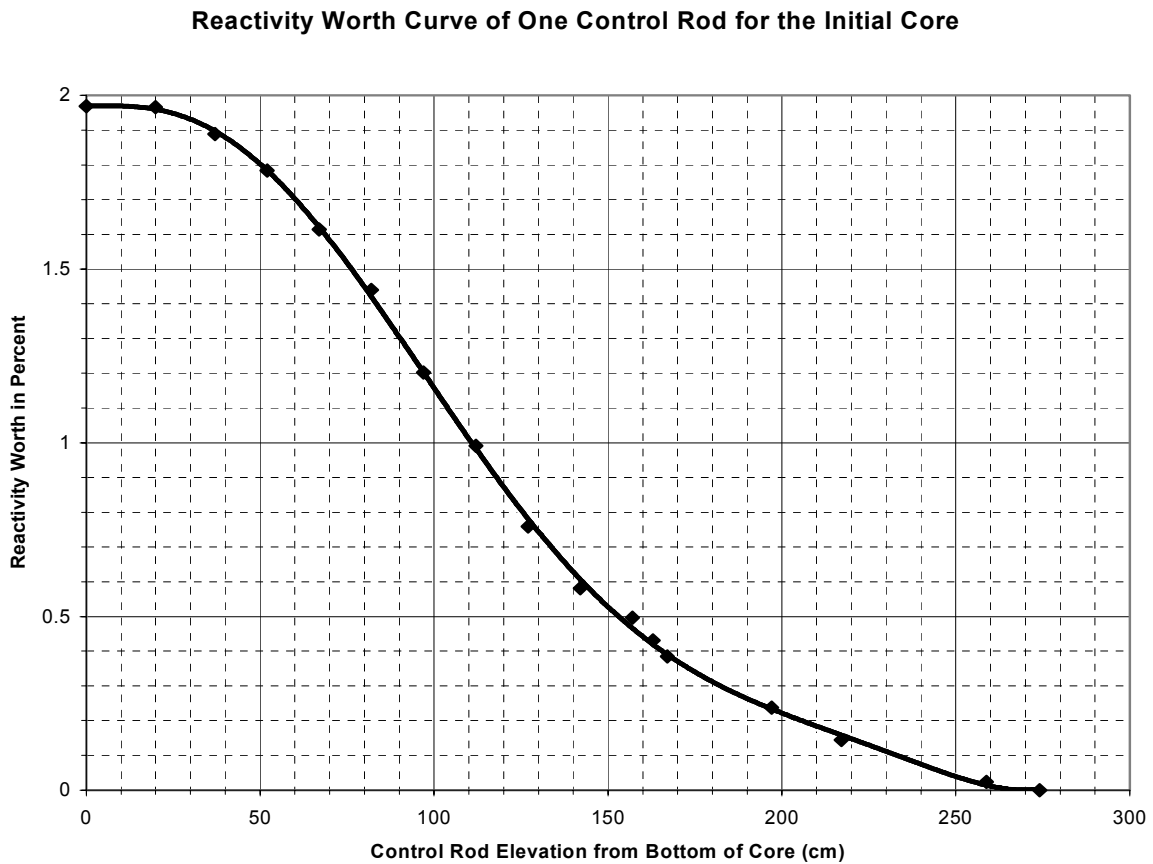


FIG. 4.49. Reactivity Worth Curve of One Control Rod (S1) for the HTR-10 Initial Core  
(Original Benchmark Problem B42).

#### 4.2.9.7. Calculational Results for the Deviated Benchmark Problems

It turns out that the HTR-10 got critical with 16890 pebbles in the core, 9627 fuel pebbles and 7263 moderator pebbles, under air condition and being loaded with another kind of moderator pebbles than defined in the original benchmark description. The core temperature was 15<sup>0</sup> C and the critical core height was: **H<sub>crit.</sub> =123.06 cm**. Compared to the description of the original benchmark problems three conditions have been changed:

- Density of dummy balls: 1.73→1.84 g/cm<sup>3</sup>
- B<sub>imp</sub> in dummy balls: 1.3→0.125 ppm
- Core atmosphere at initial criticality: helium→humid air

When considering these revised data in the unit cell calculations and in the whole core diffusion calculations the first criticality is determined to:

- in the case of the 2-d diffusion calculations: **H<sub>crit.</sub> = 121.0 cm**,
- in the case of the 3-d diffusion calculations: **H<sub>crit.</sub> = 123.3 cm**.

The latter result is in excellent agreement with the experiment. All results for the deviated benchmark problems are summarised in Table 4-66. The differential reactivity worth of one control rod at a core loading height of 126 cm is given in Table 4-67. Similar tendencies as observed in the results for the original benchmark problems, e.g. strong temperature dependence of the multiplication constants, a quite good agreement with the Monte Carlo results of the INET concerning the bank worth of the ten control rods, and a relatively high reactivity worth of one control rod, can be noticed also in the results for the deviated benchmark problems.

Table 4-66. All Calculational Results for the Deviated Benchmark Problems of the HTR-10 Initial Core

Benchmark Problem		Deviated Benchmark	
		VSOP in 2-d r,z Geometry	VSOP in 3-d r,φ,z Geometry
B1		121.0 cm	123.3 cm
B2	B21	1.1468	1.1368
	B22	1.1334	1.1232
	B23	1.1160	1.1054
B3	B31		15.73%
	B32		1.48%
B4	B41		19.31%
	B42		1.86%

Table 4-67. Differential Worth of One Control Rod at 126 cm Core Height (Deviated Benchmark Problem B42)

Axial Position (cm)	230.32	279.02	282.62	331.32	334.92	383.62	394.20
Rod Worth ρ[%Δk/k]	0.4355	0.9703	1.017	1.736	1.762	1.852	1.865

Table 4-68. All Computational Results for the Original Benchmark Problems of the HTR-10 Initial Core

Benchmark Problem		Original Benchmark	
		VSOP in 2-d r,z Geometry	VSOP in 3-d r, $\phi$ ,z Geometry
B1		124.2 cm	126.8 cm
B2	B21	1.1373	1.1266
	B22	1.1240	1.1133
	B23	1.1069	1.0959
B3	B31		16.60%
	B32		1.56%
B4	B41		20.55%
	B42		1.97%

#### 4.2.9.8. Conclusion

The calculational results of the original and the deviated benchmark problems are summarised in Tables 4-68 and 4-66, respectively. It can be noticed that there is a discrepancy of about 1% between the 2-d VSOP and the 3-d VSOP calculations considering the neutron streaming in the channels of the control rods and small absorber balls explicitly. It has to be pointed out that there is an excellent agreement between the 3-d diffusion calculation and the experiment concerning the critical core height. Furthermore, the strong temperature dependence of the effective multiplication constant is remarkable, and this effect has to be investigated in further calculations. Moreover, it turns out that the bank worth of the ten control rods is in good agreement with Monte Carlo results, whereas the reactivity worth of one control rod overestimates the corresponding value obtained by the Monte Carlo code MCNP. The reason for this difference has to be investigated furthermore.

### ACKNOWLEDGEMENT

The authors would like to thank Dr. W. Scherer and Mr. K.A. Haas for very useful discussions and comments.

## 4.2.10. South Africa [4-65]

### 4.2.10.1. Introduction

In the first section an overview is presented of the calculated equilibrium cycle based on the materials data specification as supplied in [4-62]. The normal parameters as calculated with the VSOP-PBMR design codes [4-63] will be presented and could be considered as basis for comparison of a design review.

The following benchmark problems have been calculated in the subsequent sections:

1. B1 - Loading to first criticality in air – neglecting the humidity;
2. B2 – Effective reactivity worths,  $k_{eff}$ , at different temperatures – in helium.

Even though most calculations had been performed with diffusion-based design suites of codes in use at the PBMR it should be mentioned that some transport theory was applied in deriving energy-dependant diffusion coefficients for simulating the reactivity worths of the control rods. Here the so-called, method of equivalent cross-sections (MECS) developed at FZJ [4-58] was applied.

### 4.2.10.2. Modeling of the Reactor

The most important design parameters are listed in Table 4-69.

Table 4-69. Design Parameters of the HTR-10 Experimental Reactor

Reactor thermal power	MW	10
Primary helium pressure	Mpa	3.0
Reactor core diameter	cm	180
Average core height	cm	197
Average helium temperature at reactor outlet	°C	700
Average helium temperature at reactor inlet	°C	250
Helium mass flow rate at full power	kg/s	4.3
Number of control rods in side reflector		10
Number of absorber ball units in side reflector		7
Nuclear fuel		UO <sub>2</sub>
Heavy metal loading per fuel element	g	5
Enrichment of fresh fuel element	%	17
Number of fuel elements in equilibrium core		27,000
Fuel loading mode		5 x multi-pass

### **Resonance integral**

The code ZUT-DGL [4-51], was used to analyse the effect of fuel burn-up and associated change in the atom densities on the resonance integral for the following material groups:

- (1) <sup>238</sup>U;
- (2) The other heavy metals (<sup>235</sup>U and Pu isotopes);
- (3) Fission products.

The resonance integral was influenced by the changes in these groups due to burn-up as follows:

- (1) During the course of the burn-up from 0 → 80 000 MWd/t<sub>HM</sub> the atom density of <sup>238</sup>U is reduced by 2.51 %. The resonance integral will therefore change correspondingly.
- (2) In a separate parametric investigation the <sup>235</sup>U was completely removed. The resultant influence of the resonance integral was found to be smaller by two orders of magnitude in comparison to the change of <sup>238</sup>U concentration. This is comparable to the effect of a small temperature change of ~1°C. Since the scattering properties of the emerging Pu isotopes are similar to that of the <sup>235</sup>U, it could be inferred that all these heavy metals be neglected.
- (3) At elevated burn-up the number density of the sum of all fission products was found to be of the order of 10 % of that of the oxygen contained in the UO<sub>2</sub>. Its moderating effect was low, since the atomic weights were higher than that of the oxygen. Upon investigation of the effect of a 10 % increase of the oxygen atom density it could be concluded that the impact of fission products on the resonance integral was even overestimated.

Once again the change of the resonance integral was lower by about two orders of magnitude compared to the changing <sup>238</sup>U, which therefore also justifies ignoring the influence of the fission products.

Due to the above results it was decided to investigate an average enrichment of 18%, since the <sup>238</sup>U on average was somewhat depleted. Pu was modeled as a fission product and its effect on  $k_{eff}$  found to be in the order of 0.3 Niles.

### ***Fuel element design***

The code, DATA2 [4-64], was used to model the double heterogeneous pebble fuel design.

### ***Reactor geometry***

The geometric modeler in 2-D, BIRGIT, part of VSOP, was used to model the R-Z core geometry, including the pebble flow lines. Furthermore, the many reflector regions had been included and designated according to the documentation provided by INET, Tsinghua University [4-62].

### ***Main models***

The reactor materials and spectral regions were calculated in 4 energy groups with the VSOP code by means of a diffusion approach. Spectral temperatures were iteratively updated for the equilibrium layout by means of the THERMIX code, included in VSOP. The reactor description and material characteristics were extracted from reference document [4-62] by Jing and Sun. Intermediate restart files were saved to provide initial conditions for follow-up case studies to be performed, such as the depressurized loss of forced cooling (DLOFC) event.

### Fuel element life history

The code LIFE, which is a part of VSOP was used for evaluating the decay heat produced in the reactor. This is important in the analysis of the DLOFC upset event used as design base accident.

#### 4.2.10.3. Calculated Results for the Equilibrium Cycle

In Figure 4.50 a depiction is provided of the HTR-10 calculational model. A five-channel pebble flow model is introduced.

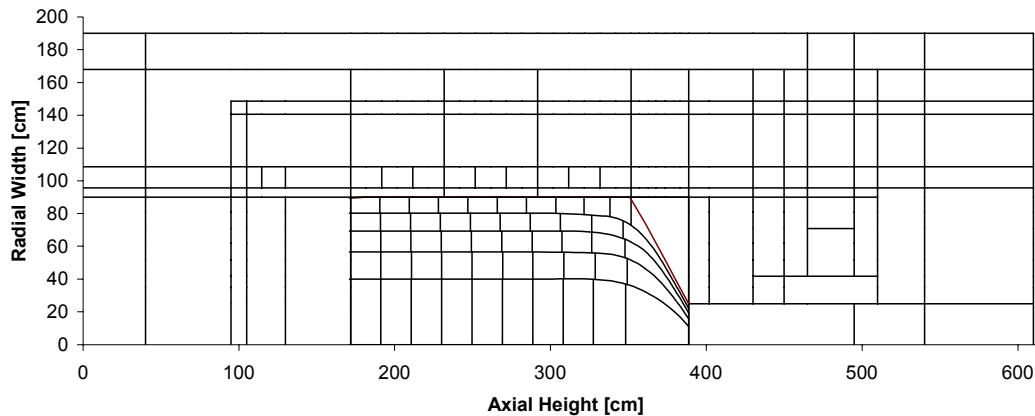


FIG. 4.50. VSOP Model for the HTR-10 in 2-D.

In Figure 4.51 the temperature-dependent resonance integral is depicted for a heavy metal loading of 5 g per fuel sphere. The design enrichment in  $^{235}\text{U}$  of 17% thus implies about 0.85 g of  $^{235}\text{U}$  per fuel sphere, which is perfectly in line with the German fuel fabrication technology, which was always below 1 g of  $^{235}\text{U}$  per fuel sphere.

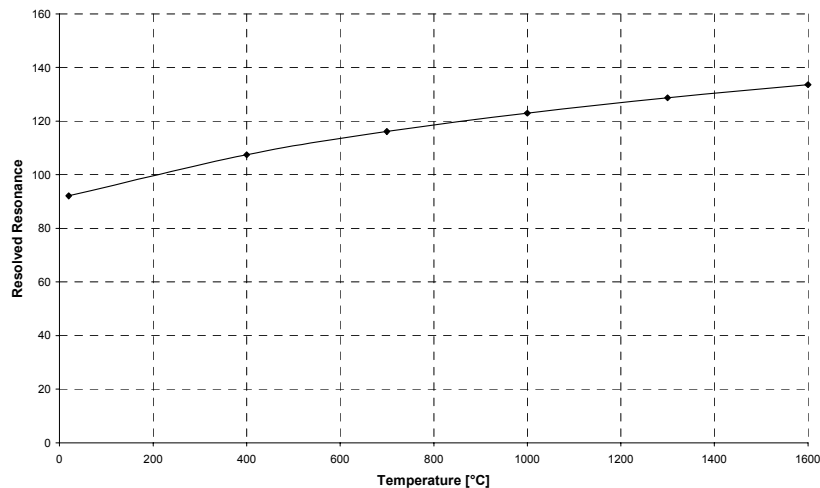


FIG. 4.51. Temperature-dependent resonance integral for 5g<sub>MH</sub>/FS and 18% enrichment.

In Figure 4.52 the radial power distribution is provided based on the integral channel power.

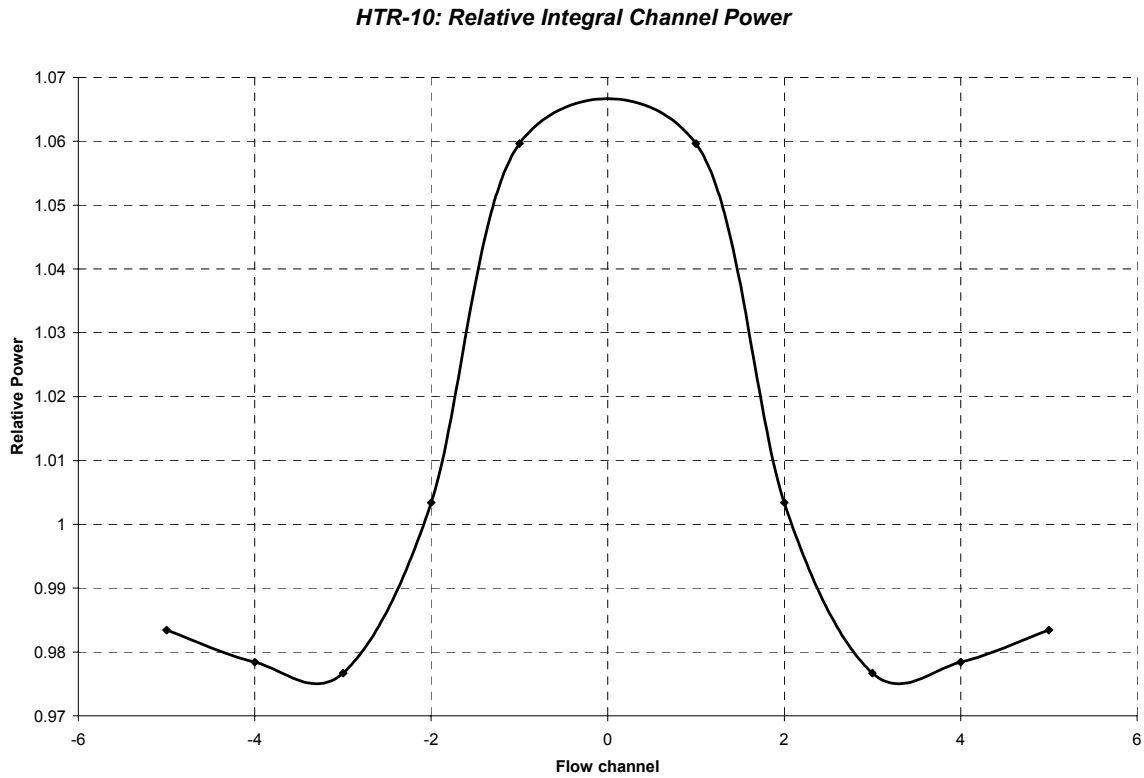


FIG. 4.52. Integral radial power distribution over the pebble flow channels.

Table 4.70 provides a summary of the neutron balance. Here it is seen that the energy down-scattering is depicted within the 4 broad energy groups, i.e. one thermal, two epi-thermal, and a fast group. The high neutron leakage of 31.7% must be observed, which is characteristic of a small reactor design due to the surface to volume ratio of the core.

Table 4.70. Neutron balance per one lost neutron

GROUP	ABSORPTION	SCATTERING	SOURCE	LEAKAGE
1	3.4061E-03	7.3025E-01	9.8439E-01	2.5074E-01
2	5.6363E-02	5.4537E-01	7.4586E-01	1.4413E-01
3	8.1015E-02	4.5541E-01	5.4537E-01	8.9400E-03
4	5.4195E-01	0.0000E+00	4.5541E-01	-8.6535E-02
TOTAL	6.8273E-01			3.1727E-01

An overview is provided in Table 4.71 of the calculated plant performance data.

Table 4.71: Performance Data

GLOBAL DATA:			
K-EFF			1.0001
FISSIONS/ENERGY	E+10 (FISS/WS)		3.070
POWER PEAKING MAX./AVG.			1.46
MAX. POWER PER BALL	KW/BALL		0.54
AVG. FUEL RESIDENCE TIME	DAYS		1080.2
AVG. BURNUP	MWD/T		80000.6
CONVERSION RATIO			0.226
FAST DOSIS SPENT FUEL ELEM.	E+21/CM2		1.21
NEUTRON DOSIS:			
FAST NEUTRON EXPOSURE (>0.1 MEV)			
MAX. UPPER EDGE	E+21/(CM2*360D)		0.13
MAX. LOWER EDGE	E+21/(CM2*360D)		0.21
MAX. OUTER EDGE	E+21/(CM2*360D)		0.26
NEUTRON BALANCE:			
FRACTIONAL FISSIONS OF			
U -235	%		85.59
U -236	%		0.01
U -238	%		0.19
PU-239	%		12.71
PU-241	%		1.49
NEUTRON LOSSES IN HEAVY METALS			
ESP. IN FISSION ISOTOPES	%		62.08
ESP. IN U -235	%		50.32
ESP. IN U -236	%		42.54
ESP. IN U -238	%		0.28
ESP. IN U -238	%		10.02
ESP. IN PU-239	%		7.09
ESP. IN PU-240	%		1.41
ESP. IN PU-241	%		0.68
ESP. IN PU-242	%		0.01
ESP. IN NP-237	%		0.04
IN FISSION PRODUCTS	%		4.22
ESP. IN XE-135	%		1.61
CORE-LEAKAGE	%		31.62
FUEL INVENTORY (KG/GW(TH)) :			
U -235			1563.92
PU-239			59.23
PU-241			7.34
U -238			11135.64
U -236			113.61
NP-239			0.88
PU-240			17.71
PU-242			1.22
NP-237			2.47
HEAVY METAL			12902.01

FUEL SUPPLY - DISCHARGE (KG/GWD(TH)) :		
U -235		2.0641 - 0.9662
PU-239		0.0000 - 0.0749
PU-241		0.0000 - 0.0173
U -238		10.4386 - 10.1768
U -236		0.0000 - 0.1849
PU-240		0.0000 - 0.0332
PU-242		0.0000 - 0.0044

U308 REQUIREMENT	KG/GWD(T)	531.2
SEPARATIVE WORK	KG SWU/GWD(T)	412.5

ECONOMY :		
FISSILE AND FERTILE MATERIAL	MILL/KWHE	9.474
FABRICATION, REPROCESSING	MILL/KWHE	1.575
FUEL CYCLE COSTS	MILL/KWHE	11.049

The maximum fuel temperature during operation was observed at 864 °C with the maximum power rating per fuel sphere at 0.54 kW.

An overview is provided in Figure 4.53 of the DLOFC temperature distribution evolved over 120 hours. It is clearly demonstrated that fuel temperatures remain well within safe limits if it is assumed that the control rods are inserted. The case where the control rods remain outside, i.e. stuck in position or even stepping out remains to be analyzed.

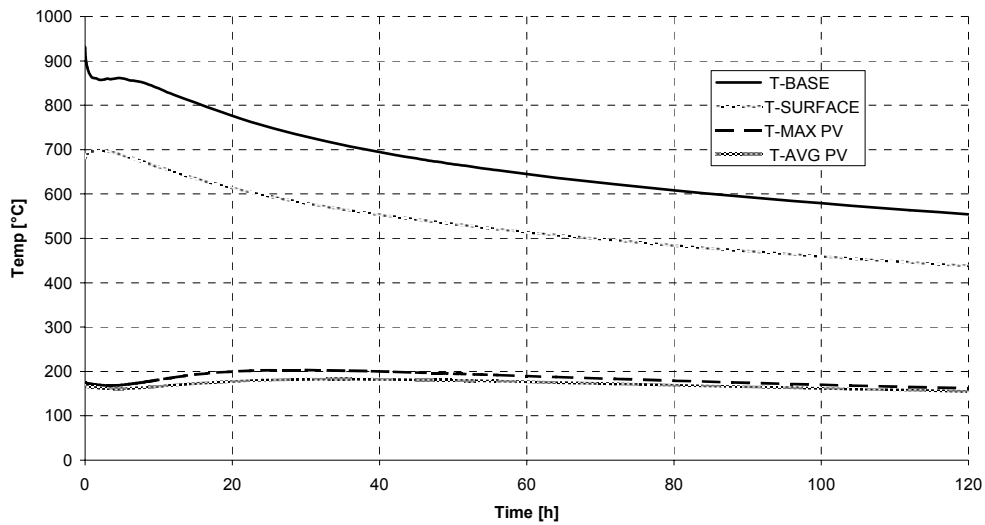


FIG. 4.53. Fuel and RPV temperature distribution following DLOFC.

In Figure 4.54 a depiction is presented of the reactivity distribution *versus* the relative xenon absorption. It should be noted that at the point where the core becomes re-critical the xenon concentration appears to be rather high still. This means that a high temperature contribution is to be expected.

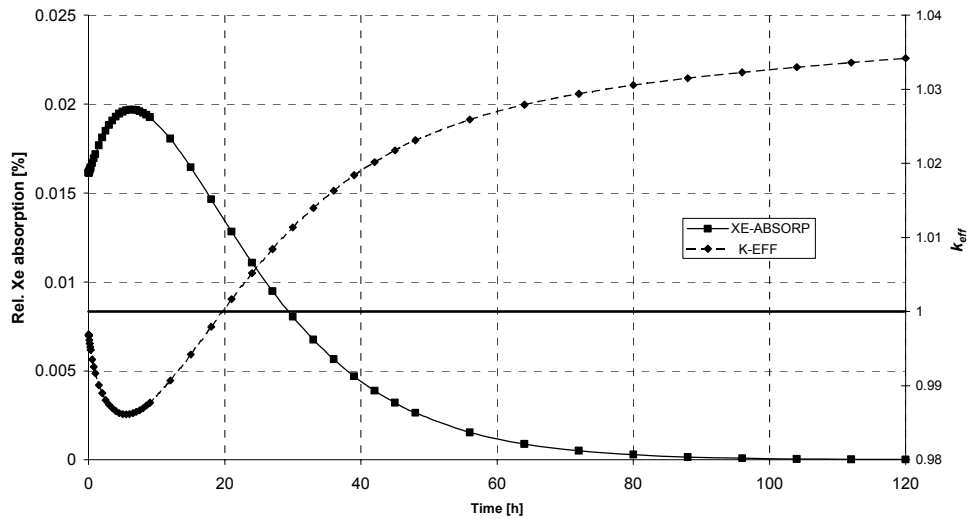


FIG. 4.54. Xenon absorption versus  $k_{eff}$ .

#### 4.2.10.4. Benchmark Problems

For purposes of the benchmark calculations a finer pebble mesh/flow division had been prepared, i.e. a 3 times increase in axial direction sub-division. A depiction of the calculational model is provided in Figure 4.55.

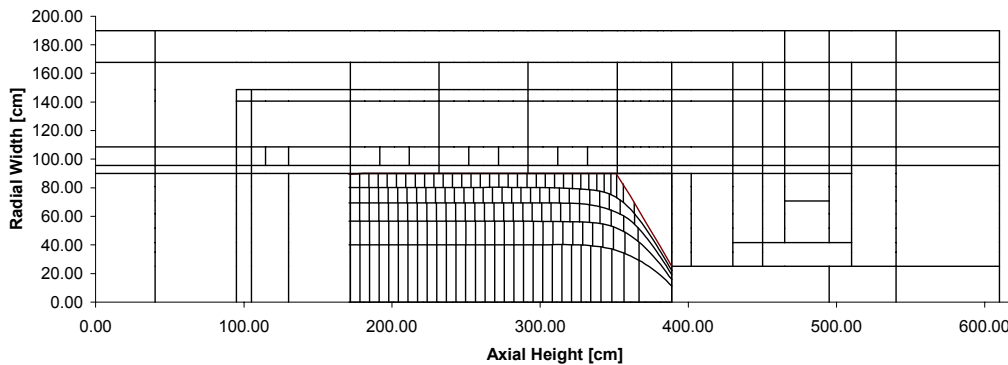


FIG. 4.55. HTR-10 loading to 1<sup>st</sup> criticality.

The following assumptions for the loading to 1<sup>st</sup> criticality calculations were:

1. As defined in [4-62], but with the following deviations included,
  - Density of graphite spheres: 1.84 g/cm<sup>3</sup>;
  - Boron equivalent of impurities in graphite spheres: 0.125 ppm;
  - Core atmosphere during initial criticality: air with oxygen and nitrogen compositions of 23.14% and 75.53%, respectively.

2. The density of air assumed to be  $1.149\text{E-}3 \text{ g/cm}^3$ .
3. A pebble packing fraction of 61% is assumed.
4. The influence of humidity in the air was neglected.

**Problem B1**

Initial criticality calculations were performed with VSOP-PBMR. The results are presented in Table 4.72.

Table 4.72. HTR-10 Initial Criticality in Non-humid Air Atmosphere

Loading height (cm)	Number of fuel spheres	Number of graphite spheres	$K_{eff}$ (27 °C)
124.80	9764	7366	1.00731
118.30	9255	6982	0.98631

Linear interpolation of the calculated values, yield the critical loading height of 122.537 cm, or a corresponding loading of 16819 spheres in total.

**Problem B2**

Initial criticality calculations were performed with VSOP-PBMR for a core in helium atmosphere. For a core with cylindrical height of 180.117 cm the calculated results are presented in Table 4.73.

Table 4.73. VSOP-PBMR Full-core Criticality in Helium Atmosphere

	$K_{eff}$ (27 °C)	$K_{eff}$ (120 °C)	$K_{eff}$ (250 °C)
VSOP-PBMR	1.12861	1.11956	1.10469

*4.2.10.5. Discussion and Suggestions*

The nuclear data used in VSOP is based on JEF-1 and ENDF/B-IV and –V data. Fission yield from ENDF/B-IV and –V are used. Furthermore, due to some historical reasons the absorption cross-section in VSOP is given as 3.88 mb.

An input possibility had been introduced into VSOP to allow the 2200-absorption cross-section for carbon to be multiplied by 0.87628866 to yield 3.40 mb. With impurities known one could then calculate the correct absorption rate.

## REFERENCES TO CHAPTER 4

- [4.1.] JING, X., SUN, Y., “Evaluation of High Temperature Gas Cooled Reactor Performance”, INET, Tsinghua University, Beijing, March 2000.
- [4.2.] INTERNATIONAL ATOMIC ENERGY AGENCY, “Current Status and Future Development of Modular High Temperature Gas Cooled Reactor Technology”, IAEA-TECDOC-1198, Vienna, February 2001.
- [4.3.] SUN, Y., XU, Y., “Relevant Safety Issues in Designing the HTR-10 Reactor”, Safety Related Design and Economic Aspects of HTGRs, IAEA-TECDOC-1210 Vienna, April 2001.
- [4.4.] ZHONG, D., QIN, Z., “Overview of the 10MW High Temperature Gas-Cooled Reactor Test Module”, (Proc. Seminar on HTGR Application and Development), INET, Tsinghua University, Beijing, March 2001.
- [4.5.] ZHONG, D., XU, Y., “Progress of the HTR-10 Project”, Design and Development of Gas Cooled Reactors with Closed Cycle Gas Turbines”, IAEA-TECDOC-899, Vienna, August 1996
- [4.6.] TANG, C., ZHU, J., QUI, X., XU, Z., ZHANG, C., NI, X., “Fabrication of the First Loading Fuel of 10 MW High Temperature Gas cooled Reactor-Test Module-HTR-10”, (Proceedings of the Seminar on HTGR Application and Development), INET, Tsinghua University, Beijing, March 2001.
- [4.7.] INSTITUTE OF NUCLEAR ENERGY TECHNOLOGY, “Contribution from INET on HTR-10 Core Physics Benchmark” (Presented at Second RCM of CRP on Evaluation of HTGR Performance, Beijing, 2001), INET, Tsinghua University, Beijing, 2001
- [4.8.] XU, Y., “China’s HTGR Programme”, INET, (Proc. 15<sup>th</sup> Meeting of the International Working Group on Gas Cooled Reactors, held at Risley, U.K., 1999), IAEA, Vienna, 1999.
- [4.9.] YAMASHITA, K., et.al., “Nuclear Design of the High-Temperature Engineering Test Reactor (HTTR)”, Nucl. Sci. Eng. 122, pp. 212-228, 1996.
- [4.10.] SHINDO, R., YAMASHITA, K., MURATA, I., “DELIGHT-7; One-Dimensional Fuel Cell Burnup Analysis Code for Height Temperature Gas-Cooled Reactor (HTGR)”, JAERI-M 90-048, Japan, 1990
- [4.11.] LATHROP, K.D., BRINKLEY, F.W., “TWOTRAN-II: An Interfaced, Exportable Version of the TWOTRAN Code for Two-Dimensional Transport,” LA-4848-MS, Los Alamos, USA, 1973.
- [4.12.] HARADA, H., YAMASHITA, K., “The Reactor Core Analysis Code CITATION-1000VP for High Temperature Engineering Test Reactor,” JAERI-M 89-135, Japan, 1989.
- [4.13.] JING, X., SUN, Y., “Benchmark Problem of HTR-10 Initial Core”, Draft Version, INET, Tsinghua University, Beijing, 1998.
- [4.14.] GERWIN, H., SCHERER, W., “Treatment of Upper Cavity in a Pebble-Bed High Temperature Gas-Cooled Reactor by Diffusion Theory,” Nucl. Sci. Eng., 97, pp. 9-19, 1987.
- [4.15.] AZIZ, F., LASMAN, A. N., “Analysis of Benchmark Calculation on HTR-10 Core First Criticality”, National Nuclear Energy Agency of Indonesia, BATAN, Indonesia, 2000.
- [4.16.] OKUMURA, K., et al, “SRAC95: The Comprehensive Neutronics Calculation Code System”, JAERI, Japan, 1995

- [4.17.] FUJIMOTO, N., AZIZ, F. NOJIRI, N., YAMASHITA, K., "JAERI's Benchmark Calculation Results of HTR-10", JAERI, (Proc. Third RCM for the CRP on Evaluation of HTGR Performance, held at Oarai, Japan, March 2001), IAEA, Vienna, 2001, (CD-ROM).
- [4.18.] FUJIMOTO, N., AZIZ, F. NOJIRI, N., YAMASHITA, K., "JAERI's Benchmark Calculation Results of HTR-10 –Revised Calculation", JAERI, Oarai, Japan, December 2001.
- [4.19.] LIEBEROTH, J. and STOJADINOVIC, A, "Neutron streaming in pebble bed", Nuclear Science and Engineering 76, pp. 336-344, 1980.
- [4.20.] GERWIN, H. and SCHERER, W., "Treatment of the upper cavity in a pebble-bed High-Temperature Gas-cooled Reactor by diffusion theory", Nuclear Science and Engineering 97, pp. 9-19, 1987.
- [4.21.] JING, X., SUN, Y., "Benchmark Problem of the HTR-10 Initial Core," INET, Tsinghua University, Beijing, China, December, 1998
- [4.22.] OPPE, J., De HAAS, J.B.M. and KUIJPER, J.C., "PANTHERMIX-THERMIX Interaction" Technical Report ECN-I-96-022, Netherlands Energy Research Foundation (ECN), Petten, Netherlands, May 1996.
- [4.23.] MITENKOVA E.F., NOVIKOV N.V., (IBRAE), SUKHAREV YU.P.,(OKBM), "Study of neutron physical performance of HTGR pebble bed core by Monte-Carlo method," A.Э., v.77, iss.3, Russia, September, 1994.
- [4.24.] KUZAVKOV, N., MAROVA, E., SUKHAREV, YU.P., (OKBM), MITENKOVA, E., NOVIKOV, N., (IBRAE), "Benchmark Problems of HTTR and HTR-10 Core Physics (Phase 2)," (Proc. Second RCM of CRP on Evaluation of HTGR Performance, held at Beijing, 1999), IAEA, Vienna, 1999
- [4.25.] HUTT, P.K., "Overview Functional Specification of PANTHER: A Comprehensive Thermal Reactor Code for Use in Design, Assessment and Operation," Technical Report PANTHER/FSPEC/OVERVIEW 2.0, Nuclear Electric Plc., UK, December 1992.
- [4.26.] STRUTH, S., "THERMIX-DIREKT: A programme code for unsteady 2d simulation of thermohydraulic transients," Forschungszentrum Juelich GmbH, Germany, September 1995, (in German).
- [4.27.] AEA TECHNOLOGY, "The ANSWERS Software Package WIMS. (A WIMS Modular Scheme for Neutronics Calculations)", User Guide ANSWERS/WIMS. Atomic Energy Agency Technology (AEA), Winfrith, UK, 1997.
- [4.28.] BENDE, E.E., HOGENBIRK, A.H., KLOOSTERMAN, J.L. and VAN DAM, H., "Analytical Calculation of the Average Dancoff-factor for a Fuel Kernel in a Pebble-Bed High Temperature Reactor," Nuclear Science and Engineering, 133: pp. 147-162, October 1999.
- [4.29.] ZEHNER, P. and SCHLUDER, E.U., "Impact of heat radiation and pressure on the heat-transfer in particle beds without gas", Chemie-Ing.-Technik, 44:1303, 1972, (in German).
- [4.30.] LEBENHAFT, J.R., and DRISCOLL, M.J., "Physics Benchmark Analysis of the HTR-10 Reactor using the Monte-Carlo Code MCNP", Excerpts from MIT-ANP-TR-070, Cambridge, Massachusetts, USA, March 2000.
- [4.31.] LEBENHAFT, J.R., and DRISCOLL, M.J., "MCNP4B Analysis of the HTR-10 Startup Core", (Proc. 2001 ANS Annual Meeting), MIT, Cambridge, Massachusetts, USA, October 2001.
- [4.32.] BRIESMEISTER, J.F. (Ed.), "MCNP—A General Monte Carlo N-Particle Transport Code, Version 4B," Los Alamos National Laboratory, LA-12625-M, USA, March 1997.

- [4.33.] JERAJ, R. *et al.*, "Monte Carlo Simulation of the TRIGA Mark II Benchmark Experiment", Nuclear Technology 120, pp. 179, 1997.
- [4.34.] CUMBERLAND, D.J. and CRAWFORD, R.J., "The Packing of Particles," Elsevier, Amsterdam, 1987.
- [4.35.] MURATA, I. *et al.*, "New Sampling Method in Continuous Energy Monte Carlo Calculation for Pebble Bed Reactors," J. of Nuclear Science and Technology, 34(8), pp. 734-744, August 1997.
- [4.36.] PARRINGTON, J.R. *et al.*, "Nuclides and Isotopes," Fifteenth Edition, General Electric Co. and KAPL Inc., USA, 1996.
- [4.37.] MACFARLANE, R.E. and MUIR, D.W., "The NJOY Nuclear Data Processing System", Los Alamos National Lab., LA-12740, USA, 1994.
- [4.38.] SUN, Y., Institute of Nuclear Energy Technology, Private communication, Beijing, China, June 24, 1999.
- [4.39.] TEUCHERT, E. *et al.*, "V.S.O.P. ('94): Computer Code System for Reactor Physics and Fuel Cycle Simulation—Input Manual and Comments," Forschungszentrum Jülich, Jül-2897, April 1994.
- [4.40.] ASKEW, J.R. *et al.*, "A General Description of the Lattice Code WIMS," Journal of British Nuclear Society, 5, pp. 564, 1966.
- [4.41.] MATHEWS, D. and CHAWLA, R., "LEU-HTR PROTEUS Computational Benchmark Specifications," Paul Scherrer Institute, TM-41-90-32, Switzerland, October 1990.
- [4.42.] MURATA, I. and TAKAHASHI, A., "Analysis of Critical Assembly Experiments by Continuous Energy Monte Carlo Method with Statistical Geometry Model," Technology Reports of the Osaka University, 48(2304), pp. 19-31, April 1998.
- [4.43.] JING, X. and SUN, Y., "Benchmark Problem of the HTR-10 Initial Core", INET, (Proc. Third RCM of CRP on Evaluation of HTGR Performance, held at Oarai, March 2000), IAEA, Vienna, 2000, (CD-ROM).
- [4.44.] JORDAN, W.C. and BOWMAN, S. M., "SCALE Cross Section Libraries," ORNL/NUREG/CSD-2/V3/R6, Oak Ridge, USA, 1998.
- [4.45.] SEN, S., SIKIK, U. E., DUKMEN, H., CECEN, Y., KADIROGLU, O. K., COLAK, U., "HTR-10 CORE PHYSICS BENCHMARK PROBLEM RESULTS", Hacettepe University Nuclear Engineering Department, Ankara , Turkey, 2001
- [4.46.] SANCHEZ, R., HEBERT, A., STANKOVSKI, Z., COSTE, M., LOUBIERE, S., VAN DER GUCHT, C. and ZMIJAREVIC, I., "APOLLO2 Twelve Years Later", Mathematics and Computation, Reactor Physics and Environmental Analysis in Nuclear Applications, Madrid, September, 1999
- [4.47.] BOTH, J.P., PENELIAU, Y., "The Monte Carlo code TRIPOLI4 and its first benchmark interpretations ", International Conference PHYSOR 96, Mito, Ibaraki, Japan, September, 1996
- [4.48.] INTERNATIONAL ATOMIC ENERGY AGENCY, "Evaluation of High Temperature Gas Cooled Reactor Performance – Part 1: Benchmark Analyses related to initial testing of the HTR and HTR-10 ", Initial Draft, IAEA TECDOC-TBD, Vienna, 2001.
- [4.49.] OHLIG, U. and BROCKMANN, H., "Calculational Results for the Benchmark Problems of the HTR-10 Initial Core", ISR, Juelich, Germany, September 15, 2002.
- [4.50.] RUTTEN, H. J., *et. al.*, "VSOP (99) Computer Code System for Reactor Physics and Fuel Cycle Simulation, Jul-3820, October 2000.
- [4.51.] TEUCHERT, E. and HAAS, K.A., "ZUT-DGL-V.S.O.P.: A computer code system for resonance absorption calculations in heterogeneous configurations," FZ-Juelich, IRE-70-1. 1970, (in German).
- [4.52.] JOANOU, C.D. and DUDEK, J.S., "GAM-A Consistent P<sub>1</sub> Multigroup Code for the Calculation of Fast Neutron Spectra and Multigroup Constants," GA-1850, 1961.

- [4.53.] HONEK, H.C., „THERMOS-A Thermalization Transport Theory Code for Reactor Lattice Calculations“, BNL-5826, USA, 1961.
- [4.54.] FOWLER, T.B., et. al., „Nuclear Reactor Core Analysis Code: CITATION“, ORNL-TM-2496, Rev.2, Oak Ridge, USA, July 1971.
- [4.55.] ROWLANDS, J. And TUBBS, N., „The joint evaluated file: A new data resource for reactor calculations“, (Proc. Int. Conf. On Nuclear Data for Basic and Applied Science, Santa Fe), JEF-1 Nuclear Data Library, Edited 1985.
- [4.56.] BROCKMANN. H. and OHLIG, U., „Generation of a 68 group cross section library in the GAM-I format and of a 96 group cross section library in the THERMALIZATION format,“ FZ-Jülich, Germany, KFA-IRE-IB-3/89, 1989, (in German).
- [4.57.] LIEBEROTH, J. and STOJADINOVIC, A., „Neutron Streaming in Pebble Beds, „ Nuc. Sci. Eng. 76, pp. 336-344, 1980.
- [4.58.] SCHERER. W. and NEEF, H.J., „Determination of Equivalent Cross Sections for Representation of Control Rod Regions in Diffusion Calculations“, Jül-1311, Germany, 1976.
- [4.59.] BROCKMANN, H., „TOTMOS: An Integral Transport Code for Spectrum Calculations“, FZ-Jülich, Germany, ISR, 1995.
- [4.60.] SCHERER, W., „Modelling of absorber rods in pebble bed reactors“, KFA- IRE-IB-21/80, Germany, 1980, (in German).
- [4.61.] YING, X. and SUN, Y., „Benchmark Problems of the HTR-10 Initial Core“, INET, (Proc. Third RCM of CRP on Evaluation of HTGR Performance, Oarai, Japan, 16-19 March 2001), IAEA, Vienna, 2001, (CD-ROM).
- [4.62.] XINGQING, J. and SUN, Y., „Contribution from INET on HTR-10 Core Physics Benchmark“, INET, Tsinghua University, Beijing, 2001.
- [4.63.] MULDER, E.J. and TEUCHERT, E., „VSOP-PBMR – Computer Code System for Reactor Physics and Fuel Cycle Simulation“, PBMR-009894-328/A, PBMR (Pty) Ltd. Centurion, South Africa, August 2001.
- [4.64.] DARVAS, J., „DATA2, An auxiliary code of the VSOP code system for HTR’s calculation“, Forschungszentrum Jülich, KFA-IRE-IB-70-4, Germany, 1970, (in German).
- [4.65.] MULDER, E.J., „HTR-10 Benchmark Calculations“, PBMR (Pty) Ltd., Centurion, South Africa, 2002.

## Chapter 5

### RESULTS, CONCLUSIONS AND RECOMMENDATIONS

This Coordinated Research Programme provides the unique opportunity for Member States to both share in the code-to-code evaluation of selected benchmark problems, and also to compare their individual analyses to tests performed on the HTTR and HTR-10 reactors.

This chapter includes a collation of the benchmark problem results obtained by each organization coupled with the actual results achieved on the HTTR and HTR-10 test reactors. It also includes a synopsis by the Chief Scientific Investigators as to the areas of uncertainty and diverse modeling options that may have contributed to differences in individual Member State results as well as recommendations for code and model improvements that can be applied to future reactor design and development activities.

#### 5.1 HTTR REACTOR PHYSICS BENCHMARKS

This section contains a review of the HTTR core physics benchmark problem results obtained by individual Member States. In many cases, the participating organizations performed these benchmarks using both diffusion and Monte Carlo methodologies which are reported herein on separate tables in section 5.1.2.

##### 5.1.1. Collation of Codes and Models

Analyses by individual CSIs related to the HTTR reactor physics benchmark problem calculations included a wide variety of codes, models and methods. These are described in detail in chapter 2 by each Member State. A summary listing of the models and methods utilized for diffusion and Monte Carlo calculations are provided below.

*France* utilized the reactor physics code system SAPHYR. This includes several codes developed at CEA including APOLLO2 (transport), based on a data base produced with THEMIS/NJOY, CRONOS2 (diffusion-transport) and FLICA4 (3D thermal hydraulics). The Monte-Carlo code TRIPOLI4 was also used.

*Indonesia* utilized the CITATION model of SRAC-EWS.

*Turkey* utilized the MCNP-4B code in the HTTR calculations.

*USA* core physics calculations were performed utilizing the MCNP-4A Monte-Carlo code.

Tables 5.1 and 5.2 present additional details on codes and models utilized by selected Member States for diffusion and Monte Carlo calculations, respectively.

Table 5.1. Analysis method and model for diffusion calculations

Items	Germany	Russia	Japan	Netherlands	
	FZJ	OKBM	HTTR	NRG	IRI
Nuc. Data File	JEF-2.2	ENDF/B6	ENDF/B-4	JEF2.2	JEF2.2
Fuel Cell Code	TOTMOS	WIMS-D/4	DELIGHT	WIMS	SCALE4
Theory	Col.	S4	Col.	Col.	Transport
Model	Cyl.	Cyl.	Cyl.	Cyl.	Cyl.
No. of Groups	123	69	40	69	172
BP Cell Code	TOTMOS DORT	WIMS-D/4	TWOTRAN	WIMS	SCALE4
Theory	Transport	S4	Transport	Col.	Transport
Model	Cyl.	Cyl.	Cyl.	Hex.	Cyl.
No. of Groups	123	69	6	16	172
Core Cal. Code	CITATION	JAR-3D	CITATION-1000VP	PANTHER	BOLD-VENTURE
Model	Tri. (24mesh)	Tri. (6 mesh)	Tri. (24mesh)	Hex.	
No. of Groups (Fast +Thermal)	26	1 + 1	6 (3+3)	2	13
Cut-off Energy (eV)	1.86	0.625	2.38	2.1	2.1

Col. = Collision Probability  
Cyl. = Cylindrical

Table 5.2. Analysis method and model description for Monte Carlo calculations

Items	Russia		Japan	Netherlands	
	RRC KI	IBRAE	HTTR	NRG	IRI
Nuc. Data File	DLC/MCUDAT-1.0	ENDF/B6	JENDL-3.2	--	JEF2.2
Energy Struct.	Continuous	Continuous	Continuous		Group
Code	MCU	MCNP 4A	MVP	--	KENO V.a
History	200	2000 (up to 16000)	20000		10000
Batches	5000	1000	150		200
Skipped-Batches	1	10	5		1

### 5.1.2. Collation of Benchmark Analysis Results

A collation of the results obtained by each Member State for the HTTR core physics benchmark problems are provided in Tables 5.3 through 5.12. Investigation of these benchmarks by many of the participating organizations included analyses utilizing both diffusion and Monte Carlo methodologies. Also included are the actual experimental results obtained on the HTTR.

#### 5.1.2.1. Initial Criticality (HTTR FC)

The number of fuel columns are evaluated for first criticality, with the fuel columns charged from the outer region of the core. They are loaded clockwise, one by one. A small

excess reactivity at the first criticality is also evaluated. The following effects are considered in Phase 2 to improve benchmark problem calculation accuracy: 1) Air in void of graphite, 2) Revised impurity contents in dummy block, 3) Aluminum in the temporary neutron detector holders. Tables 5.3 and 5.4 provide the results for the HTTR FC benchmark problem for diffusion and Monte Carlo calculations, respectively.

Table 5.3. HTTR FC (diffusion calculation)

Member state	Number of fuel columns	Keff	Excess(%dk/k)
Japan	17	1.0005	0.05
France	17	1.0061	0.61
Germany	18	1.008	0.79
Indonesia	18	1.0058	0.577
Russia (OKBM)	16	1.005	0.498
Experimental results	19		

Table 5.4. HTTR FC (Monte-Carlo Calculation)

Member state	Number of fuel columns	Keff	Excess(%dk/k)
Japan	18	1.0061	0.61
France	18	1.0085	0.85
Netherlands(IRI)	17	1.0062	0.62
Russia(IBRAE)	16	1.006	0.596
Russia(RRCKI)	17	1.004	0.398
Turkey	15	1.005	0.50
Experimental results	19		

#### 5.1.2.2. Control Rod Position at Criticality (HTTR CR)

The control rod insertion depths are evaluated at the critical condition for three cases. All control rod insertion levels are adjusted on the same level except three pairs of control rods in the most outer region in the side reflectors. These three pairs of control rods should be fully withdrawn for the calculation at: 1) 18 columns (thin annular core), 2) 24 columns (thick annular core), 3) 30 columns (fully-loaded core). Tables 5.5 and 5.6 provide the results for the HTTR CR benchmark problem for diffusion and Monte Carlo calculations, respectively.

Table 5.5. HTTR CR (diffusion calculation)

Member State	Control rod position at critical (mm)		
	18 col.	24 col.	30 col.
Japan	3035	2055	1665
France			1787
Netherlands (NRG)			1615
Russia (OKBM)	2710	1960	1660
Experimental results		2215	1775

Table 5.6. HTTR CR (Monte Carlo calculation)

Member State	Control rod position at critical (mm)		
	18 col.	24 col.	30 col.
Japan	2810	2080	1800
France			1779
Netherlands (IRI)			1705
Russia (IBRAE)	2590	1950	1700
Russia (RRCKI)	3060	2010	1540
Turkey	2850	2100	1640
USA			1590
Experimental results		2215	1775

### 5.1.2.3. Excess Reactivity (HTTR EX)

The excess reactivity is evaluated for the three cases mentioned above. The room temperature of 300 K is to be assumed as the moderator and fuel temperatures for the benchmark problem. One atmospheric pressure of helium is to be used as the primary coolant condition. Tables 5.7 and 5.8 provide the results for the HTTR EX benchmark problem for diffusion and Monte Carlo calculations, respectively.

Table 5.7. HTTR EX (diffusion calculation)

Member State	% dk/k		
	18 col.	24 col.	30 col.
Japan	1.2	9.2	12.6
France	1.7 to 2.7	9.1 to 9.9	12.0 to 12.7
Germany	0.79	8.6	11.8
Indonesia	0.577	6.472	8.517
Netherlands (NRG)			13.8
Netherlands (IRI)			16.5
Russia (OKBM)	2.68	9.73	11.14
Experimental results		7.7	12.0

Table 5.8. HTTR EX (Monte Carlo calculation)

Member State	% dk/k		
	18 col.	24 col.	30 col.
Japan	0.61	9.06	12.5
France	0.85		12.15
Netherlands (IRI)	2.4		13.8
Russia (IBRAE)	2.7	10.83	13.55
Russia (RRCKI)	1.7	9.8	13.4
Turkey	2.981	10.689	13.525
USA			12.28
Experimental results		7.7	12.0

#### 5.1.2.4. Scram Reactivity (HTTR SC)

The Scram reactivity is evaluated for the following two cases: 1) All reflector CRs are inserted at the critical condition, 2) All CRs in reflector and core are inserted at the critical condition. The core condition for this benchmark problem is as follows:

- Fully-loaded core (30 column fuel core)
- Fresh fuel core

Tables 5.9 and 5.10 provide the results for the HTTR SC benchmark problem for diffusion and Monte Carlo calculations, respectively.

Table 5.9. HTTR SC (diffusion calculation)

Member State	% dk/k	
	Ref.CR	All CR.
Japan	8.3 CR-block and 8.94 for CR-hex	44.6
France	10.83	56.31
Netherlands (NRG)		37.5
Russia (OKBM)	8.43	52.37
Experimental results	12.0	46.0

Critical position at 480K, C, R1, R2 and R3 calculated at 1825 mm(full out) by Japan

Table 5.10. HTTR SC (Monte Carlo calculation)

Member State	% dk/k	
	Ref. CR	All CR.
Japan	9.53	45.1
France	8.56	46.32
Netherlands (IRI)	9.88	47.78
Russia (IBRAE)	9.61	40.40
Russia (RRCKI)	9.55	50.81
Turkey	7.75	37.96
USA		45.0
Experimental Results	12.0	46.0

#### 5.1.2.5. Isothermal Temperature Coefficient (HTTR TC)

Isothermal temperature coefficients for the fully-loaded core are evaluated from the effective multiplication. The critical control rod positions are changed with temperature elevation in actual reactor operation. However, the control rod position is not to be changed in the calculation to obtain the reactivity difference. Critical control rod positions are to be evaluated at a temperature of 480K. Tables 5.11 and 5.12 provide the results for the HTTR TC benchmark problem for diffusion and Monte Carlo calculations, respectively.

Table 5.11. HTTR TC (diffusion calculation)

Member State	% dk/k/K x 10 <sup>-4</sup>					
	290	320	360	400	440	470
Japan	-1.15 to - 1.39 over entire range					
France	-1.5 to -1.6 between 300 and 420K					
Netherlands (NRG)	-1.52(Average)					
Russia (OKBM)		-2.33	-2.19	-1.97	-1.82	-1.81
Experimental results	-1.3 to -1.4*					

\*Evaluated from measured control rod positions and calculated control rod worth curve

Table 5.12. HTTR TC (Monte Carlo calculation)

Member State	% dk/k/K x 10 <sup>-4</sup>					
	290	320	360	400	440	470
Japan		-1.23	-1.66	-1.63	-1.56	-0.91
Netherlands (IRI)	-1.47 (Average)					
Russia (IBRAE)		-1.95	-1.73	-1.65	-1.77	-1.45
Russia (RRCKI)		-1.1	-1.7	-0.9	-1.8	-1.3
Turkey	~ -1.2@ 450K					
USA	-.75 @ 550K					
Experimental results	-1.3 to -1.4					

### 5.1.3. Discussion of Results and General Conclusions

The Chief Scientific Investigators cited the following areas of uncertainty and different modeling options that may have contributed to differences in the results obtained by the participating organizations. These include:

1. Uncertainties in the level of impurities in the dummy blocks
2. Uncertainties in water and air or nitrogen content of graphite pores
3. Uncertainties in Monte Carlo modeling of coated fuel particles and differences in geometry representation, which may include any of the following options:
  - Explicit geometry
    - Regular array placement
    - Random placement
  - Statistical geometry
  - Homogeneous representation of coated particle region, explicit geometry elsewhere.
4. Choice of selected cross section data library and version (JEF, ENDF, JENDL, etc.)
5. Uncertainties in the modeling of neutron streaming with diffusion methods
6. Difficulty in modeling harmonics in thin annular cores with diffusion methods. This can be mitigated by:
  - Detailed leakage feedback
  - Use of fine group constants or super cell calculations

#### 5.1.4. Recommendations

A comparative review and analysis of the results obtained by the individual Member States was performed by the CSIs at the 4<sup>th</sup> Research Coordination Meeting. The following recommendations are suggested for incorporation into future reactor research and development activities:

1. Perform a comparison of results from different END/FB libraries (END/FB-VI-4 with older ones). Old libraries have poor graphite scattering data. This will help evaluate magnitude of error.
2. Further investigation of coated fuel particle modeling.
3. Additional experiments and analyses for temperature and burnup dependence of temperature coefficients.
4. Investigation of streaming especially in empty control rod channels and of methods used to calculate anisotropic diffusion coefficients for whole core calculations.
5. Two core physics benchmarks will be proposed after authorization from JAERI, namely:
  - HTTR – PCR: Calculation of control rod insertion depth at 15 and 30 MW powers.
  - HTTR – PTC: Calculation of temperature coefficients at 15 and 30 MW powers.

#### 5.2 HTTR THERMAL HYDRAULIC BENCHMARKS

This section includes a summary of the Member State analyses and the experimental results for the thermal hydraulic benchmark problems of vessel cooling and loss of off-site electric power on the HTTR.

##### 5.2.1. HTTR Vessel Cooling (HTTR-VC)

The vessel cooling benchmark problem included participation by four Member States (Japan, Russia, France and the USA). Reactor data was provided by JAERI for HTTR operation at 9 MW and 30 MW (850°C avg. reactor outlet temp.).

###### 5.2.1.1. Collation of HTTR-VC Codes and Models

###### *Japan*

Heat removal of the Vessel Cooling System was calculated using the SSPHEAT code which was developed to analyze the temperature distribution in the in-core structure test section (T2) of HENDEL with complicated passages of helium flow [3-2]. The helium flow was simulated by a thermal-flow element, which is a uniaxial element in three-dimensional space with the ability to conduct heat and transmit fluid between its nodal points. The element has two parameters, temperature and pressure, at each nodal point. Within the computer code, the model is solved by the finite element method (FEM).

###### *Russia*

SM-1, GTAS-M and DUPT codes were used for computation of power transferred from the reactor vessel to the reactor cavity cooling system and temperature distribution on the side panel. The SM-1 code is intended for computation of transient temperatures in

structures with arbitrary geometry and based on solution of the heat conduction equation by heat balance method.

### *USA*

The ORNL Graphite Reactor Severe Accident Code (GRSAC) was used for the IAEA CRP-5 HTTR-VC and HTTR-LP benchmark problems, utilizing both steady state and dynamic code features. These calculations relate to the HTTR initial rise to power sequence and safety demonstration tests. An existing HTTR model in GRSAC [3-15] was upgraded to provide more detail in certain critical areas.

### *France*

A model of the High Temperature Engineering Test Reactor was developed for the benchmark concerning the evaluation of the Performance of Vessel Cooling System during normal operation. The CAST3M code [3-17] has been used to model the HTTR. CAST3M is a multi-purpose finite element code developed at CEA, which allows 3D, 2D and R-Z axisymmetric calculations.

#### *5.2.1.2. Collation of HTTR-VC Benchmark Analysis Results*

Table 5.13 summarizes the calculated and experimental results for VCS power removal at 30 and 100% power levels.

Table 5.13: Comparison between analytical results and experimental results

Country		Analytical results				Experimental Results
		Japan	Russia	USA	France	
9MW operation	VCS heat removal	0.2 MW	0.133 MW	0.180 MW	0.178 MW	0.22 MW
	RPV temperature (EL. 19-27 m)*	~170°C	165°C	159°C		~ 170°C
30MW operation	VCS heat removal	0.77 MW	0.494 MW	0.67 MW	0.555 MW	0.81 MW
	RPV temperature (EL. 19-27 m)*	370-380°C	330-360°C	330°C		340-360°C

\* EL = Elevation (See Figure 3.6)

#### *5.2.1.3. Discussion of Results and General Conclusions*

In all cases, power removed by the VCS was underestimated by the calculations. JAERI had observed that hot cavity air leakage and circulation behind the cooling panels was considerably greater than initially expected. This degraded the effectiveness of radiation shields that were to reduce power removed by the VCS. Modeling of the effects of this leakage problem appeared to underestimate this effect to a greater or lesser extent in each of the calculations. The models used ranged from very detailed CFD calculations (France) to simplified empirically-derived models based on the JAERI scaled VCS experiment analyzed in CRP-3 (US).

Predictions of maximum vessel temperatures were generally good; however, the vessel temperatures are more dependent on conditions within the vessel than on VCS performance. The predictions for VCS power at the two operating conditions ranged from ~10% low to ~40% low compared to the measured values. This indicates a typical uncertainty range for VCS performance predictions – based on previous experience with CRP-3 benchmarks for the JAERI VCS mockup experiments. Clearly, additional experience in VCS performance calculations would be useful.

### **5.2.2. HTTR Loss of Off-site Electric Power (HTTR-LP)**

The loss of off-site electrical power from HTTR operating conditions of 15 and 30 MW was the basis for this benchmark problem. Four Member States (Japan, Russia, South Africa and the USA) participated in this activity.

#### *5.2.2.1. Collation of HTTR-LP Codes and Models*

##### ***Japan***

The pre-estimation results of the benchmark problem concerning the loss of off-site electric power simulation of the HTTR were determined utilizing the ‘ACCORD’ code and included the transition of the hot plenum block temperature, reactor inlet and outlet coolant temperatures, primary coolant pressure, reactor power and heat removal of the auxiliary heat exchanger. The estimated duration is for 3600s from the beginning of the loss of off-site electric power.

##### ***Russia***

Russia used the VGM-code for the HTTR-LP benchmark. This code is intended for calculating normal and emergency transients in nuclear power plants cooled by water or helium.

##### ***South Africa***

The HTTR system was modeled and analysed using the code “Flownet Nuclear” which is comprised of a graphite-moderated prismatic block reactor, a primary cooling circuit, secondary cooling circuit and an auxiliary cooling circuit. (helium is used as the working fluid).

##### ***USA***

The ORNL Graphite Reactor Severe Accident Code (GRSAC) was used for the HTTR-LP benchmark problem. An existing HTTR model in GRSAC [3-15] was upgraded to provide more detail in certain critical areas.

#### *5.2.2.2. Collation of HTTR-LP Benchmark Analysis Results*

Due to the time related nature of this benchmark problem, a concise collation of results is not a realistic option for this chapter. Therefore, the resulting curves and data obtained by the participating organizations is referenced below by table, figure and page number.

Japan has detailed the plant conditions for the HTTR before the LP test in Tables 3-22 through 3-28 (pages 182-184). The analyzed LP transient is described in Section 3.1.1.2 with the pre-event scenario for the LP transient depicted as Figure 3.4 (page 173). Japan's experimental results of the loss of the off-site electric power from 15 MW and 30 MW is shown as Figures 3.7 and 3.8 (page 182), respectively.

Russia's analysis of HTTR behaviour during the LP event is provided in a family of curves with Figures 3.20–3.32 for the transient from 15 MW and Figures 3.24–3.27 for the transient from full power (see pages 200–203)

South Africa's analysis using Flownet Nuclear includes Figures 3.28–3.43 (pages 223-225) for the LP event from 15 MW and Figures 3.44-3.49 (pages 226-228) for the transient from 30 MW.

Analyses by the USA are depicted in Figures 3.51 and 3.52 for the LP event from 100% power and Figures 3.53 and 3.54 from 50% power. Figures 3.55 and 3.56 provide the results of HTTR loss of off-site electric power even with no auxiliary cooling flow in the pressurized and depressurized conditions, respectively (pages 237-242).

### *5.2.2.3. Discussion of Results and General Conclusions*

The LP tests proved to be rather uneventful, as predicted, with the core temperatures decreasing gradually from the start of the transient. Following the reactor scram and main circulator coastdown, the two auxiliary cooling system circulators started up and ran for the first 40 minutes. After that, one of the two auxiliary circulators was stopped to reduce core thermal stresses associated with a rapid cooldown.

Analyses of the cooldown transients by Russia (VGM code), Japan (ACCORD code), South Africa (Flownet Nuclear code), and USA (GRSAC code) were presented and found to be in general agreement with the experimental results. For the 30 MW case, however, a discrepancy was observed between the Japanese and South African calculations and measurement of auxiliary cooler heat removal rate versus that predicted by both the Russian and USA codes. There are also some discrepancies between the calculated cooldown rates for the core. These differences are being investigated by the parties involved.

## **5.3 HTR-10 REACTOR PHYSICS BENCHMARKS**

This section contains a review of the HTR-10 core physics benchmark problem results obtained by individual Member States. This includes organizations from China, France, Germany, Indonesia, Japan, the Netherlands, Russia, South Africa, Turkey and the USA. In many cases, the participating organizations performed these benchmarks using both diffusion and Monte Carlo methodologies which are reported herein in separate tables.

### **5.3.1 Analysis Methods and Models**

This section includes an overall summary of the codes and models utilized by the participating Member States in their investigation of the benchmark problems associated with HTR-10 core physics

China employed the VSOP code system for calculation of HTR-10 criticality using the diffusion approach. The code system includes GAM for the calculation of fast and epithermal spectrums and THERMOS for the calculation of thermal spectrum. The finite mesh diffusion code CITATION in the code system calculates the eigenvalue problem in four energy groups and in two or three dimensional reactor geometry. Cross-sections of the resolved and unresolved resonances are generated by the ZUT-DGL code. For the Monte Carlo Calculation, the code version of MCNP-4A has been used in the criticality calculation. Nuclear data are based on ENDF/B-V.

The French reactor physics code system SAPHYR used by CEA. SAPHYR gathers several codes developed at CEA like APOLLO2 [4-46] (transport) based on a database produced with THEMIS/NJOY, CRONOS2 (diffusion-transport), and FLICA4 (3D-thermal hydraulics), which are interconnected. The Monte-Carlo code, TRIPOLI4 [4-47], has also been used throughout the study.

In Germany, the HTR-10 benchmark problems were calculated using the following parts of the VSOP code system: the ZUT [4-51], GAM-1 [4-52], THERMOS [4-53], and the CITATION [4-54] code.

BATAN of Indonesia used the WIMS/D4 nuclear design code in calculating HTR-10 first criticality. In addition, a code system consisting of DELIGHT [3-10], TWOTRAN-II [3-11] and CITATION-1000VP [3-12] codes were also used in collaboration between Indonesia and Japan.

In Japan, the HTR-10 core physics calculations were carried out using the HTTR nuclear evaluation code system. This code system consists of DELIGHT, TWOTRAN-II and CITATION-1000VP codes. The DELIGHT code is a one dimensional cell burnup code. Nuclear data was based on ENDF-IV, and III. TWOTRAN-II code was used for control rod cell calculation. CITATION-1000VP code was used for two-dimensional core calculations.

In the Netherlands the HTR-10 was modeled in the PANTHERMIX code, a combination of the 3-D diffusion reactor code PANTHER 5.1 coupled to the 2-D thermal hydraulics code THERMIX./DIREKT. The nuclear data necessary for the PANTHER code was generated by means of the WIMS8 code system.

Russia utilized the WIMS-D/4 code for the diffusion model. This was used to calculate the few-group macrosections characterizing the fuel cells and reflector blocks. The main results of diffusion approximation were obtained in two-group with a thermal cut-off energy of 0,625 eV. The JAR-code of 3D reactor calculation was used for estimation of multiplication coefficients. The nuclear data file was from ENDF/B6. The MCNP4A code was used for the Monte Carlo calculations with the nuclear data files from ENDF/B6 and NJOY.

At Hacettepe University in Turkey, Monte Carlo calculations were carried out using the KENOva module of the SCALE4.4 code system. Diffusion calculations were performed using VSOP'94.

The MCNP4B code was employed in the USA for criticality analysis using ENDF/B-VI cross-section data evaluated at 300 K, and the University of Texas at Austin (UTXS) cross-section library for the temperature-dependent calculations.

South Africa used the VSOP-PBMR design code with DATA2 to model the heterogeneous pebble fuel, the 2-D BIRGIT for reactor geometry and THERMIX for spectral temperature

### 5.3.2 Collation of Results

The results collation deals with two cases: (1) calculation results of the original defined benchmark problems, and (2) calculation results of the revised (deviated) benchmark problems. The differences between these two cases lie in the following: in the revised (deviated) benchmark problems, the following parameter changes have been considered in comparison to the original defined benchmark problems:

- ✧ Density of dummy balls: 1.73 → 1.84 g/cm<sup>3</sup>
- ✧ Boron equivalent of impurities in dummy ball: 1.3 → 0.125 ppm
- ✧ Core atmosphere: Helium → Air; Temperature: 20°C → 15°C

Available experimental results are also included in the collation tables.

Table 5-14: Collation of Results for Benchmark Problem B1 (Given in loading height, cm)

	Original Benchmark Problems		Revised (Deviated) Benchmark Problems	
	Diffusion/Transport	Monte Carlo	Diffusion/Transport	Monte Carlo
China	125.8	126.1	122.558	122.874
France <sup>1</sup>	-	-	-	115.36 117.37
Germany <sup>2</sup>	124.2 126.8	-	121.0 123.3	-
Indonesia <sup>3</sup>	107 120	-	-	-
Japan	113	-	-	-
Netherlands	125.3	-	122.1	-
Russia	136	137.3	-	-
South Africa	-	-	122.537	-
Turkey <sup>4</sup>	119.27	129.7 135.3	-	-
USA <sup>5</sup>	-	127.5 128	-	-
<b><i>Experimental result of critical loading height: 123.06cm. It is noted that the experimental conditions are those conditions for the revised (deviated) benchmarks except the temperature is 15°C instead of 20°C (or 27°C).</i></b>				

1. The first row of data is obtained with simplified PB modeling, and the second row of data with improved PB modeling.
2. The first row of data is obtained with 2-dimensional VSOP, and the second row of data with 3-dimensional VSOP.
3. The first row of data is obtained with the DELIGHT code, and the second row of data with SRAC code.
4. The first row of data in the Monte Carlo approach is obtained with the ENDF/B-IV nuclear data set, and the second row of data with ENDF/B-V nuclear data set.
5. The first row of data is obtained with the UTXS nuclear data set, and the second row of data with ENDF/B-VI nuclear data set.

### 3.3.2.1. Initial Criticality (Benchmark Problem B1)

This benchmark problem involved calculating the amount of loading (given in loading height, starting from the upper surface of the conus region) for the first criticality:  $K_{\text{eff}} = 1.0$  under the atmosphere of helium and core temperature of 20 °C, without any control rod being inserted. A collation of results by Member States is provided in Table 5-14.

Table 5-15: Collation of Results for Benchmark Problem B2, (original)

	B21 ( $K_{\text{eff}}$ at 20 or 27°C)		B22 ( $K_{\text{eff}}$ at 120°C)		B23 ( $K_{\text{eff}}$ at 250°C)	
	D/T	M	D/T	M	D/T	M
China	1.1197	-	1.1104	-	1.0960	-
Germany <sup>1</sup>	1.13725 1.12665	-	1.12404 1.11331	-	1.10693 1.09588	-
Indonesia <sup>2</sup>	1.2193 1.1381	-	1.1983 1.1149	-	1.1748 1.0844	-
Netherlands	1.1176	-	1.1085	-	1.0963	-
Russia	1.1182	1.1076	1.1079	1.0933	1.0927	1.0794
Turkey <sup>3</sup>	-	1.0941 1.0809	-	1.0802 1.0380	-	1.0671 1.0035
USA <sup>4</sup>	-	1.1319 1.1298	-	1.1279	-	1.1245

D/T: Diffusion and Transport approach, M: Monte Carlo approach

1. The first row of data is obtained with 2-dimensional VSOP, and the second row of data with 3-dimensional VSOP.
2. The first row of data is obtained with the DELIGHT code, and the second row of data with SRAC code.
3. The first row of data in the Monte Carlo approach is obtained with the ENDF/B-IV nuclear data set, and the second row of data with ENDF/B-V nuclear data set.
4. The first row of data is obtained with the UTXS nuclear data set, and the second row of data with ENDF/B-VI nuclear data set.

Table 5-16: Collation of Results for Benchmark Problem B2, Revised (deviated)

	B21 ( $K_{\text{eff}}$ at 20 or 27°C)		B22 ( $K_{\text{eff}}$ at 120°C)		B23 ( $K_{\text{eff}}$ at 250°C)	
	D/T	M	D/T	M	D/T	M
China	1.1358	1.1381	1.1262	-	1.1111	-
France <sup>1</sup>	-	1.15679 1.14737	-	-	-	-
Germany <sup>2</sup>	1.1468 1.1368	-	1.1334 1.1232	-	1.1160 1.1054	-
South Africa	1.12861	-	1.11956	-	1.10469	-

D/T: Diffusion and Transport approach, M: Monte Carlo approach

1. The first row of data is obtained with simplified PB modeling, and the second row of data with improved PB modeling.
2. The first row of data is obtained with 2-dimensional VSOP, and the second row of data with 3-dimensional VSOP.

### 3.3.2.2. Temperature Coefficient (Benchmark Problem B2)

This benchmark problem was to calculate the effective multiplication factor  $K_{\text{eff}}$  of the full core ( $5\text{m}^3$ ) under helium atmosphere and core temperatures as follows:  $20^\circ\text{C}$ (B21),  $120^\circ\text{C}$ (B22) and  $250^\circ\text{C}$ (B23) respectively, without any control rods being inserted. A collation of results by Member States is provided in Table 5-15 and 5-16 for the original and deviated benchmark, respectively.

### 3.3.2.3. Control Rod Worth for Full Core (Benchmark Problem B3)

This problem included calculating the reactivity worth of the ten fully inserted control rods (B31), and of one fully inserted control rod (B32, the other rods are in the withdrawn position) under helium atmosphere and a core temperature of  $20^\circ\text{C}$  for the full core. A collation of results by Member States is provided in Table 5-17.

Table 5-17. Collation of Results for Benchmark Problem B3

	Original Benchmark Problems				Revised (Deviated) Benchmark Problems			
	B31 (%)		B32 (%)		B31 (%)		B32 (%)	
	D/T	M	D/T	M	D/T	M	D/T	M
China	15.24	16.56	-	1.413	14.46	15.31	1.277	1.343
France <sup>1</sup>	-	-	-	-	-	13.06 13.44	-	1.35 1.31
Germany	16.6	-	1.56	-	15.73	-	1.48	-
Japan	18.0	-	-	-	-	-	-	-
Netherlands	11.86	-	-	-	-	-	-	-
Russia	15.50	17.90	-	-	-	-	-	-
Turkey <sup>2</sup>	-	18.73 21.88	-	2.53 4.60				
USA <sup>3</sup>	-	16.50 16.56	-	-	-	-	-	-

D/T: Diffusion and Transport approach, M: Monte Carlo approach

1. The first row of data is obtained with simplified PB modeling, and the second row of data with improved PB modeling.
2. The first row of data in the Monte Carlo approach is obtained with the ENDF/B-IV nuclear data set, and the second row of data with ENDF/B-V nuclear data set.
3. The first row of data is obtained with the UTXS nuclear data set, and the second row of data with ENDF/B-VI nuclear data set.

### 3.3.2.4. Control Rod Worth for the Initial Core (Benchmark Problem B4)

This benchmark problem involves calculation of the reactivity worth of the ten fully inserted control rods (B41) under helium atmosphere and core temperature of  $20^\circ\text{C}$  for a loading height of 126cm, and the differential worth of one control rod (B42, with the other rods in the withdrawn position). The differential reactivity worth is calculated when the lower end of the rod is at the following axial positions: 394.2cm, 383.618cm, 334.918cm, 331.318cm, 282.618cm, 279.018cm, 230.318cm.) under helium atmosphere and core temperature of  $20^\circ\text{C}$  for a loading height of 126cm. A collation of results by Member States is provided in Table 5-18.

Table 5-18: Collation of Results for Benchmark Problem B4

	Original Benchmark Problems				Revised (Deviated) Benchmark Problems			
	B41 (%)		B42 (%)		B41 (%)		B42 (%)	
	D/T	M	D/T	M	D/T	M	D/T	M
China	18.27	19.36	1.619	1.793	17.23	18.28	1.540	1.572
France <sup>1</sup>	-	-	-	-	-	13.66 13.80	-	1.52
Germany	20.50	-	1.97	-	19.31	-	1.86	-
Netherlands	13.61	-	-	-	-	-	-	-

*Experimental result of one rod (S3 rod) at initial core (B42): 1.4368%. It is noted that the experiment result is not directly to be compared with calculated data, as the control rod movement in the experiment is not exactly the same as benchmark definition. For detailed reasons please refer to Section 3.2.1.6.*

D/T: Diffusion and Transport approach, M: Monte Carlo approach

1. The first row of data is obtained with simplified PB modeling, and the second row of data with improved PB modeling.

### 5.3.3. Analysis and Conclusion

It is readily observed that the analyses by the Member State organizations can be factually divided as follows:

1. There are cases where good agreement exists between (1) different approaches (2) different participating institutions (3) calculation and experiment.
2. Generally and statistically speaking, the differences are huge between (1) different approaches (2) different participating institutions (3) calculation and experiment.

An analysis of why there are large statistical differences in the results between participating organizations is as follows:

1. Some cell calculations for preparing control rod cross-sections are more appropriate for rod array evaluations rather than single rod worth, due to boundary conditions used.
2. Control rod evaluations in partially fuelled core where some parts of the rod are adjacent to fuel and some he/air.
3. Uncertainty in the modeling of neutron streaming (directional diffusion calculations are required)
4. Choice of selected cross section library (JEFF, ENDF, JENDL, etc.)
5. Water content of graphite pores (assured zero but some may remain)
6. Investigation of library dependent cross-sections for temperature coefficients
7. Effective fuel homogenization methods for deterministic approach
8. Uncertainties in the modeling of fuel with Monte Carlo calculations including:
  - Explicit geometry
    - (ア) Coated particles, uniform distribution of particles is important throughout the pebbles
    - (イ) Pebbles, placement and distribution is important
  - Some analysis were performed using homogeneous cross-sections representing the fuel region containing particles, explicit geometry was used elsewhere as a hybrid method
  - The modeling of the fuel/dummy ball ratio

#### **5.3.4. Recommendations**

A comparative review and analysis of the results obtained by the individual Member States was performed by the CSIs at the 4<sup>th</sup> Research Coordination Meeting. The following recommendations are suggested for incorporation in future reactor research and development activities:

1. Perform a comparison of results from different ENDFB libraries (ENDF/B-VI-4 with older ones). Old libraries have poor graphite scattering data. This will help evaluate magnitude of error.
2. Further investigation of pebble modeling
3. Investigation of streaming especially in empty channels in graphite reflectors. Need to determine how to prepare directional diffusion coefficient for whole core calculations.

## Appendix

### RELATED IAEA PUBLICATIONS

- 1996 Design and Development of Gas Cooled Reactors with Closed Cycle Gas Turbines (IAEA-TECDOC-899)
- 1996 Graphite Moderator Lifecycle Behaviour (IAEA-TECDOC-901)
- 1997 Non-electric Applications of Nuclear Energy (IAEA-TECDOC-923)
- 1997 Fuel Performance and Fission Product Behaviour in Gas Cooled Reactors (IAEA-TECDOC-978)
- 1997 High Temperature Gas Cooled Reactor Development (IAEA-TECDOC-988)
- 1999 Hydrogen as an Energy Carrier and Its Production by Nuclear Power (IAEA-TECDOC-1085)
- 2000 Irradiation Damage in Graphite Due to Fast Neutrons in Fission and Fusion Systems (IAEA-TECDOC-1154)
- 2001 Heat Transport and Afterheat Removal for Gas Cooled Reactors under Accident Conditions (TECDOC-1163)
- 2001 Current Status and Future Development of Modular High Temperature Gas Cooled Reactor Technology (IAEA-TECDOC-1198)
- 2001 Safety Related Design and Economic Aspects of HTGRs (IAEA-TECDOC-1210)
- 2001 Gas Turbine Power Conversion Systems for Modular HJTGRs (IAEA-TECDOC-1238)
- 2001 Design and Evaluation of Heat Utilization Systems for the High Temperature Engineering Test Reactor (IAEA-TECDOC-1236)
- 2001 Validation of Safety Related Physics Calculations for Low Enriched HTGRs (TECDOC-1249)

## CONTRIBUTORS TO DRAFTING AND REVIEW

Aziz, F.	BATAN, Indonesia
Badulescu, A.	International Atomic Energy Agency, Vienna
Ball, S.	Oak Ridge National Laboratory, United States of America
Brey, H.	Nuclear Power Consultant to JAERI, United States of America
Brey, V.	United States of America
Brockmann, H.	Forschungszentrum Jülich, Germany
Colak, U.	Nuclear Engineering Dept., Hacettepe University, Turkey
de Haas, J.B.M..	NRG, Netherlands,
Du Toit, J.	Potchefstroom University, South Africa
Emslie, F.	PBMR (Pty) Ltd., Centurion, South Africa
Gougar, H.	Idaho National Engineering and Environmental Lab., United States of America
Jing, X.	Institute of Nuclear Energy Technology, China
Kadak, A.	Massachusetts Institute of Technology, United States of America
Kadiroglu, O.	Hacettepe University, Turkey,
Kendall, J.	International Atomic Energy Agency
Kunitomi, K.	JAERI, Japan
Kuzavkov, N.	OKBM, Russian Federation
Methnani, M.	International Atomic Energy Agency
Mulder, E.	PBMR, South Africa
Ohlig, U.	ISR, Forschungszentrum Jülich, Germany
Raepsaet, X.	CEA, France
Sun, Y.	INET, China
Tachibana, Y.	High Temperature Engineering Test Reactor, JAERI, Japan

Turkcan, E. Delft University of Technology (IRI), Netherlands  
Yamashita, K. High Temperature Engineering Test Reactor, JAERI, Japan

### **Research Coordination Meetings**

Vienna, Austria: 24–28 August 1998, 30 September–4 October 2002  
Beijing, China: 18–22 October 1999  
Oarai, Japan: 12–16 March 2001